

This Page Is Inserted by IFW Operations
and is not a part of the Official Record

BEST AVAILABLE IMAGES

Defective images within this document are accurate representation of
The original documents submitted by the applicant.

Defects in the images may include (but are not limited to):

- BLACK BORDERS
- TEXT CUT OFF AT TOP, BOTTOM OR SIDES
- FADED TEXT
- ILLEGIBLE TEXT
- SKEWED/SLANTED IMAGES
- COLORED PHOTOS
- BLACK OR VERY BLACK AND WHITE DARK PHOTOS
- GRAY SCALE DOCUMENTS

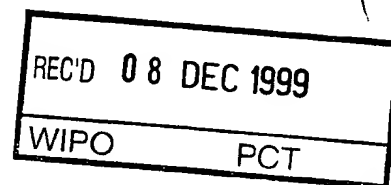
IMAGES ARE BEST AVAILABLE COPY.

**As rescanning documents *will not* correct images,
please do not report the images to the
Image Problem Mailbox.**

THIS PAGE BLANK (USPTO)



PCT/AU99/00894



Patent Office
Canberra

I, LEANNE MYNOTT, TEAM LEADER EXAMINATION SUPPORT AND SALES hereby certify that annexed is a true copy of the Provisional specification in connection with Application No. PP6538 for a patent by SILVERBROOK RESEARCH PTY LTD filed on 16 October 1998.

WITNESS my hand this
First day of December 1999

LEANNE MYNOTT
TEAM LEADER EXAMINATION
SUPPORT AND SALES



PRIORITY
DOCUMENT
SUBMITTED OR TRANSMITTED IN
COMPLIANCE WITH RULE 17.1(a) OR (b)

THIS PAGE BLANK (USPTO)

AUSTRALIA
Patents Act 1990

PROVISIONAL SPECIFICATION

Applicant(s) :

SILVERBROOK RESEARCH PTY LTD

Invention Title: Micromechanical Device and Method (IJ46f)

The invention is described in the following statement:

MICROMECHANICAL DEVICE AND METHOD (IJ46F)

Field of the Invention

The present invention relates to the construction of micro-electromechanical systems and in particular
5 discloses A method of manufacture of an out of plane bend actuator.

Background of the Invention

Recently, for example, in PCT Application No. PCT/AU98/00550 the present applicant has proposed an inkjet
10 printing device which utilizes micro-electromechanical (MEMS) processing techniques in the construction of a thermal bend actuator type device for the ejection of fluid from a nozzle chamber.

In the utilization of bend actuators within
15 (MEMS) devices, it is extremely important to have a highly efficient form of operation of the bend actuator. Unfortunately, the construction of (MEMS) devices often proceeds by the deposition and etching of multiple layers which in turn commonly results in a wafer surface, on a
20 microscopic scale, becoming uneven and having a number of hills and valleys in accordance with the masking and etching of lower layers. Unfortunately, such hills and valleys are likely to have a substantial operational influence on any mechanical type devices such as a thermal
25 actuator which is formed on top of a previously deposited substrate layer.

Summary of the Invention

It is an object of the present invention to provide for an effective form of operation of (MEMS)
30 mechanical devices such as bend actuators when formed on a substrate which is substantially non-planar at a microscopic level.

In accordance with a first aspect of the present invention, there is provided in a moveable micromechanical
35 device including a bending member having a first bending direction having a planar bottom surface, the bending member formed on a plane substrate on top of a number of

deposited lower layers, a method of forming the bending member comprising the step of: forming a series of structures in the deposited lower layers, the series of structures having a surface profile including a series of elongated ribs running in a direction substantially transverse to the bending direction.

The bending member can comprise a thermal bend actuator. The deposited layers can include a conductive circuitry layer and can be interconnected to the bending member for activation of the bending member. The bending member can be attached to a paddle member and actuated for the ejection of ink from an ink ejection nozzle of an ink jet printing device. The deposited layer, located under the bending member can include a power transistor for the control of operation of the bending member.

Brief Description of the Drawings

Notwithstanding any other forms which may fall within the scope of the present invention, preferred forms of the invention will now be described, by way of example only, with reference to the accompanying drawings in which:

Fig. 1 illustrates schematically a single ink jet nozzle in a quiescent position;

Fig. 2 illustrates schematically a single ink jet nozzle in a firing position;

Fig. 3 illustrates schematically a single ink jet nozzle in a refilling position;

Fig. 4 illustrates a bi-layer cooling process;

Fig. 5 illustrates a single-layer cooling process;

Fig. 6 is a top view of an aligned nozzle;

Fig. 7 is a sectional view of an aligned nozzle;

Fig. 8 is a top view of an aligned nozzle;

Fig. 9 is a sectional view of an aligned nozzle;

Fig. 10 is a sectional view of a process on constructing an ink jet nozzle;

Fig. 11 is a sectional view of a process on constructing an ink jet nozzle after Chemical Mechanical

Planarization;

Fig. 12 illustrates the steps involved in the preferred embodiment in preheating the ink;

Fig. 13 illustrates the normal printing clocking
5 cycle;

Fig. 14 illustrates the utilization of a preheating cycle;

Fig. 15 illustrates a graph of likely printhead operation temperature;

Fig. 16 illustrates a graph of likely printhead operation temperature;

Fig. 17 illustrates one form of driving a printhead for preheating

Fig. 18 illustrates a sectional view of a portion
15 of an initial wafer on which an ink jet nozzle structure is to be formed;

Fig. 19 illustrates the mask for N-well processing;

Fig. 20 illustrates a sectional view of a portion
20 of the wafer after N-well processing;

Fig. 21 illustrates a side perspective view partly in section of a single nozzle after N-well processing;

Fig. 22 illustrates the active channel mask;

Fig. 23 illustrates a sectional view of the field
25 oxide;

Fig. 24 illustrates a side perspective view partly in section of a single nozzle after field oxide deposition;

Fig. 25 illustrates the poly mask;

Fig. 26 illustrates a sectional view of the deposited poly;

Fig. 27 illustrates a side perspective view partly in section of a single nozzle after poly deposition;

Fig. 28 illustrates the n⁺ mask;

Fig. 29 illustrates a sectional view of the n⁺ implant;

Fig. 30 illustrates a side perspective view partly in section of a single nozzle after n+ implant;

Fig. 31 illustrates the p+ mask;

Fig. 32 illustrates a sectional view showing the
5 effect of the p+ implant;

Fig. 33 illustrates a side perspective view partly in section of a single nozzle after p+ implant;

Fig. 34 illustrates the contacts mask;

Fig. 35 illustrates a sectional view showing the
10 effects of depositing ILD 1 and etching contact vias;

Fig. 36 illustrates a side perspective view partly in section of a single nozzle after depositing ILD 1 and etching contact vias;

Fig. 37 illustrates the Metal 1 mask;

Fig. 38 illustrates a sectional view showing the
15 effect of the metal deposition of the Metal 1 layer;

Fig. 39 illustrates a side perspective view partly in section of a single nozzle after metal 1 deposition;

Fig. 40 illustrates the Via 1 mask;

Fig. 41 illustrates a sectional view showing the effects of depositing ILD 2 and etching contact vias;

Fig. 42 illustrates the Metal 2 mask;

Fig. 43 illustrates a sectional view showing the
25 effects of depositing the Metal 2 layer;

Fig. 44 illustrates a side perspective view partly in section of a single nozzle after metal 2 deposition;

Fig. 45 illustrates the Via 2 mask;

Fig. 46 illustrates a sectional view showing the
30 effects of depositing ILD 3 and etching contact vias;

Fig. 47 illustrates the Metal 3 mask;

Fig. 48 illustrates a sectional view showing the effects of depositing the Metal 3 layer;

Fig. 49 illustrates a side perspective view
35 partly in section of a single nozzle after metal 3 deposition;

Fig. 50 illustrates the Via 3 mask;

Fig. 51 illustrates a sectional view showing the effects of depositing passivation oxide and nitride and etching vias;

5 Fig. 52 illustrates a side perspective view partly in section of a single nozzle after depositing passivation oxide and nitride and etching vias;

Fig. 53 illustrates the heater mask;

10 Fig. 54 illustrates a sectional view showing the effect of depositing the heater titanium nitride layer;

Fig. 55 illustrates a side perspective view partly in section of a single nozzle after depositing the heater titanium nitride layer;

15 Fig. 56 illustrates the actuator / bend compensator mask;

Fig. 57 illustrates a sectional view showing the effect of depositing the actuator glass and bend compensator titanium nitride after etching;

20 Fig. 58 illustrates a side perspective view partly in section of a single nozzle after depositing and etching the actuator glass and bend compensator titanium nitride layers;

Fig. 59 illustrates the nozzle mask;

25 Fig. 60 illustrates a sectional view showing the effect of the depositing of the sacrificial layer and etching the nozzles;

Fig. 61 illustrates a side perspective view partly in section of a single nozzle after depositing and initial etching the sacrificial layer;

30 Fig. 62 illustrates the nozzle chamber mask;

Fig. 63 illustrates a sectional view showing the etched chambers in the sacrificial layer;

35 Fig. 64 illustrates a side perspective view partly in section of a single nozzle after further etching of the sacrificial layer;

Fig. 65 illustrates a sectional view showing the deposited layer of the nozzle chamber walls;

Fig. 66 illustrates a side perspective view partly in section of a single nozzle after further deposition of the nozzle chamber walls;

5 Fig. 67 illustrates a sectional view showing the process of creating self aligned nozzles using Chemical Mechanical Planarization (CMP);

Fig. 68 illustrates a side perspective view partly in section of a single nozzle after CMP of the nozzle chamber walls;

10 Fig. 69 illustrates a sectional view showing the nozzle mounted on a wafer blank;

Fig. 70 illustrates the back etch inlet mask;

Fig. 71 illustrates a sectional view showing the etching away of the sacrificial layers;

15 Fig. 72 illustrates a side perspective view partly in section of a single nozzle after etching away of the sacrificial layers;

Fig. 73 illustrates a side perspective view partly in section of a single nozzle after etching away of the sacrificial layers taken along a different section line;

Fig. 74 illustrates a sectional view showing a nozzle filled with ink;

25 Fig. 75 illustrates a side perspective view partly in section of a single nozzle ejecting ink;

Fig. 76 illustrates a schematic of the control logic for a single nozzle;

Fig. 77 illustrates a CMOS implementation of the control logic of a single nozzle;

30 Fig. 78 illustrates a legend or key of the various layers utilized in the described CMOS/MEMS implementation;

Fig. 79 illustrates the CMOS levels up to the poly level;

35 Fig. 80 illustrates the CMOS levels up to the metal 1 level;

Fig. 81 illustrates the CMOS levels up to the

metal 2 level;

Fig. 82 illustrates the CMOS levels up to the metal 3 level;

Fig. 83 illustrates the CMOS and MEMS levels up to the MEMS heater level;

Fig. 84 illustrates the Actuator Shroud Level;

Fig. 85 illustrates a side perspective partly in section of a portion of an ink jet head;

Fig. 86 illustrates an enlarged view of a side perspective partly in section of a portion of an ink jet head;

Fig. 87 illustrates a number of layers formed in the construction of a series of actuators;

Fig. 88 illustrates a portion of the back surface of a wafer showing the through wafer ink supply channels;

Fig. 89 illustrates the arrangement of segments in a printhead;

Fig. 90 illustrates schematically a single pod numbered by firing order;

Fig. 91 illustrates schematically a single pod numbered by logical order;

Fig. 92 illustrates schematically a single tripod containing one pod of each color;

Fig. 93 illustrates schematically a single podgroup containing 10 tripods;

Fig. 94 illustrates schematically, the relationship between segments, firegroups and tripods;

Fig. 95 illustrates clocking for AEnable and BEnable during a typical print cycle;

Fig. 96 illustrates an exploded perspective view of the incorporation of a printhead into an ink channel molding support structure;

Fig. 97 illustrates a side perspective view partly in section of the ink channel molding support structure;

Fig. 98 illustrates a side perspective view partly in section of a print roll unit, printhead and

platen; and

Fig. 99 illustrates a side perspective view of a print roll unit, printhead and platen;

Fig. 100 illustrates a side exploded perspective view of a print roll unit, printhead and platen;

Description of Preferred and Other Embodiments

The preferred embodiment utilizes a 4-inch width printhead suitable for incorporation into small printers and in print on demand camera systems. The printhead will be herein after referred to generically as Memjet.

The preferred embodiment relies on the utilization of a thermally actuated lever arm which is utilized for the ejection of ink. The nozzle chamber in which ink ejection occurs includes a thin nozzle rim around which a surface meniscus is formed. A nozzle rim is formed utilizing a self aligning deposition mechanism. The preferred embodiment also includes the advantageous feature of a flood prevention rim around the ink ejection nozzle.

Turning initially to Fig. 1 to Fig. 3, there will be now initially explained the operation of principles of the ink jet printhead of the preferred embodiment. In Fig. 1, there is illustrated a single nozzle arrangement 1 which includes a nozzle chamber 2 which is supplied via an ink supply channel 3 so as to form a meniscus 4 around a nozzle rim 5. A thermal actuator mechanism 6 is provided and includes an end paddle 7 which can be a circular form. The paddle 7 is attached to an actuator arm 8 which pivots at a post 9. The actuator arm 8 includes two arms 10, 11 which are formed from a conductive material having a high degree of stiffness, such as titanium nitride. The bottom arm 10 forms a conductive circuit interconnect to post 9 and further includes a thinned portion near the end post 9. Hence, upon passing a current through the bottom layer 10, the bottom layer is heated in the area adjacent the post 9.

Without the heating, the two arms 10, 11 are in thermal balance with one another. The heating of the bottom arm 10 causes the overall actuator mechanism 6 to bend generally

upwards and hence paddle 7 as indicated in Fig. 2 undergoes a rapid upward movement. The rapid upward movement results in an increase in pressure around the rim 5 which results in a general expansion of the meniscus 4 as ink flows outside the chamber. The conduction to the bottom arm 10 is turned off. The actuator arm 6, as illustrated in Fig. 3 begins to return to its quiescent position. The return results in a movement of the panel 7 in a downward direction. This in turn results in a general sucking back of the ink around the nozzle 5. The forward momentum of the ink outside the nozzle in addition to the backward momentum of the ink within the nozzle chamber results in a drop 14 being formed as a result of a necking and breaking of the meniscus 4. Subsequently, due to surface tension effects across the meniscus 4, ink is drawn into the nozzle chamber 2 from the ink supply channel 3.

The operation of the preferred embodiment has a number of significant features. Firstly, there is the aforementioned balancing of the arm 10, 11. The utilization of a second arm 11 allows for more efficient thermal operation of the actuator device 6. Further, the two arm operation ensures thermal stresses are not a problem upon cooling during manufacture, thereby reducing the likelihood of "lift off" during fabrication. This is illustrated in Fig. 4 and Fig. 4. In Fig. 4, there is shown the process of cooling off a thermal actuator arm having two balanced material layers 20, 21 surrounding a central material layer 22. The cooling process affects each of the conductive layers 20, 21 equally resulting in a stable configuration. In Fig. 5, a thermal actuator arm having only one conductive layer 20 as shown. Upon cooling after manufacture, the upper arm 20 is going to bend with respect to the lower arm 22. This is likely to cause problems due to the instability of the final arrangement and variations and thickness of various layers which will result in different degrees of bending.

Further, the arrangement described with reference

to Fig. 1 to Fig. 3 includes an ink jet spreading prevention rim 25 which is constructed so as to provide for a pit around the nozzle rim 5. Any ink which should flow outside of the nozzle rim 5 is generally caught within the pit 26 around the rim and thereby prevented from flowing across the surface of the ink jet head and influencing operation.

Further, the nozzle rim 5 and ink spread prevention rim 25 are formed via a unique chemical mechanical planarization technique. This arrangement can be understood by reference to Fig. 6 to Fig. 9. Ideally, an ink ejection nozzle rim is highly symmetrical in form as illustrated 30 in Fig. 6. The utilization of a thin highly regular rim is desirable when it is time to eject ink. For example, in Fig. 7 there is illustrated a drop being ejected from a rim during the necking and breaking process. The necking and breaking process is a high sensitive one, complex chaotic forces being involved. Should standard lithography be utilized to form the nozzle rim, it is likely that the regularity or symmetry of the rim can only be guaranteed to within a certain degree of variation in accordance with the lithographic process utilized. This may result in a variation of the rim as illustrated 35 in Fig. 8. The rim variation leads to a non-symmetrical rim 35 as illustrated in Fig. 8. This variation is likely to cause problems when forming a droplet. The problem is illustrated in Fig. 9 wherein the meniscus 36 creeps along the surface 37 where the rim is bulging. This results in an ejected drop likely to have a higher variants in direction of ejection.

In the preferred embodiment, to overcome this problem, a self aligning chemical mechanical planarization (CMP) technique is utilized. A simplified illustration of this technique will now be discussed with reference to Fig. 10. In Fig. 10, there is illustrated a silicon substrate 40 upon which is deposited a first sacrificial layer 41 and a thin layer of material such as titanium nitride 42 shown

in exaggerated form. The sacrificial layer is first deposited and etched so as to form a "blank" for the titanium nitride layer 42 which is deposited over all surfaces conformally utilizing, for exmaple, sputtered TiN or low temperature MOCVD TiN, depending on the choice of the sacrificial materials. In an alternative manufacturing process, a further sacrificial material layer can be deposited on top of the titanium nitride layer.

Next, the critical step is to chemically mechanically planarize the titanium nitride and sacrificial layers down to a first level eg. 44. The chemical mechanical planarization process acts to effectively "chop off" the top layers down to level 44. Through the utilization of conformal TiN deposition, a regular rim is produced. The result, after chemical mechanical planarization, is illustrated schematically in Fig. 11.

The description of the preferred embodiments will now proceed by first describing an ink jet preheating step preferably utilized in the memjet device.

20 Ink Preheating

In the preferred embodiment, an ink preheating step is utilized so as to bring the temperature of the printhead arrangement to be within a predetermined bound. The steps utilized are illustrated 101 in Fig. 12.

25 Initially, the decision to initiate a printing run is made 102. Before any printing has begun, the current temperature of the printhead is sensed to determine whether it is above a predetermined threshold. If the heated temperature is too low, a preheat cycle 104 is applied 30 which heats the printhead by means of heating the thermal actuators to be above a predetermined temperature of operation. Once the temperature has achieved a predetermined temperature, the normal print cycle 105 has begun.

35 The utilization of the preheating step 104 results in a general reduction in possible variation in factors such as viscosity etc. allowing for a narrower

operating range of the device and, the utilization of lower thermal energies in ink ejection.

The preheating step can take a number of different forms. Where the ink ejection device is of a thermal bend actuator type, it would normally receive a series of clock pulses as illustrated in Fig. 13 with the ejection of ink requiring a clock pulses 110 of a predetermined thickness so as to provide enough energy for ejection.

As illustrated in Fig. 14, when it is desired to provide for preheating capabilities, these can be provided through the utilization of a series of shorter pulses eg. 111 which whilst providing thermal energy to the printhead, failed to cause ejection of the ink from the ink ejection nozzle.

Fig. 16 illustrates an example graph of the printhead temperature during a printing operation. Assuming the printhead has been idle for a substantial period of time, the printhead temperature initially 115 will be the ambient temperature. When it is desired to print, a preheating step (104 of Fig. 12) is executed such that the temperature rises 116 to an operational temperature T_2 , 117 at which point printing can begin and the temperature left to fluctuate in accordance with usage requirements.

Alternately, as illustrated in Fig. 16, the printhead temperature can be continuously monitored such that should the temperature fall below a threshold eg. 120, a series of preheating cycles are injected into the printing process so as to increase the temperature 121 above a threshold.

Assuming the ink utilized has properties substantially similar to that water, the utilization of the preheating step can take advantage of the substantial fluctuations in ink viscosity with temperature. Of course, other operational factors may be significant and the stabilisation to a narrower temperature range provides for advantageous effects. As the viscosity changes with

changing temperature, it would be readily evident that the degree of preheating required above the ambient temperature will be dependant upon the ambient temperature and the equilibrium temperature of the printhead during printing operations. Hence, the degree of preheating may be varied in accordance with the measured ambient temperature so as to provide for optimal results.

A simple operational schematic is illustrated in Fig. 17 with the printhead 130 including an on-board series of temperature sensors which are connected to a temperature determination unit 131 for determining the current temperature which in turn outputs to an ink ejection drive unit 132 which determines whether preheating is required at any particular stage. The on chip temperature sensors can be simple MEMS temperature sensors, the construction of which is well known to those skilled in the art.

Memjet Manufacturing Process

The Memjet device manufacture can be constructed from a combination of standard CMOS processing, and MEMS postprocessing. Ideally, no exotic materials are used. The only materials are PECVD glass, sputtered TiN, and a sacrificial material (which may be polyimide, BPSG, aluminum, or other materials). Ideally, to fit corresponding drive circuits between the nozzles without increasing chip area, the minimum process is a 0.5 micron, one poly, 3 metal CMOS process with aluminum metalization. However, any more advanced process can be used instead. Alternatively, NMOS, bipolar, BiCMOS, or other processes may be used. CMOS is recommended only due to its prevalence in the industry, and the availability of large amounts of CMOS fab capacity.

The CMOS process implements a simple circuit consisting of 19,200 stages of shift register, 19,200 bits of transfer register, 19,200 enable gates, and 19,200 drive transistors. There are also some clock buffers and enable decoders. The clock speed of a photo print head is only 3.8 MHz, and a 30 ppm A4 print head is only 14 MHz, so the CMOS

performance is not critical. The CMOS process is fully completed, including passivation and opening of bond pads before the MEMS processing begins. This allows the CMOS processing to be completed in a standard CMOS fab, with the MEMS processing being performed in a separate facility.

Reasons for Process Choices

It will be understood from those skilled in the art of manufacture of MEMS devices that there are many possible process sequences for the manufacture of a Memjet nozzle printhead. The process sequence described here is based on a 'generic' 0.5 micron (drawn) n-well CMOS process with 1 poly and three metal layers. This table outlines the reasons for some of the choices of this 'nominal' process, to make it easier to determine the effect of any alternative process choices.

Nominal Process	Reason
CMOS	Wide availability
0.5 micron or less	0.5 micron is required to fit drive electronics without increasing chip area
0.5 micron or more	Fully amortized fabs, low cost
N-well	Performance of n-channel is more important than p-channel transistors
6" wafers	Minimum practical for 4" monolithic printheads
1 polysilicon layer	2 poly layers are not required, as there is little low current connectivity
3 metal layers	To supply high currents, most of metal 3 also provides sacrificial structures
Aluminum metalization	Low cost, standard for 0.5 micron processes (copper may be more efficient)

Mask Summary

Mask #	Mask	Notes	Type	Pattern	Align to	CD
1	N-well		CMOS 1	Light	Flat	4 μm
2	Active	Includes nozzle chamber	CMOS 2	Dark	N-Well	1 μm
3	Poly		CMOS 3	Dark	Active	0.5 μm
4	N+		CMOS 4	Dark	Poly	4 μm
5	P+		~CMOS 4	Light	Poly	4 μm
6	Contact	Includes nozzle chamber	CMOS 5	Light	Poly	0.5 μm
7	Metal 1		CMOS 6	Dark	Contact	0.6 μm
8	Via 1	Includes nozzle chamber	CMOS 7	Light	Metal 1	0.6 μm
9	Metal 2	Includes sacrificial aluminum	CMOS 8	Dark	Via 1	0.6 μm
10	Via 2	Includes nozzle chamber	CMOS 9	Light	Metal 2	0.6 μm
11	Metal 3	Includes sacrificial aluminum	CMOS 10	Dark	Poly	1 μm
12	Via 3	Overcoat, but 0.6 μm CD	CMOS 11	Light	Poly	0.6 μm
13	Heater		MEMS 1	Dark	Poly	0.6 μm
14	Actuator		MEMS 2	Dark	Heater	1 μm
15	Nozzle	For CMP cut region control	MEMS 3	Dark	Poly	2 μm
16	Chamber		MEMS 4	Dark	Nozzle	2 μm
17	Inlet	Backside deep silicon etch	MEMS 5	Light	Poly	4 μm

Example Process Sequence (Including CMOS Steps)

Although many different CMOS and other processes can be used, this process description is combined with an example CMOS process to show where MEMS features are integrated in the CMOS masks, and show where the CMOS process may be simplified due to the low CMOS performance requirements.

Process steps described below are part of the example 'generic' 1P3M 0.5µm CMOS process.

As shown in Fig. 18, processing starts with a standard 6" p-type <100> wafers. (8" wafers can also be used, giving a substantial increase in primary yield).

Using the n-well mask of Fig. 19, implant the n-well transistor portions 210 of Fig. 20.

Grow a thin layer of SiO₂ and deposit Si₃N₄ forming a field oxide hard mask.

Etch the nitride and oxide using the active mask of Fig. 22. The mask is oversized to allow for the LOCOS bird's beak. The nozzle chamber region is incorporated in this mask, as field oxide is excluded from the nozzle chamber. The result is a series of oxide regions 212, illustrated in Fig. 23.

Implant the channel-stop using the n-well mask with a negative resist, or using a complement of the n-well mask.

Perform any required channel stop implants as required by the CMOS process used.

Grow 0.5 micron of field oxide using LOCOS.

Perform any required n/p transistor threshold voltage adjustments. Depending upon the characteristics of the CMOS process, it may be possible to omit the threshold adjustments. This is because the operating frequency is only 3.8 MHz, and the quality of the p-devices is not critical. The n-transistor threshold is more significant,

as the on-resistance of the n-channel drive transistor has a significant effect on the efficiency and power consumption while printing.

Grow the gate oxide

Deposit 0.3 microns of poly, and pattern using the poly mask illustrated in Fig. 25 so as to form poly portions 214 shown in Fig. 26.

5 Perform the n+ implant shown e.g. 216 in Fig. 29 using the n+ mask shown in Fig. 28. The use of a drain engineering processes such as LDD should not be required, as the performance of the transistors is not critical.

10 Perform the p+ implant shown e.g. 218 in Fig. 32, using a complement of the n+ mask shown in Fig. 31, or using the n+ mask with a negative resist. The nozzle chamber region will be doped either n+ or p+ depending upon whether it is included in the n+ mask or not. The doping of this silicon region is not relevant as it is
15 subsequently etched, and the STS ASE etch process recommended does not use boron as an etch stop.

Deposit 0.6 microns of PECVD TEOS glass to form ILD 1, shown e.g. 220 in Fig. 35.

20 Etch the contact cuts using the contact mask of Fig. 34. The nozzle region is treated as a single large contact region, and will not pass typical design rule checks. This region should therefore be excluded from the DRC.

Deposit 0.6 microns of aluminum to form metal 1.

25 Etch the aluminum using the metal 1 mask shown in Fig. 37 so as to form metal regions e.g. 224 shown in Fig. 38. The nozzle metal region is covered with metal 1 e.g. 225. This aluminum 225 is sacrificial, and is etched as part of the MEMS sequence. The inclusion of metal 1 in the
30 nozzle is not essential, but helps reduce the step in the neck region of the actuator lever arm.

Deposit 0.7 microns of PECVD TEOS glass to form ILD 2 regions e.g. 228 of Fig. 41.

Etch the contact cuts using the via 1 mask shown
35 in Fig. 40. The nozzle region is treated as a single large via region, and again it will not pass DRC.

Deposit 0.6 microns of aluminum to form metal 2.

Etch the aluminum using the metal 2 mask shown in Fig. 42 so as to form metal portions e.g. 230 shown in Fig. 43. The nozzle region 231 is fully covered with metal 2. This aluminum is sacrificial, and is etched as part of the MEMS sequence. The inclusion of metal 2 in the nozzle is not essential, but helps reduce the step in the neck region of the actuator lever arm. Sacrificial metal 2 is also used for another fluid control feature. A relatively large rectangle of metal 2 is included in the neck region 233 of the nozzle chamber. This is connected to the sacrificial metal 3, so is also removed during the MEMS sacrificial aluminum etch. This undercuts the lower rim of the nozzle chamber entrance for the actuator (which is formed from ILD 3). The undercut adds 90 degrees to angle of the fluid control surface, and thus increases the ability of this rim to prevent ink surface spread.

Deposit 0.7 microns of PECVD TEOS glass to form ILD 3.

Etch the contact cuts using the via 2 mask shown in Fig. 45 so as to leave portions e.g. 236 shown in Fig. 46. As well as the nozzle chamber, fluid control rims are also formed in ILD 3. These will also not pass DRC.

Deposit 1.0 microns of aluminum to form metal 3.

Etch the aluminum using the metal 3 mask shown in Fig. 47 so as to leave portions e.g. 238 as shown in Fig. 48. Most of metal 3 e.g. 239 is a sacrificial layer used to separate the actuator and paddle from the chip surface. Metal 3 is also used to distribute V+ over the chip. The nozzle region is fully covered with metal 3 e.g. 240. This aluminum is sacrificial, and is etched as part of the MEMS sequence. The inclusion of metal 3 in the nozzle is not essential, but helps reduce the step in the neck region of the actuator lever arm.

Deposit 0.5 microns of PECVD TEOS glass to form the overglass.

35 Deposit 0.5 microns of Si_3N_4 to form the passivation layer.

Etch the passivation and overglass using the via

3 mask shown in Fig. 50 so as to form the arrangement of Fig. 51. This mask includes access 242 to the metal 3 sacrificial layer, and the vias e.g. 243 to the heater actuator. Lithography of this step has 0.6 micron critical dimensions (for the heater vias) instead of the normally relaxed lithography used for opening bond pads. This is the one process step which is different from the normal CMOS process flow. This step may either be the last process step of the CMOS process, or the first step of the MEMS process, depending upon the fab setup and transport requirements.

Wafer Probe. Much, but not all, of the functionality of the chips can be determined at this stage. If more complete testing at this stage is required, an active dummy load can be included on chip for each drive transistor. This can be achieved with minor chip area penalty, and allows complete testing of the CMOS circuitry. Transfer the wafers from the CMOS facility to the MEMS facility. These may be in the same fab, or may be distantly located.

Deposit 0.9 microns of magnetron sputtered TiN. Voltage is -65V, magnetron current is 7.5 A, argon gas pressure is 0.3 Pa, temperature is 300 °C. This results in a coefficient of thermal expansion of $9.4 \times 10^{-6} / ^\circ\text{C}$, and a Young's modulus of 600 GPa [*Thin Solid Films* 270 p 266, 1995], which are the key thin film properties used.

Etch the TiN using the heater mask shown in Fig. 53. This mask defines the heater element, paddle arm, and paddle. There is a small gap 247 shown in Fig. 54 between the heater and the TiN layer of the paddle and paddle arm. This is to prevent electrical connection between the heater and the ink, and possible electrolysis problems. Sub-micron accuracy is required in this step to maintain a uniformity of heater characteristics across the wafer. This is the main reason that the heater is not etched simultaneously with the other actuator layers. CD for the heater mask is 0.5 microns. Overlay accuracy is +/- 0.1 microns. The bond pads are also covered with this layer of TiN. This is to

prevent the bond pads being etched away during the sacrificial aluminum etch. It also prevents corrosion of the aluminum bond pads during operation. TiN is an excellent corrosion barrier for aluminum. The resistivity of TiN is low enough to not cause problems with the bond pad resistance.

Deposit 2 microns of PECVD glass. This is preferably done at around 350 °C to 400 °C to minimize intrinsic stress in the glass. Thermal stress could be reduced by a lower deposition temperature, however thermal stress is actually beneficial, as the glass is sandwiched between two layers of TiN. The TiN/glass/TiN tri-layer cancels bend due to thermal stress, and results in the glass being under constant compressive stress, which increases the efficiency of the actuator.

Deposit 0.9 microns of magnetron sputtered TiN. This layer is deposited to cancel bend from the differential thermal stress of the lower TiN and glass layers, and prevent the paddle from curling when released from the sacrificial materials. The deposition characteristics should be identical to the first TiN layer.

Anisotropically plasma etch the TiN and glass using actuator mask as shown in Fig. 56. This mask defines the actuator and paddle. CD for the actuator mask is 1 micron. Overlay accuracy is +/- 0.1 microns. The results of the etching process is illustrated in Fig. 57 with the glass layer 250 sandwiched between TiN layers 251, 248. Electrical testing can be performed by wafer probing at this time. All CMOS tests and heater functionality and resistance tests can be completed at wafer probe.

Deposit 15 microns of sacrificial material. There are many possible choices for this material. The essential requirements are the ability to deposit a 15 micron layer without excessive wafer warping, and a high etch selectivity to PECVD glass and TiN. Several possibilities are borophosphosilicate glass (BPSG), polymers such as polyimide, and aluminum. Either a close CTE match to

silicon (BPSG with the correct doping, filled polyimide) or a low Young's modulus (aluminum) is required. This example uses BPSG. Of these issues, stress is the most demanding due to the extreme layer thickness. BPSG normally has a CTE well below that of silicon, resulting in considerable compressive stress. However, the composition of BPSG can be varied significantly to adjust its CTE close to that of silicon. As the BPSG is a sacrificial layer, its electrical properties are not relevant, and compositions not normally suitable as a CMOS dielectric can be used. Low density, high porosity, and a high water content are all beneficial characteristics as they will increase the etch selectivity versus PECVD glass when using an anhydrous HF etch.

Etch the sacrificial layer to a depth of 2 microns using the nozzle mask as defined in Fig. 59 so as to form the structure 254 illustrated in section in Fig. 60. The mask of Fig. 59 defines all of the regions where a subsequently deposited overcoat is to be polished off using CMP. This includes the nozzles themselves, and various other fluid control features. CD for the nozzle mask is 2 microns. Overlay accuracy is +/- 0.5 microns.

Anisotropically plasma etch the sacrificial layer down to the CMOS passivation layer using the chamber mask as illustrated in Fig. 62. This mask defines the nozzle chamber and actuator shroud including slots 255 as shown in Fig. 63. CD for the chamber mask is 2 microns. Overlay accuracy is +/- 0.2 microns.

Deposit 0.5 microns of fairly conformal overcoat material 257 as illustrated in Fig. 65. The electrical properties of this material are irrelevant, and it can be a conductor, insulator, or semiconductor. The material should: be chemically inert, be strong, have a high etch selectivity with respect to the sacrificial material, be suitable for CMP planarization, and be suitable for conformal deposition at temperatures below 500 °C. Suitable materials include: PECVD glass, MOCVD TiN, ECR CVD TiN, PECVD Si₃N₄, and many others. The choice for this example

is PECVD TEOS glass. This must have a very low water content if BPSG is used as the sacrificial material and anhydrous HF is used as the sacrificial etchant, as the anhydrous HF etch relies on water content to achieve 1000:1
5 etch selectivity of BPSG over TEOS glass.

Planarize the wafer to a depth of 1 micron using CMP as illustrated in Fig. 67. The CMP processing should be maintained to an accuracy of +/- 0.5 microns over the wafer surface. Dishing of the sacrificial material is not
10 relevant. This opens the nozzles 259 and fluid control regions e.g. 260. The rigidity of the sacrificial layer relative to the nozzle chamber structures during CMP is one of the key factors which may affect the choice of sacrificial materials.

15 Turn the print head wafer over and securely mount the front surface on an oxidized silicon wafer blank 262 illustrated in Fig. 69 having an oxidized surface 263. The mounting can be by way of glue 265. The blank wafers 262 can be recycled.

20 Thin the print head wafer to 300 microns using backgrinding (or etch) and polish. The wafer thinning is performed to reduce the subsequent processing duration for deep silicon etching from around 5 hours to around 2.3 hours. The accuracy of the deep silicon etch is also
25 improved, and the hard-mask thickness is halved to 2.5 microns. The wafers could be thinned further to improve etch duration and print head efficiency. The limitation to wafer thickness is the print head fragility after sacrificial BPSG etch.

30 Deposit a SiO₂ hard mask (2.5 microns of PECVD glass) on the backside of the wafer and pattern using the inlet mask as shown in Fig. 67. The hard mask of Fig. 67 is used for the subsequent deep silicon etch, which is to a depth of 315 microns with a hard mask selectivity of 150:1.

35 This mask defines the ink inlets, which are etched through the wafer. CD for the inlet mask is 4 microns. Overlay accuracy is +/- 2 microns. The inlet mask is undersize by

5.25 microns on each side to allow for a re-entrant etch angle of 91 degrees over a 300 micron etch depth.

Lithography for this step uses a mask aligner instead of a stepper. Alignment is to patterns on the front of the

5 wafer. Equipment is readily available to allow sub-micron front-to-back alignment.

Back-etch completely through the silicon wafer (using, for example, an ASE Advanced Silicon Etcher from Surface Technology Systems) through the previously
10 deposited hard mask. The STS ASE is capable of etching highly accurate holes through the wafer with aspect ratios of 30:1 and sidewalls of 90 degrees. In this case, a re-entrant sidewall angle of 91 degrees is taken as nominal. A re-entrant angle is chosen because the ASE performs better,
15 with a higher etch rate for a given accuracy, with a slightly re-entrant angle. Also, a re-entrant etch can be compensated by making the holes on the mask undersize. Non-re-entrant etch angles cannot be so easily compensated, because the mask holes would merge. This etch will take
20 approximately 2.2 hours, meaning that 40 of these machines would be required for a fab processing 10,000 wafers per month. While this is a significant outlay, such a fab could produce 18 million print heads per annum on 6" wafers, resulting in an amortized cost contribution of the ASE of
25 less than 50 cents per print head. The wafer is also preferably diced by this etch. The final result is as illustrated in Fig. 69 including back etched ink channel portions 264.

Etch all exposed aluminum. Aluminum on all three
30 layers is used as sacrificial layers in certain places.

Etch all of the sacrificial material. The nozzle chambers are cleared by this etch with the result being as shown in Fig. 71. If BPSG is used as the sacrificial material, it can be removed without etching the CMOS glass
35 layers or the actuator glass. This can be achieved with 1000:1 selectivity against undoped glass such as TEOS, using anhydrous HF at 1500 sccm in a N₂ atmosphere at 60 °C

[L. Chang et al, "Anhydrous HF etch reduces processing steps for DRAM capacitors", *Solid State Technology* Vol. 41 No. 5, pp 71-76, 1998]. The actuators are freed and the chips are separated from each other, and from the blank wafer, by this etch. If aluminum is used as the sacrificial layer instead of BPSG, then its removal is combined with the previous step, and this step is omitted.

Pick up the loose print heads with a vacuum probe, and mount the print heads in their packaging. This must be done carefully, as the unpackaged print heads are fragile. The front surface of the wafer is especially fragile, and should not be touched. This process should be performed manually, as it is difficult to automate. The package is a custom injection molded plastic housing incorporating ink channels that supply the appropriate color ink to the ink inlets at the back of the print head. The package also provides mechanical support to the print head. The package is especially designed to place minimal stress on the chip, and to distribute that stress evenly along the length of the package. The print head is glued into this package with a compliant sealant such as silicone.

Form the external connections to the print head chip. For a low profile connection with minimum disruption of airflow, tape automated bonding (TAB) may be used. Wire bonding may also be used if the printer is to be operated with sufficient clearance to the paper. All of the bond pads are along one 100 mm edge of the chip. There are a total of 504 bond pads, in 8 identical groups of 63 (as the chip is fabricated using 8 stitched stepper steps). Each bond pad is 100 x 100 micron, with a pitch of 200 micron. 256 of the bond pads are used to provide power and ground connections to the actuators, as the peak current is 6.58 Amps at 3V. There are a total of 40 signal connections to the entire printhead (24 data and 16 control), which are mostly bussed to the eight identical sections of the print head.

Hydrophobize the front surface of the print heads. This can be achieved by the vacuum deposition of 50 nm or more of polytetrafluoroethylene (PTFE). However, there are also many other ways to achieve this. As the fluid is fully controlled by mechanical protuberances formed in previous steps, the hydrophobic layer is an 'optional extra' to prevent ink spreading on the surface if the print head becomes contaminated by dust.

Plug the print heads into their sockets. The socket provides power, data, and ink. The ink fills the print-head by capillarity. Allow the completed print heads to fill with ink, and test. Fig. 74 illustrates the filling of ink 268 into the nozzle chamber.

Process Parameters used for this Implementation Example

The CMOS process parameters utilized can be varied to suit any CMOS process of 0.5 micron dimensions or better. The MEMS process parameters should not be varied beyond the tolerances shown below. Some of these parameters affect the actuator performance and fluidics, while others have more obscure relationships. For example, the wafer thin stage affects the cost and accuracy of the deep silicon etch, the thickness of the back-side hard mask, and the dimensions of the associated plastic ink channel molding. Suggested process parameters can be as follows:

Parameter	Type	Min.	Nom.	Max.	Unit s	Tol.
Wafer resistivity	CMOS	15	20	25	Ω cm	± 25 %
Wafer thickness	CMOS	600	650	700	μ m	± 8 %
N-Well Junction depth	CMOS	2	2.5	3	μ m	± 20 %
n+ Junction depth	CMOS	0.15	0.2	0.25	μ m	± 25 %
p+ Junction depth	CMOS	0.15	0.2	0.25	μ m	± 25 %

Parameter	Type	Min.	Nom.	Max.	Unit s	Tol.
Field oxide thickness	CMOS	0.45	0.5	0.55	μm	±10 %
Gate oxide thickness	CMOS	12	13	14	nm	±7 %
Poly thickness	CMOS	0.27	0.3	0.33	μm	±10 %
ILD 1 thickness (PECVD glass)	CMOS	0.5	0.6	0.7	μm	±16 %
Metal 1 thickness (aluminum)	CMOS	0.55	0.6	0.65	μm	±8 %
ILD 2 thickness (PECVD glass)	CMOS	0.6	0.7	0.8	μm	±14 %
Metal 2 thickness (aluminum)	CMOS	0.55	0.6	0.65	μm	±8 %
ILD 3 thickness (PECVD glass)	CMOS	0.6	0.7	0.8	μm	±14 %
Metal 3 thickness (aluminum)	CMOS	0.9	1.0	1.1	μm	±10 %
Overcoat (PECVD glass)	CMOS	0.4	0.5	0.6	μm	±20 %
Passivation (Si ₃ N ₄)	CMOS	0.4	0.5	0.6	μm	±20 %
Heater thickness (TiN)	MEMS	0.85	0.9	0.95	μm	±5 %
Actuator thickness (PECVD glass)	MEMS	1.9	2.0	2.1	μm	±5 %
Bend compensator thickness (TiN)	MEMS	0.85	0.9	0.95	μm	±5 %
Sacrificial layer thickness (low stress	MEMS	13.5	15	16.5	μm	±10 %

Parameter	Type	Min.	Nom.	Max.	Unit s	Tol.
BPSG)						
Nozzle etch (BPSG)	MEMS	1.6	2.0	2.4	μm	±20 %
Nozzle chamber and shroud (PECVD glass)	MEMS	0.3	0.5	0.7	μm	±40 %
Nozzle CMP depth	MEMS	0.7	1	1.3	μm	±30 %
Wafer thin (back-grind and polish)	MEMS	295	300	305	μm	±1.6 %
Back-etch hard mask (SiO ₂)	MEMS	2.25	2.5	2.75	μm	±10 %
STS ASE back- etch (stop on aluminum)	MEMS	305	325	345	μm	±6 %

Turning over to Fig. 76, there is illustrated the associated control logic for a single ink jet nozzle. The control logic 280 is utilized to activate a heater element 281 on demand. The control logic 280 includes a shift register 282, a transfer register 283 and a firing control gate 284. The basic operation is to shift data from one shift register 282 to the next until it is in place. Subsequently, the data is transferred to a transfer register 283 upon activation of a transfer enable signal 286. The data is latched in the transfer register 283 and subsequently, a firing phase control signal 289 is utilized to activate a gate 284 for output of a heating pulse to heat an element 281.

As the preferred implementation utilizes a CMOS layer for implementation of all control circuitry, one form of suitable CMOS implementation of the control circuitry will now be described. Turning now to Fig. 77, there is illustrated a schematic block diagram of the corresponding

CMOS circuitry. Firstly, shift register 282 takes an inverted data input and latches the input under control of shift clocking signals 291, 292. The data input 290 is output 294 to the next shift register and is also latched
5 by a transfer register 283 under control of transfer enable signals 296, 297. The enable gate 284 is activated under the control of enable signal 299 so as to drive a power transistor 300 which allows for resistive heating of resistor 281. The functionality of the shift register 282,
10 transfer register 283 and enable gate 284 are standard CMOS components well understood by those skilled in the art of CMOS circuit design. The ink jet printhead can consist of a large number of replicated unit cells each of which has basically the same design. This design will now be
15 discussed.

Turning initially to Fig. 78, there is illustrated a general key or legend of different material layers utilized in subsequent discussions.

Fig. 79 illustrates the unit cell 305 on a $1\mu m$
20 backing grid 306. The unit cell 305 is copied and replicated a large number of times with Fig. 79 illustrating the diffusion and poly-layers in addition to vias e.g. 308. The signals 290, 291, 292, 296, 297 and 299 are as previously discussed with reference to Fig. 77. A
25 number of important aspects of Fig. 79 include the general layout including the shift register, transfer register and gate and drive transistor. Importantly, the drive transistor 300 includes an upper poly-layer e.g. 309 which is laid out having a large number of perpendicular traces
30 e.g. 312. The perpendicular traces are important in ensuring that the corrugated nature of a heater element formed over the power transistor 300 will have a corrugated bottom with corrugations running generally in the
~~perpendicular direction of trace 112. The effect of the~~
35 corrugations being more clearly illustrated in the earlier figures describing the manufacturing steps in the construction of an actuator.

In Fig. 80, there is illustrated the addition of the first level metal layer which includes enable lines 296, 297.

5 In Fig. 81, there is illustrated the second level metal layer which includes data in-line 290, SClock line 91, ~SClock 292, ~Q 294, Ten 296 and ~Ten 297, V- 320, VDD 321, VSS 322, in addition to associated reflected components 323 to 328. The portions 330 and 331 are utilized as a sacrificial etch.

10 Turning now to Fig. 82 there is illustrated the third level metal layer which includes a portion 340 which is utilized as a sacrificial etch layer underneath the heater actuator. The portion 341 is utilized as part of the actuator structure with the portions 342 and 343
15 providing for electrical interconnector.

Turning now to Fig. 83, there is illustrated the heater actuator layer including heater arms 350 and 351 which are interconnected to the lower layers. The second portion of the heater arm 352 is electrically isolated from
20 the arms 350 and 351 and provides for structural support for the main paddle.

In Fig. 84 there is illustrated the portions of the shroud and nozzle layer including shroud 350 and outer nozzle chamber 351.

25 Turning to Fig. 85, there is illustrated a portion 360 of a array of ink ejection nozzles which are divided into three groups 361 - 363 with each group providing separate color output (cyan, magenta and yellow) so as to provide full three color printing. A series of
30 standard cell clock buffers and address decoders 364 is also provided in addition to bond pads 365 for interconnection with the external circuitry.

Each color group 361, 363 consists of two spaced apart rows of ink ejection nozzles e.g. 367 each having a
35 heater actuator element.

Fig. 87 illustrates one form of overall layout in a cut away manner with a first area 370 illustrating the

layers up to the poly-level. A second area 371 illustrating the layers up to the first level metal, the area 372 illustrating the layers up to the second level metal and the area 373 illustrating the layers up to the heater actuator layer.

The ink ejection nozzles are grouped in two groups of 10 nozzles sharing a common ink channel through the wafer. Turning to Fig. 88, there is illustrated the back surface of the wafer which includes a series of ink supply channels 380 for supplying ink to a front surface.

Replication

The unit cell is replicated 19,200 times on the 4" print head, in the hierarchy as shown in the replication hierarchy table below. The layout grid is 1/2 1 at 0.5 micron (0.125 micron). Many of the ideal transform distances fall exactly on a grid point. Where they do not, the distance is rounded to the nearest grid point. The rounded numbers are shown with an asterisk.. The transforms are measured from the center of the corresponding nozzles in all cases. The transform of a group of five even nozzles into five odd nozzles also involves a 180° rotation. The translation for this step occurs from a position where all five pairs of nozzle centers are coincident.

Replication Hierarchy Table

R ep lic ati o n	Replication stage	Rotat ion (°)	Repli catio n ratio	Tota l noz zles	X Transform	Y Transfor m				
					Pixels	Grid units	Actual (micron)	Pixel s	Gri d unit s	Actual (micro n)
0	Initial rotation	45	1:1	1	0	0	0	0	0	0
1	Even nozzles in a pod	0	5:1	5	2	254	31.75	$\frac{1}{10}$	13*	1.625 *
2	Odd nozzles in a pod	180	2:1	10	1	127	15.875	$1\frac{9}{16}$	198 *	24.75 *
3	Pods in a CMY tripod	0	3:1	30	$5\frac{1}{2}$	699*	87.375*	7	889	111.1 25
4	Tripods per podgroup	0	10:1	300	10	1270	158.75	0	0	0
5	Podgroups per firegroup	0	2:1	600	100	12700	1587.5	0	0	0
6	Firegroups per segment	0	4:1	240 0	200	25400	3175	0	0	0
7	Segments per print head	0	8:1	192 00	800	101600	12700	0	0	0

3.1 COMPOSITION

5 Taking the example of a 4-inch print head
suitable for use in camera photoprinting as illustrated in
Fig. 89, a 4-inch print head 380 consists of 8 segments eg.
381, each segment is $\frac{1}{2}$ an inch in length. Consequently
each of the segments prints bi-level cyan, magenta and
10 yellow dots over a different part of the page to produce

the final image. The positions of the 8 segments are shown in Fig. 89. In this example, the print head is assumed to print dots at 1600 dpi, each dot is 15.875 μm in diameter. Thus each half-inch segment prints 800 dots, with the 8 segments corresponding to positions as illustrated in the following table:

Segment	First dot	Last dot
0	0	799
1	800	1599
2	1600	2399
3	2400	3199
4	3200	3999
5	4000	4799
6	4800	5599
7	5600	6399

Although each segment produces 800 dots of the final image, each dot is represented by a combination of bi-level cyan, magenta, and yellow ink. Because the printing is bi-level, the input image should be dithered or error-diffused for best results.

Each segment 381 then, contains 2,400 nozzles: 800 each of cyan, magenta, and yellow. A four-inch print head contains 8 such segments for a total of 19,200 nozzles.

The nozzles within a single segment are grouped for reasons of physical stability as well as minimization of power consumption during printing. In terms of physical stability, as shown in Fig. 88 groups of 10 nozzles are grouped together and share the same ink channel reservoir. In terms of power consumption, the groupings are made so that only 96 nozzles are fired simultaneously from the entire printhead. Since the 96 nozzles should be maximally distant, 12 nozzles are fired from each segment. To fire all 19,200 nozzles, 200 different sets of 96 nozzles must

be fired.

Fig. 90 shows schematically, a single pod 395 which consists of 10 nozzles numbered 1 to 10 sharing a common ink channel supply. 5 nozzles are in one row, and 5
5 are in another. Each nozzle produces dots 15.875mm in diameter. The nozzles are numbered according to the order in which they must be fired.

Although the nozzles are fired in this order, the relationship of nozzles and physical placement of dots on
10 the printed page is different. The nozzles from one row represent the even dots from one line on the page, and the nozzles on the other row represent the odd dots from the adjacent line on the page. Fig. 91 shows the same pod 395 with the nozzles numbered according to the order in which
15 they must be loaded.

The nozzles within a pod are therefore logically separated by the width of 1 dot. The exact distance between the nozzles will depend on the properties of the ink jet firing mechanism. In the best case, the print head could be
20 designed with staggered nozzles designed to match the flow of paper. In the worst case there is an error of 1/3200 dpi. While this error would be viewable under a microscope for perfectly straight lines, it certainly will not be an apparent in a photographic image.

25 As shown in Fig. 92, three pods representing Cyan 398, Magenta 197, and Yellow 396 units, are grouped into a tripod 400. A tripod represents the same horizontal set of 10 dots, but on different lines. The exact distance between different color pods depends on the inkjet operating
30 parameters, and may vary from one inkjet to another. The distance can be considered to be a constant number of dot-widths, and must therefore be taken into account when printing: the dots printed by the cyan nozzles will be for different lines than those printed by the magenta or yellow
35 nozzles. The printing algorithm must allow for a variable distance up to about 8 dot-widths.

As illustrated in Fig. 93, 10 tripods eg. 404 are

organized into a single *podgroup* 405. Since each tripod contains 30 nozzles, each podgroup contains 300 nozzles: 100 cyan, 100 magenta and 100 yellow nozzles. The arrangement is shown schematically in Fig. 93, with tripods
5 numbered 0-9. The distance between adjacent tripods is exaggerated for clarity.

As shown in Fig. 94, two podgroups (PodgroupA 410 and PodgroupB 411) are organized into a single *firegroup* 414, with 4 firegroups in each segment 415. Each segment
10 415 contains 4 firegroups. The distance between adjacent firegroups is exaggerated for clarity.

Name of Grouping	Composition	Replication Ratio	Nozzle Count
Nozzle	Base unit	1:1	1
Pod	Nozzles per pod	10:1	10
Tripod	Pods per CMY tripod	3:1	30
Podgroup	Tripods per podgroup	10:1	300
Firegroup	Podgroups per firegroup	2:1	600
Segment	Firegroups per segment	4:1	2,400
Print head	Segments per print head	8:1	19,200

3.2 LOAD AND PRINT CYCLES

The print head contains a total of 19,200
15 nozzles. A *Print Cycle* involves the firing of up to all of these nozzles, dependent on the information to be printed. A *Load Cycle* involves the loading up of the print head with the information to be printed during the subsequent Print Cycle.

20 Each nozzle has an associated *NozzleEnable* (289 of Fig. 76) bit that determines whether or not the nozzle will fire during the Print Cycle. The *NozzleEnable* bits (one per nozzle) are loaded via a set of shift registers.

Logically there are 3 shift registers per color,

each 800 deep. As bits are shifted into the shift register they are directed to the lower and upper nozzles on alternate pulses. Internally, each 800-deep shift register is comprised of two 400-deep shift registers: one for the upper nozzles, and one for the lower nozzles. Alternate bits are shifted into the alternate internal registers. As far as the external interface is concerned however, there is a single 800 deep shift register.

Once all the shift registers have been fully loaded (800 pulses), all of the bits are transferred in parallel to the appropriate NozzleEnable bits. This equates to a single parallel transfer of 19,200 bits. Once the transfer has taken place, the Print Cycle can begin. The Print Cycle and the Load Cycle can occur simultaneously as long as the parallel load of all NozzleEnable bits occurs at the end of the Print Cycle.

In order to print a 6" x 4" image at 1600 dpi in say 2 seconds, the 4" print head must print 9,600 lines (6 x 1600). Rounding up to 10,000 lines in 2 seconds yields a line time of 200 microseconds. A single Print Cycle and a single Load Cycle must both finish within this time. In addition, a physical process external to the print head must move the paper an appropriate amount.

3.2.1 Load Cycle

The Load Cycle is concerned with loading the print head's shift registers with the next Print Cycle's NozzleEnable bits.

Each segment has 3 inputs directly related to the cyan, magenta, and yellow pairs of shift registers. These inputs are called *CDataIn*, *MDataIn*, and *YDataIn*. Since there are 8 segments, there are a total of 24 color input lines per print head. A single pulse on the *SRClock* line (shared between all 8 segments) transfers 24 bits into the appropriate shift registers. Alternate pulses transfer bits to the lower and upper nozzles respectively. Since there are 19,200 nozzles, a total of 800 pulses are required for the transfer. Once all 19,200 bits have been transferred, a

single pulse on the shared *PTransfer* line causes the parallel transfer of data from the shift registers to the appropriate NozzleEnable bits. The parallel transfer via a pulse on *PTransfer* must take place after the Print Cycle has finished. Otherwise the NozzleEnable bits for the line being printed will be incorrect.

Since all 8 segments are loaded with a single SRClock pulse, the printing software must produce the data in the correct sequence for the print head. As an example, the first SRClock pulse will transfer the C, M, and Y bits for the next Print Cycle's dot 0, 800, 1600, 2400, 3200, 4000, 4800, and 5600. The second SRClock pulse will transfer the C, M, and Y bits for the next Print Cycle's dot 1, 801, 1601, 2401, 3201, 4001, 4801 and 5601. After 800 SRClock pulses, the *PTransfer* pulse can be given.

It is important to note that the odd and even C, M, and Y outputs, although printed during the same Print Cycle, do not appear on the same physical output line. The physical separation of odd and even nozzles within the print head, as well as separation between nozzles of different colors ensures that they will produce dots on different lines of the page. This relative difference must be accounted for when loading the data into the print head. The actual difference in lines depends on the characteristics of the inkjet used in the print head. The differences can be defined by variables D_1 and D_2 where D_1 is the distance between nozzles of different colors (likely value 4 to 8), and D_2 is the distance between nozzles of the same color (likely value = 1). Table 3 shows the dots transferred to segment n of a print head on the first 4 pulses.

Pulse	Yellow		Magenta		Cyan	
	Line	Dot	Line	Dot	Line	Dot
1	N	800S	$N+D_1$	800S	$N+2D_1$	800S
2	$N+D_2$	800S+1	$N+D_1+D_2$	800S+1	$N+2D_1+D_2$	800S+1
3	N	800S+2	$N+D_1$	800S+2	$N+2D_1$	800S+2

4	$N+D_2$	$800S+3$	$N+D_1+D_2$	$800S+3$	$N+2D_1+D_2$	$800S+3$
---	---------	----------	-------------	----------	--------------	----------

And so on for all 800 pulses. The 800 SRClock pulses (each clock pulse transferring 24 bits) must take place within the 200 microseconds line time. Therefore the average time to calculate the bit value for each of the 19,200 nozzles must not exceed $200\text{ms} / 19200 = 10\text{ns}$. Data can be clocked into the print head at a maximum rate of 10 MHz, which will load the data in 80ms. Clocking the data in at 4 MHz will load the data in 200ms.

10 3.2.2 Print Cycle

The print head contains 19,200 nozzles. To fire them all at once would consume too much power and be problematic in terms of ink refill and nozzle interference. A single print cycle therefore consists of 200 different phases. 96 maximally distant nozzles are fired in each phase, for a total of 19,200 nozzles.

- 4 bits *TripodSelect* (select 1 of 10 tripods from a firegroup)

The 96 nozzles fired each round equate to 12 per segment (since all segments are wired up to accept the same print signals). The 12 nozzles from a given segment come equally from each firegroup. Since there are 4 firegroups, 3 nozzles fire from each firegroup. The 3 nozzles are one per color. The nozzles are determined by:

- 25 • 4 bits *NozzleSelect* (select 1 of 10 nozzles from a pod)

The duration of the firing pulse is given by the *AEnable* and *BEnable* lines, which fire the PodgroupA and PodgroupB nozzles from all firegroups respectively. The duration of a pulse depends on the viscosity of the ink (dependent on temperature and ink characteristics) and the amount of power available to the print head. The *AEnable* and *BEnable* are separate lines in order that the firing pulses can overlap. Thus the 200 phases of a Print Cycle consist of 100 A phases and 100 B phases, effectively giving 100 sets of Phase A and Phase B.

When a nozzle fires, it takes approximately 100 microseconds to refill. This is not a problem since the entire Print Cycle takes 200 microseconds. The firing of a nozzle also causes perturbations for a limited time within the common ink channel of that nozzle's pod. The perturbations can interfere with the firing of another nozzle within the same pod. Consequently, the firing of nozzles within a pod should be offset by at least this amount. The procedure is to therefore fire three nozzles from a tripod (one nozzle per color) and then move onto the next tripod within the podgroup. Since there are 10 tripods in a given podgroup, 9 subsequent tripods must fire before the original tripod must fire its next three nozzles. The 9 firing intervals of 2 microseconds gives an ink settling time of 18 microseconds.

Consequently, the firing order is:

- TripodSelect 0, NozzleSelect 0 (Phases A and B)
- TripodSelect 1, NozzleSelect 0 (Phases A and B)
- TripodSelect 2, NozzleSelect 0 (Phases A and B)
- ...
- TripodSelect 9, NozzleSelect 0 (Phases A and B)
- TripodSelect 0, NozzleSelect 1 (Phases A and B)
- TripodSelect 1, NozzleSelect 1 (Phases A and B)
- TripodSelect 2, NozzleSelect 1 (Phases A and B)
- ...
- TripodSelect 8, NozzleSelect 9 (Phases A and B)
- TripodSelect 9, NozzleSelect 9 (Phases A and B)

Note that phases A and B can overlap. The duration of a pulse will also vary due to battery power and ink viscosity (which changes with temperature). Fig. 95 shows the AEnable and BEnable lines during a typical Print Cycle.

3.3 FEEDBACK FROM THE PRINT HEAD

The print head produces several lines of feedback (accumulated from the 8 segments). The feedback lines can be used to adjust the timing of the firing pulses. Although each segment produces the same feedback, the feedback from

all segments share the same tri-state bus lines. Consequently only one segment at a time can provide feedback. A pulse on the *SenseEnable* line ANDed with data on CYAN enables the sense lines for that segment. The
5 feedback sense lines are as follows:

- *Tsense* informs the controller how hot the print head is. This allows the controller to adjust timing of firing pulses, since temperature affects the viscosity of the ink.

10 • *Vsense* informs the controller how much voltage is available to the actuator. This allows the controller to compensate for a flat battery or high voltage source by adjusting the pulse width.

- *Rsense* informs the controller of the
15 resistivity (Ohms per square) of the actuator heater. This allows the controller to adjust the pulse widths to maintain a constant energy irrespective of the heater resistivity.

- *Wsense* informs the controller of the
20 width of the critical part of the heater, which may vary up to $\pm 5\%$ due to lithographic and etching variations. This allows the controller to adjust the pulse width appropriately.

3.4 PREHEAT MODE

25 The printing process has a strong tendency to stay at the equilibrium temperature. To ensure that the first section of the printed photograph has a consistent dot size, ideally the equilibrium temperature should be met before printing any dots. This is accomplished via a
30 preheat mode.

The Preheat mode involves a single Load Cycle to all nozzles with 1s (i.e. setting all nozzles to fire), and a number of short firing pulses to each nozzle. The duration of the pulse must be insufficient to fire the
35 drops, but enough to heat up the ink surrounding the heaters. Altogether about 200 pulses for each nozzle are required, cycling through in the same sequence as a

standard Print Cycle.

- Feedback during the Preheat mode is provided by Tsense, and continues until an equilibrium temperature is reached (about 30° C above ambient). The duration of the Preheat mode can be around 50 milliseconds, and can be tuned in accordance with the ink composition.

3.5 PRINT HEAD INTERFACE SUMMARY

The print head has the following connections:

Name	#Pins	Description
Tripod Select	4	Select which tripod will fire (0-9)
NozzleSelect	4	Select which nozzle from the pod will fire (0-9)
AEnable	1	Firing pulse for podgroup A
BEnable	1	Firing pulse for podgroup B
CDataIn[0-7]	8	Cyan input to cyan shift register of segments 0-7
MDataIn[0-7]	8	Magenta input to magenta shift register of segments 0-7
YDataIn[0-7]	8	Yellow input to yellow shift register of segments 0-7
SRClock	1	A pulse on SRClock (ShiftRegisterClock) loads the current values from CDataIn[0-7], MdataIn[0-7] and YDataIn[0-7] into the 24 shift registers.
PTransfer	1	Parallel transfer of data from the shift registers to the internal NozzleEnable bits (one per nozzle).
SenseEnable	1	A pulse on SenseEnable ANDed with data on CDataIn[n] enables the sense lines for segment n.

Name	#Pins	Description
Tsense	1	Temperature sense
Vsense	1	Voltage sense
Rsense	1	Resistivity sense
Wsense	1	Width sense
Logic GND	1	Logic ground
Logic PWR	1	Logic power
V-	Bus bars	
V+		
TOTAL	43	

Internal to the print head, each segment has the following connections to the bond pads:

Pad Connections

5 Although an entire printhead has a total of 504 connections, the mask layout contains only 63. This is because the chip is composed of eight identical and separate sections, each 12.7 mm long. Each of these sections has 63 pads at a pitch of 200 microns. There is an
10 extra 50 microns at each end of the group of 63 pads, resulting in an exact repeat distance of 12,700 microns (12.7 mm, 1/2")

Pads

No.	Name	Function
1	V-	Negative actuator supply
2	Vss	Negative drive logic supply
3	V+	Positive actuator supply
4	Vdd	Positive drive logic supply
5	V-	Negative actuator supply
6	SCLK	Serial data transfer clock
7	V+	Positive actuator supply
8	Ten	Parallel transfer enable
9	V-	Negative actuator supply
10	EPEn	Even phase enable

No.	Name	Function
11	V+	Positive actuator supply
12	OPEn	Odd phase enable
13	V-	Negative actuator supply
14	NA[0]	Nozzle Address [0] (in pod)
15	V+	Positive actuator supply
16	NA[1]	Nozzle Address [1] (in pod)
17	V-	Negative actuator supply
18	NA[2]	Nozzle Address [2] (in pod)
19	V+	Positive actuator supply
20	NA[3]	Nozzle Address [3] (in pod)
21	V-	Negative actuator supply
22	PA[0]	Pod Address [0] (1 of 10)
23	V+	Positive actuator supply
24	PA[1]	Pod Address [1] (1 of 10)
25	V-	Negative actuator supply
26	PA[2]	Pod Address [2] (1 of 10)
27	V+	Positive actuator supply
28	PA[3]	Pod Address [3] (1 of 10)
29	V-	Negative actuator supply
30	PGA[0]	Podgroup Address [0]
31	V+	Positive actuator supply
32	FGA[0]	Firegroup Address [0]
33	V-	Negative actuator supply
34	FGA[1]	Firegroup Address [1]
35	V+	Positive actuator supply
36	SEn	Sense Enable
37	V-	Negative actuator supply
38	Tsense	Temperature sense
39	V+	Positive actuator supply
40	Rsense	Actuator resistivity sense
41	V-	Negative actuator supply
42	Wsense	Actuator width sense
43	V+	Positive actuator supply
44	Vsense	Power supply voltage sense

No.	Name	Function
45	V-	Negative actuator supply
46	N/C	Spare
47	V+	Positive actuator supply
48	D[C]	Cyan serial data in
49	V-	Negative actuator supply
50	D[M]	Magenta serial data in
51	V+	Positive actuator supply
52	D[Y]	Yellow serial data in
53	V-	Negative actuator supply
54	Q[C]	Cyan data out (for testing)
55	V+	Positive actuator supply
56	Q[M]	Magenta data out (for testing)
57	V-	Negative actuator supply
58	Q[Y]	Yellow data out (for testing)
59	V+	Positive actuator supply
60	Vss	Negative drive logic supply
61	V-	Negative actuator supply
62	Vdd	Positive drive logic supply
63	V+	Positive actuator supply

Fabrication and Operational Tolerances

Parameter	Cause of variation	Compensation	Min	Nom	Max	Units
Ambient Temperature	Environmental	Real-time	-10	25	50	°C
Nozzle Radius	Lithographic	Brightness adjust	5.3	5.5	5.7	micron
Nozzle Length	Processing	Brightness adjust	0.5	1.0	1.5	micron
Nozzle Tip Contact Angle	Processing	Brightness adjust	100	110	120	°

Parameter	Cause of variation	Compensati on	Min	Nom	Max	Unit s
Paddle Radius	Lithographic	Brightness adjust	9.8	10.0	10.2	micr on
Paddle-Chamber Gap	Lithographic	Brightness adjust	0.8	1.0	1.2	micr on
Chamber Radius	Lithographic	Brightness adjust	10.8	11.0	11.2	micr on
Inlet Area (shared by 10 nozzles)	Lithographic	Brightness adjust	5500	6000	6500	micr on ²
Inlet Length	Processing	Brightness adjust	295	300	305	micr on
Inlet etch angle (re-entrant)	Processing	Brightness adjust	90.5	91	91.5	°
Heater Thickness	Processing	Real-time	0.95	1.0	1.05	micr on
Heater Resistivity	Materials	Real-time	115	135	160	mW-cm
Heater Young's's Modulus	Materials	Mask design	400	600	650	GPa
Heater Density	Materials	Mask design	5400	5450	5500	kg/m ³
Heater CTE	Materials	Mask design	9.2	9.4	9.6	10 ⁻⁶ /°C
Heater Width	Lithographic	Real-time	1.15	1.25	1.35	micr on
Heater Length	Lithographic	Real-time	27.9	28.0	28.1	micr on
Actuator Glass Thickness	Processing	Brightness adjust	1.9	2.0	2.1	micr on

Parameter	Cause of variation	Compensati on	Min .	Nom .	Max .	Unit s
Glass Young's's Modulus	Materials	Mask design	60	75	90	GPa
Glass CTE	Materials	Mask design	0.0	0.5	1.0	10 ⁻⁶ /°C
Actuator Wall Angle	Processing	Mask design	85	90	95	°
Actuator to Substrate Gap	Processing	None required	0.9	1.0	1.1	micr on
Bend Cancelling Layer Thickness	Processing	Brightness adjust	0.9 5	1.0	1.0 5	micr on
Lever Arm Length	Lithographic	Brightness adjust	87. 9	88. 0	88. 1	micr on
Chamber Height	Processing	Brightness adjust	10	11. 5	13	micr on
Chamber Wall Angle	Processing	Brightness adjust	85	90	95	°
Color Related Ink Viscosity	Materials	Mask design	-20	Nom .	+20	%
Ink Surface Tension @ 25°C	Materials	Programmed	25	35	45	mN/m
Ink Viscosity @ 25°C25°C	Materials	Programmed	0.7	0.8 9	1.2	cP
Ink Dye Concentrati on	Materials	Programmed	5	10	15	%

Parameter	Cause of variation	Compensati on	Min .	Nom .	Max .	Unit s
Ink Temperature (relative to chip)	Operation	None	-10	0	+10	°C
Ink Pressure	Operation	Programmed	-10	0	+10	kPa
Ink Drying (viscosity increase)	Materials	Programmed	+0	+2	+5	cP
Actuator Voltage	Operation	Real-time	2.75	2.8	2.85	V
Drive Pulse Width	Xtal Osc.	None required	1.299	1.300	1.301	micro seconds
Drive Transistor On Resistance	Processing	Real-time	3.6	4.1	4.6	W
Fabrication Temperature (TiN)	Processing	Correct by design	300	350	400	°C
Battery Voltage	Operation	Real-time	2.5	3.0	3.5	V

Variation with Ambient Temperature

The main consequence of a change in ambient temperature is that the ink viscosity and surface tension changes. As the bend actuator responds only to differential temperature between the actuator layer and the bend compensation layer, ambient temperature has negligible direct effect on the bend actuator. The resistivity of the TiN heater changes only slightly with temperature. The following simulations are for an water based ink, in the temperature range 0 °C to 80°C.

The drop velocity and drop volume does not increase monotonically with increasing temperature as one may expect. This is simply explained: as the temperature increases, the viscosity falls faster than the surface tension falls. As the viscosity falls, the movement of ink out of the nozzle is made slightly easier. However, the movement of the ink around the paddle - from the high pressure zone at the paddle front to the low pressure zone behind the paddle - changes even more. Thus more of the ink movement is 'short circuited' at higher temperatures and lower viscosity's.

Am bi en t Te mp er at ur c	In k Vi sc os it y	Su rf ac Te ns io n	Ac tu at or Wi dt h	Ac tu at or Th ic kn es s	Ac tu at or Le ng th	Pu ls e Vo lt ag e	Pu ls e Cu rr en t	Pu ls e Wi dt h	Pu ls e En er gy	Pe ak Te mp er at ur e	Pa dd le De fl ec ti on	Pa dd le Ve lo ci ty	Dr op Ve lo ci ty	Dr op Vo lu me
°C	cP	mN /m	mi cr on	mi cr on	mi cr on	V	mA	mi cr os ec on ds	nJ	°C	mi cr on	m/ s	m/ s	pl

0	1. 79	38 .6	1. 25	1. 0	27	2. 8	42 .4 7	1. 6	19 0	46 5	3. 16	2. 06	2. 82	0. 80
20	1. 00	35 .8	1. 25	1. 0	27	2. 8	42 .4 7	1. 6	19 0	48 5	3. 14	2. 13	3. 10	0. 88
							7							

40	0. 65	32 .6	1. 25	1. 0	27	2. 8	42 .4 7	1. 6	19 0	50 5	3. 19	2. 23	3. 25	0. 93
60	0. 47	29 .2	1. 25	1. 0	27	2. 8	42 .4 7	1. 6	19 0	52 5	3. 13	2. 17	3. 40	0. 78
80	0. 35	25 .6	1. 25	1. 0	27	2. 8	42 .4 7	1. 6	19 0	54 5	3. 24	2. 31	3. 31	0. 88

The temperature of the Memjet print head is regulated to optimize the consistency of drop volume and drop velocity. The temperature is sensed on chip for each segment. The temperature sense signal (T_{sense}) is connected to a common T_{sense} output. The appropriate T_{sense} signal is selected by asserting the Sense Enable (Sen) and selecting the appropriate segment using the $D[C_0-7]$ lines. The T_{sense} signal is digitized by the drive ASIC, and drive pulse width is altered to compensate for the ink viscosity change. Data specifying the viscosity/temperature relationship of the ink is stored in the Authentication chip associated with the ink.

Variation with Nozzle Radius

The nozzle radius has a significant effect on the drop volume and drop velocity. For this reason it is closely controlled by 0.5 micron lithography. The nozzle is formed by a 2 micron etch of the sacrificial material, followed by deposition of the nozzle wall material and a CMP step. The CMP planarizes the nozzle structures, removing the top of the overcoat, and exposed the sacrificial material inside. The sacrificial material is subsequently removed, leaving a self-aligned nozzle and nozzle rim. The accuracy internal radius of the nozzle is primarily determined by the accuracy of the lithography, and the consistency of the sidewall angle of the 2 micron etch.

The following table shows operation at various

nozzle radii. With increasing nozzle radius, the drop velocity steadily decreases. However, the drop volume peaks at around a 5.5 micron radius. The nominal nozzle radius is 5.5 micron, and the operating tolerance specification allows a $\pm 4\%$ variation on this radius, giving a range of 5.3 to 5.7 micron. The simulations also include extremes outside of the nominal operating range (5.0 and 6.0 micron). The major nozzle radius variations will likely be determined by a combination of the sacrificial nozzle etch and the CMP step. This means that variations are likely to be non-local: differences between wafers, and differences between the center and the perimeter of a wafer. The between wafer differences are compensated by the 'brightness' adjustment. Within wafer variations will be imperceptible as long as they are not sudden.

Nozzle Radius	Ink Viscosity	Surface Tension	Actuator Width	Actuator Length	Pulsed Voltage	Pulsed Current	Pulse Width	Pulse Energy	Peak Temperature	Peak Pressure	Particle Diameter	Particle Velocity	Drop Velocity	Drop Volume
micron	cP	mN/m	micron	micron	V	mA	microseconds	nJ	°C	kPa	micron	m/s	m/s	pl
5.0	0.65	32.6	1.25	25	2.8	42.36	1.4	166	482	75.9	2.81	2.18	4.36	0.84
5.3	0.65	32.6	1.25	25	2.8	42.36	1.4	166	482	69.0	2.88	2.22	3.92	0.87

5. 5	0. 65	32 .6	1. 25	25	2. 8	42 .3 6	1. 4	16 6	48 2	67 .2	2. 96	2. 29	3. 45	0. 99
5. 7	0. 65	32 .6	1. 25	25	2. 8	42 .3 6	1. 4	16 6	48 2	64 .1	3. 00	2. 33	3. 09	0. 95
6. 0	0. 65	32 .6	1. 25	25	2. 8	42 .3 6	1. 4	16 6	48 2	59 .9	3. 07	2. 39	2. 75	0. 89

A printhead constructed in accordance with the
aforementioned techniques can be utilized in a print camera
system similar to that disclosed in PCT patent application
5 No. PCT/AU98/00544. Upon such printhead arrangement
suitable for utilization in a print on demand camera system
will now be described. Starting initially with Fig. 96 and
Fig. 97, there is illustrated portions of an ink supply
unit 430 which can be utilized to supply three color ink to
10 the back surface of a printhead 431. The ink is supplied
by means of an ink distribution molding 433 which includes
a series of slots e.g. 434 for the flow of ink to the back
of the print head. The printhead 431 can be attached by
means of silicone gel or the like. A filter 436 is
15 designed to fit around the distribution molding 433 so as
to filter the ink passing through the distribution molding
433.

Molding 433 and filter 436 are in turn inserted
within baffle unit 437 again being attached by means of
20 silicone sealant such that ink is able to, for example,
flow through the holes 440 and in turn through the hole
434. The baffles 437 can be a plastic injection molded
unit which includes a number of spaced apart baffles or
slats 441-443. The baffles are formed within each ink
25 ~~channel so as to restrict the macroscopic flow of ink in~~
the lateral direction along the baffle unit 437 whilst
allowing for microscopic flows of ink between the baffles
to the distribution molding 423. The baffles are effective

in providing for portable carriage of the ink so as to minimize disruption due to flow fluctuations during handling.

5 The baffle unit 437 is in turn encased in a housing 445. The housing 445 can be ultrasonically welded to the baffle member 437 so as to seal the baffle member 437 into three separate ink chambers. The baffle member 437 further includes a series of pierceable end wall portions 450 - 452 which can be pierced by a corresponding
10 mating ink supply conduit for the flow of ink into each of the three chambers. The housing 445 also includes a series of holes 455 which are hydrophobically sealed by means of tape or the like so as to allow air within the three chambers of the baffle units to escape whilst ink remains
15 within the baffle chambers due to the hydrophobic nature of the holes eg. 455.

The housing 445 includes a series of positioning protuberances eg. 460 - 462. A first series of protuberances is designed to accurately position a tape
20 automated bonded film 470 in addition to first 465 and second 466 power and ground busbars which are interconnected to the tab 470 at a large number of locations along the surface of the tab so as to provide for low resistance power and ground distribution along the
25 surface of the tab 470 which is in turn interconnected to the chip 431. The busbars 465, 466 are in turn connected to contacts 475, 476 which are firmly clamped against the busbars 465, 466 by means of cover unit 478. The cover unit 478 also can comprise an injection molded part and
30 includes a slot 480 for the insertion of an aluminum bar for assisting in cutting a printed page.

Turning now to Fig. 98 there is illustrated a cut away view of the printhead unit 430, associated platen unit 490, print roll and ink supply unit 491 and drive power
35 distribution unit 492 which interconnects each of the units 430, 490 and 491.

The guillotine blade 495 is able to be driven by

a first motor along the aluminum blade 498 so as to cut a picture 499 after printing has occurred. The operation of the system of Fig. 98 is very similar to that disclosed in PCT patent application PCT/AU98/00544. Ink is stored in
5 the core portion 500 of a print roll former 501 around which is rolled print media 502. The print media is fed under the control of electric motor 494 between the platen 290 and printhead unit 490 with the ink being interconnected via ink transmission channels 505 to the
10 printhead unit 430. The print roll unit 491 can be as described in the aforementioned PCT specification. In Fig. 99, there is illustrated the assembled form of single printer unit 510.

The printhead obviously has other applications
15 and the technology can be readily adapted for a wide range of applications for which current digital printing technologies are not adequate. These include:

- Full quality color photographic images
- Full quality text
- 20 Wide ink and 'paper' flexibility
- High speed
- Low cost
- Low power
- Small size
- 25 Simple drive circuits
- High volume manufacture
- Low manufacturing investment
- Permanent print head

Major example applications include:

- 30 Office and SOHO color printing
- Network color printers
- Photographic printers
- Pocket printers in cameras, PDA's, phones
- Portable and notebook printers
- 35 Wide format (poster) printers
- Digital photocopiers
- Color fax machines

Digital commercial printing
Short run digital printing
Packaging and industrial printing
Fabric printing

5 As more than 50,000 nozzles are required for A4
photographic quality pagewidth printer, integration of the
drive electronics on the same chip as the print head is
essential to achieve low cost. Integration allows the
number of external connections to the print head to be
10 reduced. Over the past decade, manufacturing capability in
the field of MEMS has been steadily increasing. MEMS is
Micro-Electro-Mechanical Systems, and refers to mechanical
systems built using technologies developed for integrated
circuit fabrication. MEMS has three major advantages over
15 other manufacturing techniques:
Mechanical devices can be built with dimensions and
accuracy on the micron scale.

Millions of mechanical devices can be made
simultaneously, on the same silicon wafer.

20 The mechanical devices can incorporate
electronics.

It was also evident that both of the main current
inkjet technologies - thermal inkjet and piezoelectric
inkjet technologies - were fundamentally unable to meet
25 these project's objectives. An estimated is shown in the
following table:

Comparison of Memjet and Thermal Ink Jet (TIJ) printing
mechanisms

Factor	TIJ	Memje t	Advantage
Resolution	600	1,600	Full photographic image quality and high quality text
Printer type	Scanni ng	Pagew idth	Memjet does not scan, resulting in faster printing and smaller size

Factor	TIJ	Memjet	Advantage
Print speed	<1 ppm	30 ppm	Memjet's page width results in >30 times faster operation
Number of nozzles	512	51,200	100 times as many nozzles enables the high print speed
Manufacturing cost	~US\$20	~US\$200	Optimized MEMS construction allows low manufacturing cost
Drop volume	20 picoliters	1 picoliter	Less water on the paper, print is immediately dry, no 'cockle'
Construction	Multi-part	Monolithic	Memjet does not require precision assembly
Efficiency	<0.1%	2%	20 times increase in efficiency results in low power operation
Power supply	Mains power	Batteries	Battery operation allows portable printers, e.g. in cameras, phones
Peak pressure	>100 atm	0.6 atm	The high pressures in a thermal ink jet cause reliability problems
Ink temperature	+300 °C	+50 °C	High ink temperatures cause burnt dye deposits (fogging)
Cavitation	Problem	None	Cavitation (erosion due to bubble collapse) limits head life
Head life	Limited	Permanent	TIJ print heads are replaceable due to cavitation and fogging
Operating voltage	20 V	3 V	Allows operation from two AA batteries

Factor	TIJ	Memjet	Advantage
Energy per drop	10 μ J	160 nJ	>50 times lower drop ejection energy allows battery operation
Actuator area	40,000 μ m ²	1,764 μ m ²	Small size allows low cost manufacture

A number of advantages of the memjet technology are outlined as follows:

High Resolution

The true resolution of Memjet is 1,600 dots per inch (dpi) in both directions. This allows full photographic quality color images, and high quality text (including Kanji). Higher resolutions are possible with the technology. 2,400 dpi and 4,800 dpi versions have been investigated for special applications, but 1,600 dpi is chosen as ideal for most applications. The true resolution of advanced commercial piezoelectric and thermal inkjet devices is around 600 to 800 dpi. 'Addressable resolution' is now often quoted in advertising to give the illusion of higher resolution.

Excellent Image Quality

High image quality requires high resolution and accurate placement of drops. The monolithic pagewidth nature of Memjet allows drop placement to sub-micron precision. High accuracy is also achieved by eliminating misdirected drops, electrostatic deflection, air turbulence, and eddies, and maintaining highly consistent drop volume and velocity. Image quality is also ensured by the provision of sufficient resolution to avoid requiring multiple ink densities. Five color or 6 color 'photo' inkjet systems can introduce halftoning artifacts in mid tones (such as flesh-tones) if the dye interaction and drop sizes are not absolutely perfect. This problem is eliminated in binary three color systems such as Memjet.

High Speed (30 ppm per print head)

The pagewidth nature of the print head allows

high-speed operation, as no scanning is required. The time to print a full color A4 page is less than 2 seconds, allowing full 30 page per minute (ppm) operation per print head. Multiple print heads can be used in parallel to
5 obtain 60 ppm, 90 ppm, 120 ppm, etc. Memjet print heads are low cost and compact, so multiple head designs are practical.

Low Cost

10 A photo-width photographic print head assembly is projected to cost under US\$10, and a pagewidth A4 print head assembly (using two 4" print heads) is projected to cost less than US\$20. This is because 190 photographic print heads can be fabricated on a single 6" 0.5 micron CMOS wafer. With a CMOS cost of around US\$600 per wafer, a
15 MEMS postprocessing cost of around US\$400 per wafer, and a projected yield better than 80% (chip area is only 0.55 cm²), the projected cost is US\$6.50 per print head chip. 290 print heads fit on an 8" (200 mm) wafer. When early 300 mm fabs eventually become obsolete for leading edge CMOS,
20 more than 360 monolithic 8" print heads (or 720 4" print heads) can be fabricated on a single wafer, halving production cost.

All Digital Operation

25 The high resolution of the print head is chosen to allow fully digital operation using digital halftoning. This eliminates color non-linearity (a problem with continuous tone printers), and simplifies the design of drive ASICs.

Small Drop Volume

30 To achieve true 1,600 dpi resolution, a small drop size is required. Memjet's drop size is one picoliter (1 pl). The drop size of advanced commercial piezoelectric and thermal inkjet devices is around 10 pl to 30 pl.

Accurate Control of Drop Velocity

35 As the drop ejector is a precise mechanical mechanism, and does not rely on bubble nucleation, accurate drop velocity control is available. This allows low drop

velocities (4 m/s) to be used in applications where media and airflow can be controlled. Drop velocity can be accurately varied over a considerable range by varying the energy provided to the actuator. High drop velocities (10 to 15 m/s) suitable for plain-paper operation and relatively uncontrolled conditions can be achieved using variations of the nozzle chamber and actuator dimensions.

Fast Drying

A combination of very high resolution, very small drops, and high dye density allows full color printing with much less water ejected. Memjet ejects less than 25% of the water of a 400 dpi thermal inkjet printer. This allows fast drying and virtually eliminates paper cockle.

Wide Temperature Range

Memjet is designed to cancel the effect of ambient temperature. Only the change in ink characteristics with temperature affects operation and this can be electronically compensated. Operating temperature range is expected to be 0 °C to 50 °C for water based inks.

No Special Manufacturing Equipment Required

The manufacturing process for Memjet leverages entirely from the established semiconductor manufacturing industry. Most inkjet systems encounter major difficulty and expense in moving from the laboratory to production, as high accuracy specialized manufacturing equipment is required.

High Production Capacity Available

A 6" CMOS fab with 10,000 wafer starts per month can produce around 18 million print heads per annum. An 8" CMOS fab with 20,000 wafer starts per month can produce around 60 million print heads per annum. There are currently many such CMOS fabs in the world.

Low Factory Setup Cost

The factory set-up cost is low because existing 0.5 micron 6" CMOS fabs can be used. These fabs could be fully amortized, and essentially obsolete for CMOS logic production. Therefore, volume production can use 'old'

existing facilities. Most of the MEMS post-processing can also be performed in the CMOS fab, but at least one new piece of equipment will be required (an Advanced Silicon Etcher (ASE) from Surface Technology Systems in the UK, or equivalent).

Good Light- Fastness

As the ink is not heated, there are few restrictions on the types of dyes that can be used. This allows dyes to be chosen for optimum light-fastness. Some recently developed dyes from companies such as Zeneca Specialties and Hoechst have light-fastness of 4. This is equal to the light-fastness of many pigments, and considerably in excess of photographic dyes and of inkjet dyes in use until recently.

Good Water- Fastness

As with light-fastness, the lack of thermal restrictions on the dye allows selection of dyes for characteristics such as water-fastness. For extremely high water-fastness (as is required for washable fabrics) reactive dyes can be used.

Excellent Color Gamut

The use of transparent dyes of high color purity allows a color gamut considerably wider than that of offset printing and silver halide photography. Offset printing in particular has a restricted gamut due to light scattering from the pigments used. With three-color systems (CMY) or four-color systems (CMYK) the gamut is necessarily limited to the tetrahedral volume between the color vertices. Therefore it is important that the cyan, magenta and yellow dyes are as spectrally pure as possible. A slightly wider 'hexcone' gamut that includes pure reds, greens, and blues can be achieved using a 6 color (CMYRGB) model. Such a six-color print head can be made economically with a width of only 1 mm.

Elimination of Color Bleed

Ink bleed between colors occurs if the different primary colors are printed while the previous color is wet.

While image blurring due to ink bleed is typically insignificant at 1600 dpi, ink bleed can 'muddy' the midtones of an image. Ink bleed can be eliminated by using microemulsion-based ink, for which Memjet is highly suited.

- 5 The use of microemulsion ink can also help prevent nozzle clogging and ensure long-term ink stability.

High Nozzle Count

- Memjet has 19,200 nozzles in a monolithic CMY three-color photographic print head. While this is large compared to other print heads, it is a small number compared to the number of devices routinely integrated on CMOS VLSI chips in high volume production. It is also less than 3% of the number of movable mirrors which Texas Instruments integrates in its Digital Micromirror Device (DMD), manufactured using similar CMOS and MEMS processes.
- 15 51,200 Nozzles per A4 Pagewidth Print Head

A four color (CMYK) Memjet print head for pagewidth A4/US letter printing uses two chips. Each 0.66 cm² chip has 25,600 nozzles for a total of 51,200 nozzles.

- 20 Integration of Drive Circuits

- In a print head with as many as 51,200 nozzles, it is essential to integrate data distribution circuits (shift registers), data timing, and drive transistors with the nozzles. Otherwise, a minimum of 51,201 external connections would be required. This is a severe problem with piezoelectric ink jets, as drive circuits cannot be integrated on piezoelectric substrates. Integration of many millions of connections is common in CMOS VLSI chips, which are fabricated in high volume at high yield. It is the number of *off-chip* connections that must be limited.
- 25 30

Monolithic Fabrication

- Memjet is made as a single monolithic CMOS chip, so no precision assembly is required. All fabrication is performed using standard CMOS VLSI and MEMS (Micro-Electro-Mechanical Systems) processes and materials. In thermal inkjet and some piezoelectric inkjet systems, the assembly of nozzle plates with the print head chip is a major cause
- 35

of low yields, limited resolution, and limited size. Also, pagewidth arrays are typically constructed from multiple smaller chips. The assembly and alignment of these chips is an expensive process.

5 Modular, Extendable for Wide Print Widths

Long pagewidth print heads can be constructed by butting 'standard' 100 mm Memjet heads together. The edge of the Memjet print head chip is designed to automatically align to adjacent chips. One print head gives a
10 photographic size printer, two gives an A4 printer, and four gives an A3 printer. Larger numbers can be used for high speed digital printing, pagewidth wide format printing, and fabric printing.

Duplex Operation

15 Duplex printing at the full print speed is highly practical. The simplest method is to provide two print heads - one on each side of the paper. The cost and complexity of providing two print heads is less than that of mechanical systems to turn over the sheet of paper.

20 Straight Paper Path

As there are no drums required, a straight paper path can be used to reduce the possibility of paper jams. This is especially relevant for office duplex printers, where the complex mechanisms required to turn over the
25 pages are a major source of paper jams.

High Efficiency

Thermal inkjet printheads are only around 0.1% efficient (electrical energy input compared to drop kinetic energy and increased surface energy). Memjet is more than
30 10 times as efficient.

Self-Cooling Operation

The energy required to eject each drop is 160 nJ (0.16 microJoules), a small fraction of that required for thermal ink jet printers. The low energy allows the print
35 head to be completely cooled by the ejected ink, with only a 40 °C worst-case ink temperature rise. No heat sinking is required.

Low Pressure

The maximum pressure generated in a Memjet print head is around 60 kPa (0.6 atmospheres). The pressures generated by bubble nucleation and collapse in thermal ink jet and Bubblejet systems are typically in excess of 10 MPa (100 atmospheres), which is 160 times the maximum Memjet pressure. The high pressures in Bubblejet and thermal inkjet designs result in high mechanical stresses.

Low Power

A 30 ppm A4 Memjet print head requires about 67 Watts when printing full 3 color black. When printing 5% coverage, average power consumption is only 3.4 Watts.

Low Voltage Operation

Memjet can operate from a single 3V supply, the same as typical drive ASICs. Thermal inkjets typically require at least 20 V, and piezoelectric inkjets often require more than 50 V. The Memjet actuator is designed for nominal operation at 2.8 volts, allowing a 0.2 volt drop across the drive transistor, to achieve 3V chip operation.

Operation from 2 or 4 AA Batteries

Power consumption is low enough that a photographic Memjet print head can operate from AA batteries. A typical 6" x 4" photograph requires less than 20 Joules to print (including drive transistor losses). Four AA batteries are recommended if the photo is to be printed in 2 seconds. If the print time is increased to 4 seconds, 2 AA batteries can be used.

Battery Voltage Compensation

Memjet can operate from an unregulated battery supply, to eliminate efficiency losses of a voltage regulator. This means that consistent performance must be achieved over a considerable range of supply voltages. Memjet senses the supply voltage, and adjusts actuator operation to achieve consistent drop volume.

Small Actuator and Nozzle Area

The area required by a Memjet nozzle, actuator, and drive circuit is 1764 μm^2 . This is less than 1% of the

area required by piezoelectric ink jet nozzles, and around 5% of the area required by Bubblejet nozzles. The actuator area directly affects the print head manufacturing cost.

Small Total Print Head Size

5 An entire print head assembly (including ink supply channels) for an A4, 30 ppm, 1,600 dpi, four color print head is 210 mm x 12 mm x 7 mm. The small size allows incorporation into notebook computers and miniature printers. A photograph printer is 106 mm x 7 mm x 7 mm, 10 allowing inclusion in pocket digital cameras, palmtop PC's, mobile phone/fax, and so on. Ink supply channels take most of this volume. The print head chip itself is only 102 mm x 0.55 mm x 0.3 mm.

Miniature Nozzle Capping System

15 A miniature nozzle capping system has been designed for Memjet. For a photograph printer this nozzle capping system is only 106 mm x 5 mm x 4 mm, and does not require the print head to move.

High Manufacturing Yield

20 The projected manufacturing yield (at maturity) of the Memjet print heads is at least 80%, as it is primarily a digital CMOS chip with an area of only 0.55 cm². Most modern CMOS processes achieve high yield with chip areas in excess of 1 cm². For chips less than around 1 25 cm², cost is roughly proportional to chip area. Cost increases rapidly between 1 cm² and 4 cm², with chips larger than this rarely being practical. There is a strong incentive to ensure that the chip area is less than 1 cm². For thermal inkjet and Bubblejet print heads, the chip 30 width is typically around 5 mm, limiting the cost effective chip length to 1 to 2 cm. A major target of Memjet has been to reduce the chip width as much as possible, allowing cost effective monolithic pagewidth print heads.

Low Process Complexity

35 With digital IC manufacture, the mask complexity of the device has little or no effect on the manufacturing cost or difficulty. Cost is proportional to the number of

process steps, and the lithographic critical dimensions. Memjet uses a standard 0.5 micron single poly triple metal CMOS manufacturing process, with an additional 5 MEMS mask steps. This makes the manufacturing process less complex than a typical 0.25 micron CMOS logic process with 5 level metal. However, as the MEMS postprocessing is not standard, a significant amount of process development is required. Process development is usually difficult and expensive, and is likely to be the highest portion of the remaining development costs.

Simple Testing

Memjet includes test circuits and a test strategy that allows most testing to be completed at the wafer probe stage. Testing of all electrical properties, including the resistance of the actuator, can be completed at this stage. However, actuator motion can only be tested after release from the sacrificial materials, so final testing must be performed on the packaged chips.

Low Cost Packaging

Memjet is packaged in an injection molded polycarbonate package. All connections are made using Tape Automated Bonding (TAB) technology (though wire bonding can be used as an option). All connections are along one edge of the chip. Alpha particle emission does not need to be considered in the packaging, as there are no memory elements except static registers, and a change of state due to alpha particle tracks is likely to cause only a single extra dot to be printed (or not) on the paper.

Relaxed Critical Dimensions

The critical dimension (CD) of the Memjet CMOS drive circuitry is 0.5 microns. Advanced digital IC's such as microprocessors currently use CDs of 0.25 microns, which is two device generations more advanced than the Memjet print head requires. Most of the MEMS post processing steps have CDs of 1 micron or greater.

Low Stress during Manufacture

Devices cracking during manufacture are a

critical problem with both thermal ink jet and piezoelectric devices. This limits the size of the print head that it is possible to manufacture. The stresses involved in the manufacture of Memjet print heads are no greater than those required for CMOS fabrication.

No Scan Banding

Memjet is a full pagewidth print head, so does not scan. This eliminates one of the most significant image quality problems of inkjet printers. Banding due to other causes (mis-directed drops, print head alignment) is usually a significant problem in pagewidth print heads. These causes of banding have also been addressed.

'Perfect' Nozzle Alignment

All of the nozzles within a print head are aligned to sub-micron accuracy by the 0.5 micron stepper used for the lithography of the print head. Nozzle alignment of two 4" print heads to make an A4 pagewidth print head is achieved with the aid of mechanical alignment features on the print head chips. This allows automated mechanical alignment (by simply pushing two print head chips together) to within 1 micron. If finer alignment is required in specialized applications, 4" print heads can be aligned optically.

No Satellite Drops

The very small drop size (1 pl) and moderate drop velocity (4 m/s) eliminates satellite drops, which are a major source of image quality problems. The low drop velocity requires laminar airflow, with no eddies, to achieve good drop placement on the print medium. This is achieved by the design of the print head packaging. For 'plain paper' applications and for printing on other 'rough' surfaces, higher drop velocities are desirable. Drop velocities to 15 m/s can be achieved using variations of the design dimensions. It is possible to manufacture 3 color photographic print heads with a 4 m/s drop velocity, and 4 color plain-paper print heads with a 15 m/s drop velocity, on the same wafer. This is because both can be

made using the same process parameters.

No Misdirected Drops

Misdirected drops are eliminated by the provision of a thin rim around the nozzle, which prevents the spread of a drop across the print head surface in regions where the hydrophobic coating is compromised.

No Thermal Crosstalk

When adjacent actuators are energized in Bubblejet or other thermal inkjet systems, the heat from one actuator spreads to others, and affects their firing characteristics. In Memjet, heat diffusing from one actuator to adjacent actuators affects both the heater layer and the bend-cancelling layer equally, so has no effect on the paddle position. This virtually eliminates thermal crosstalk.

No Fluidic Crosstalk

Each simultaneously fired nozzle is at the end of a 300 micron long ink inlet etched through the (thinned) wafer. These ink inlets are connected to large ink channels with low fluidic resistance. This configuration virtually eliminates any effect of drop ejection from one nozzle on other nozzles.

No Structural Crosstalk

This is a common problem with piezoelectric print heads. It does not occur in Memjet.

Permanent Print Head

The Memjet print heads can be permanently installed. This dramatically lowers the production cost of consumables.

30 No Kogation

Kogation (residues of burnt ink, solvent, and impurities, from the Japanese 'koga' for burnt rice) is a significant problem with Bubblejet and other thermal inkjet print heads. Memjet does not have this problem, as the ink is not directly heated.

No Cavitation

Erosion caused by the violent collapse of bubbles

is another problem that limits the life of Bubblejet and other thermal inkjet print heads. Memjet does not have this problem because no bubbles are formed.

No Electromigration

5 No metals are used in Memjet actuators or nozzles, which are entirely ceramic. Therefore, there is no problem with electromigration in the actual inkjet devices. The CMOS metalization layers are designed to support the required currents without electromigration. This can be
10 readily achieved because the current considerations arise from heater drive power, not high speed CMOS switching.

Reliable Power Connections

 While the energy consumption of Memjet is fifty times less than thermal ink jet, the high print speed and
15 low voltage results in a fairly high electrical current consumption. Worst case current for a photographic Memjet head printing in two seconds from a 3 Volt supply is 4.9 Amps. This is supplied via copper busbars to 256 bond pads along the edge of the chip. Each bond pad carries a maximum
20 of 40 mA. On chip contacts and vias to the drive transistors carry a peak current of 1.5 mA for 1.3 microseconds, and a maximum average of 12 mA.

No Corrosion

 The nozzle and actuator are entirely formed of
25 glass and titanium nitride (TiN), a conductive ceramic commonly used as metalization barrier layers in CMOS devices. Both materials are at minimum chemical energy levels with respect to water, so do not corrode. Titanium nitride does not corrode or dissolve in extreme
30 environments such as molten aluminum. It is used as the coating for the electrodes in aluminum smelters. TiN is also highly wear resistant - many watches and jewellery items are coated with TiN as it looks like gold, but has much better wear properties.

35 No Electrolysis

 The ink is not in contact with any electrical potentials, so there is no electrolysis.

No Fatigue

All actuator movement is within elastic limits, and the materials used are all ceramics, so there is no fatigue.

5 No Friction

No moving surfaces are in contact, so there is no friction.

No Stiction

Memjet is designed to eliminate stiction, a
10 problem common to many MEMS devices.

No Crack Propagation

The stresses applied to the materials are less than 1% of that which leads to crack propagation with the typical surface roughness of the TiN and glass layers.
15 Corners are rounded to minimize stress 'hotspots'. The glass is also always under compressive stress, which is much more resistant to crack propagation than tensile stress.

No Electrical Poling Required

20 Piezoelectric materials must be poled after they are formed into the printhead structure. This poling requires very high electrical field strengths - around 20,000 V/cm. The high voltage requirement typically limits the size of piezoelectric print heads to around 5 cm,
25 requiring 100,000 Volts to pole. Memjet requires no poling.

No Rectified Diffusion

Rectified diffusion - the formation of bubbles due to cyclic pressure variations - is a problem that primarily afflicts piezoelectric ink jets. Memjet is
30 designed to prevent rectified diffusion, as the ink pressure never falls below zero.

Elimination of the Saw Street

The saw street between chips on a wafer is typically 200 microns. This would take 26% of the wafer
~~35 area. Instead, plasma etching is used, requiring just 4% of~~
the wafer area. This also eliminates breakage during sawing.

Lithography Using Standard Steppers

Although Memjet print heads are 100 mm long, standard steppers (which typically have an imaging field around 20 mm square) are used. This is because the print head is 'stitched' using eight identical exposures. Alignment between stitches is not critical, as there are no electrical connections between stitch regions. One segment of each of 32 print heads is imaged with each stepper exposure, giving an 'average' of 4 print heads per exposure.

Integration of Full Color on a Single Chip

Memjet integrates all of the colors required onto a single chip. This cannot be done with pagewidth 'edge shooter' designs, such as Canon Bubblejet.

Wide Variety of Inks

Memjet does not rely on the ink properties for drop ejection. Inks can be based on water, microemulsions, oils, various alcohols, MEK, hot melt waxes, or other solvents. Memjet can be 'tuned' for inks over a wide range of viscosity and surface tension. This is one significant factor allowing a wide range of applications.

Archival Quality

With the right choice of dye and media, archival permanence significantly better than color photographs can be achieved.

Laminar Air Flow with no Eddies

The print head packaging is designed to ensure that airflow is laminar, and to eliminate eddies. This is important, as eddies or turbulence could degrade image quality due to the small drop size.

Drop Repetition Rate

The nominal drop repetition rate of a photographic Memjet is 5 kHz, resulting in a print speed of 2 second per photo. The nominal drop repetition rate for an A4 print head is 10 kHz for 30+ ppm A4 printing. The maximum drop repetition rate is primarily limited by the nozzle refill rate, which is determined by surface tension

when operated using non-pressurized ink. Drop repetition rates of 50 kHz are possible using positive ink pressure (around 20 kPa). However, 34 ppm is entirely adequate for most low cost consumer applications. For very high-speed applications, such as commercial printing, multiple print heads can be used in conjunction with fast paper handling. For low power operation (such as operation from 2 AA batteries) the drop repetition rate can be reduced to reduce power.

10 Low Head-to-Paper Speed

The nominal head to paper speed of a photographic Memjet print head is only 0.076 m/sec. For an A4 print head it is only 0.16 m/sec, which is about a third of the typical scanning inkjet head speed. The low speed simplifies printer design and improves drop placement accuracy. However, this head-to-paper speed is enough for 34 ppm printing, due to the pagewidth print head. Higher speeds can readily be obtained where required.

High Speed CMOS not Required

20 The clock speed of the print head shift registers is only 14 MHz for an A4/letter print head operating at 30 ppm. For a photograph printer, the clock speed is only 3.84 MHz. This is much lower than the speed capability of the CMOS process used. This simplifies the CMOS design, and eliminates power dissipation problems when printing near-white images.

Fully Static CMOS Design

The shift registers and transfer registers are fully static designs. A static design requires 35 transistors per nozzle, compared to around 13 for a dynamic design. However, the static design has several advantages, including higher noise immunity, lower quiescent power consumption, and greater processing tolerances.

Wide Power Transistor

35 The width to length ratio of the power transistor is 688. This allows a 4 Ohm on-resistance, whereby the drive transistor consumes 6.7% of the actuator power when

operating from 3V. This size transistor fits beneath the actuator, along with the shift register and other logic. Thus an adequate drive transistor, along with the associated data distribution circuits, consumes no chip area that is not already required by the actuator.

There are several ways to reduce the percentage of power consumed by the transistor: increase the drive voltage so that the required current is less, reduce the lithography to less than 0.5 micron, use BiCMOS or other high current drive technology, or increase the chip area, allowing room for drive transistors which are not underneath the actuator. However, the 6.7% consumption of the present design is considered a cost-performance optimum.

Other Uses:

The presently disclosed ink jet printing technology is potentially suited to a wide range of printing system including: colour and monochrome office printers, short run digital printers, high speed digital printers, offset press supplemental printers, low cost scanning printers high speed pagewidth printers, notebook computers with inbuilt pagewidth printers, portable colour and monochrome printers, colour and monochrome copiers, colour and monochrome facsimile machines, combined printer, facsimile and copying machines, label printers, large format plotters, photograph copiers, printers for digital photographic "minilabs", video printers, PhotoCD printers, portable printers for PDAs, wallpaper printers, indoor sign printers, billboard printers, fabric printers, camera printers and fault tolerant commercial printer arrays.

Existing inkjet technologies

Similar capability print heads are unlikely to become available from the established inkjet manufacturers in the near future. This is because the two main contenders

- thermal inkjet and piezoelectric inkjet - each have severe fundamental problems meeting the requirements of the application.

The most significant problem with thermal inkjet is power consumption. This is approximately 100 times that required for these applications, and stems from the energy-inefficient means of drop ejection. This involves the rapid
5 boiling of water to produce a vapor bubble which expels the ink. Water has a very high heat capacity, and must be superheated in thermal inkjet applications.

The most significant problem with piezoelectric inkjet is size and cost. Piezoelectric crystals have a very
10 small deflection at reasonable drive voltages, and therefore require a large area for each nozzle. Also, each piezoelectric actuator must be connected to its drive circuit on a separate substrate. This is not a significant problem at the current limit of around 300 nozzles per
15 print head, but is a major impediment to the fabrication of pagewidth print heads with 19,200 nozzles.

It would be appreciated by a person skilled in the art that numerous variations and/or modifications may be made to the present invention as shown in the specific
20 embodiments without departing from the spirit or scope of the invention as broadly described. The present embodiments are, therefore, to be considered in all respects to be illustrative and not restrictive.

We Claim

1. In a moveable micromechanical device including a bending member having a first bending direction having a planar bottom surface, said bending member formed
5 on a plane substrate on top of a number of deposited lower layers, a method of forming the bending member comprising the step of:
forming a series of structures in said deposited lower layers, said series of structures having a surface
10 profile including a series of elongated ribs running in a direction substantially transverse to said bending direction.
2. A method as claimed in claim 1 wherein said bending member comprises a thermal bend actuator.
- 15 3. A method as claimed in claim 1 wherein said deposited layers include a conductive circuitry layer.
4. A method as claimed in claim 3 wherein said conductive circuitry layer is interconnected to said bending member for activation of said bending member.
- 20 5. A method as claimed in claim 1 wherein said bending member is attached to a paddle member and actuated for the ejection of ink from an ink ejection nozzle of an ink jet printing device.
- 25 6. A method as claimed in claim 3 wherein said deposited layer, located under said bending member include a power transistor for the control of operation of said bending member.

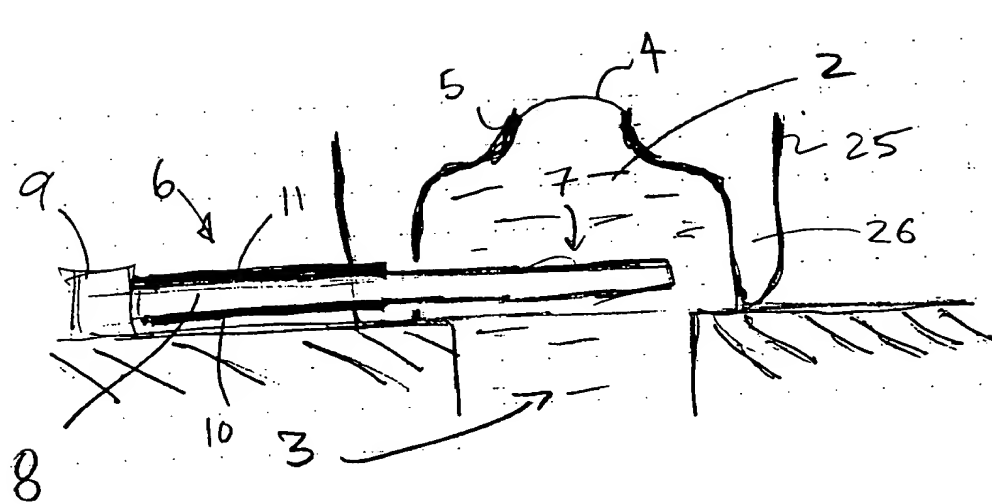


FIG. 1

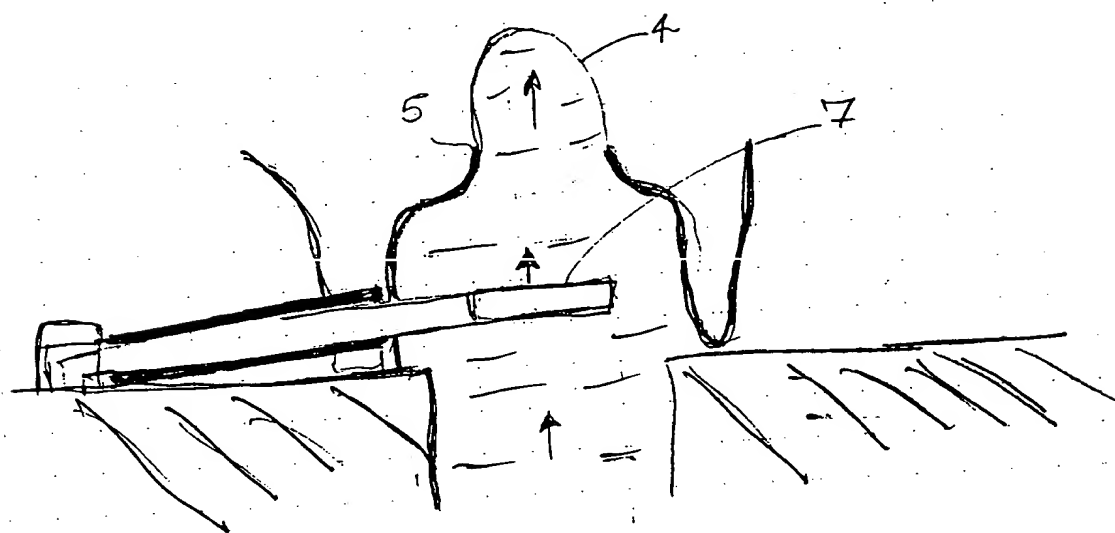
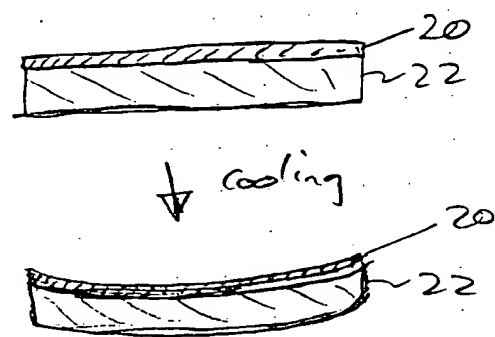
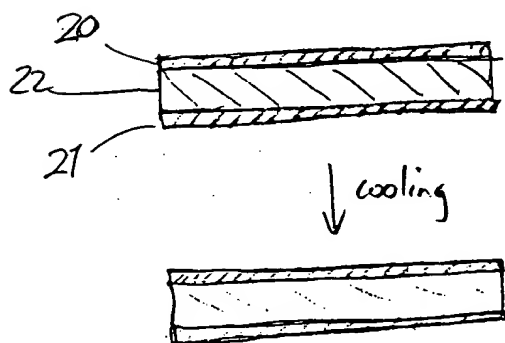
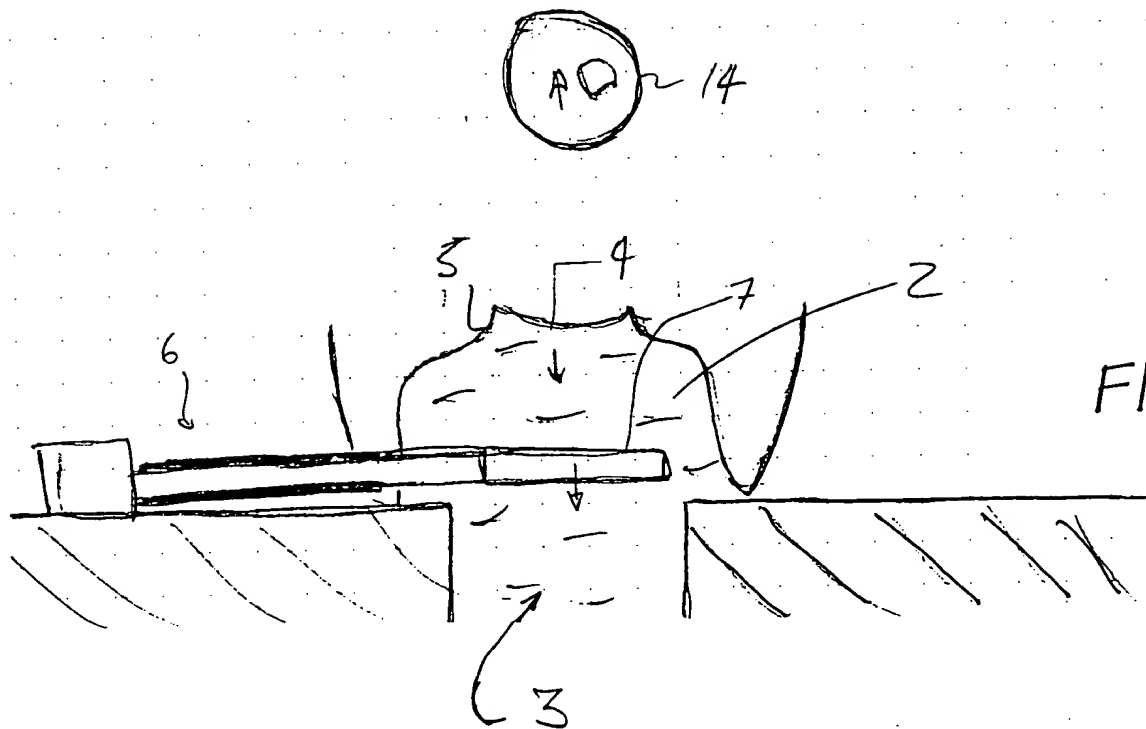


FIG. 2



30

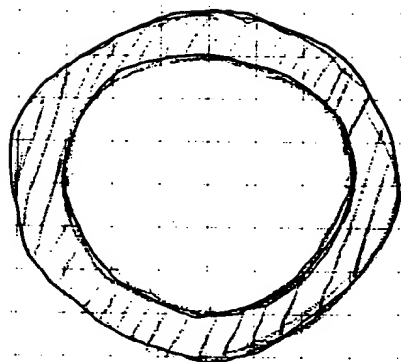


FIG. 6

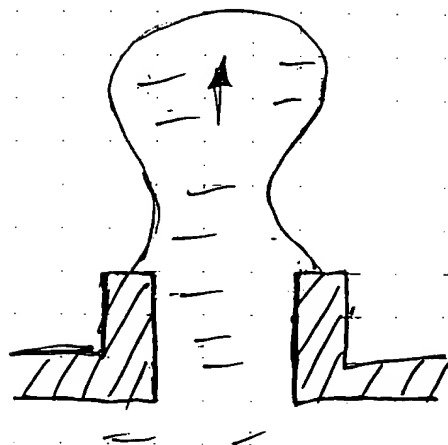


FIG. 7

35

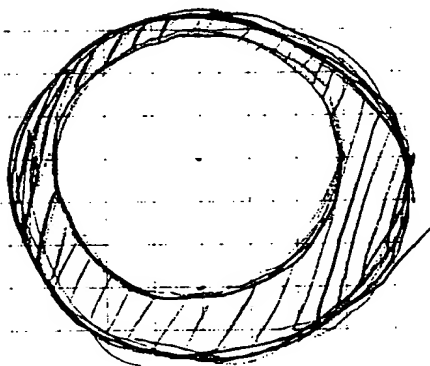


FIG. 8

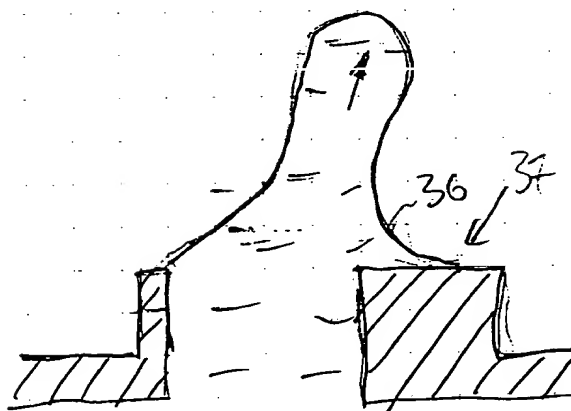


FIG. 9

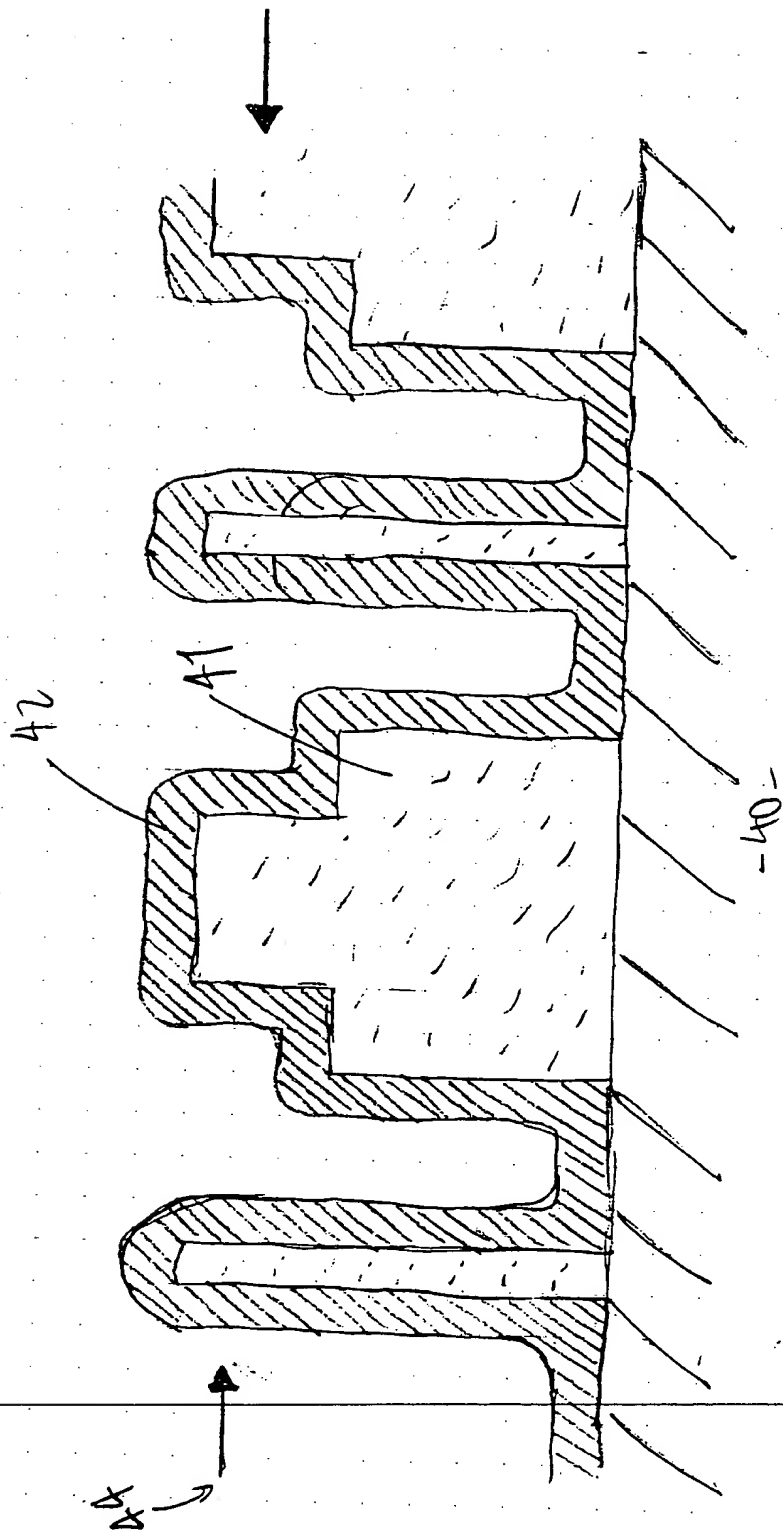


FIG. 10

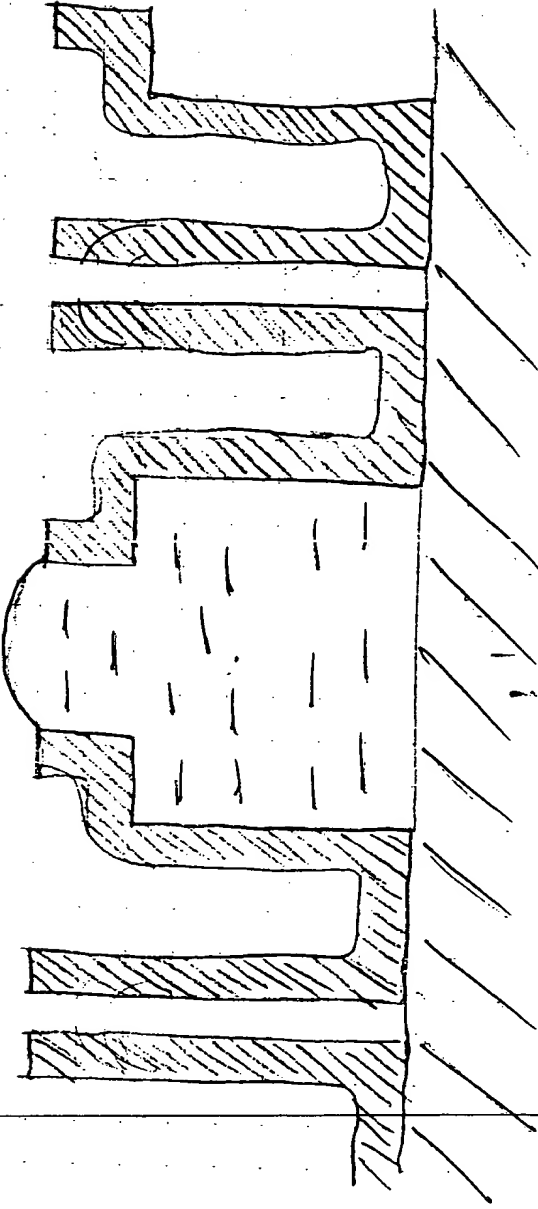


FIG. 11

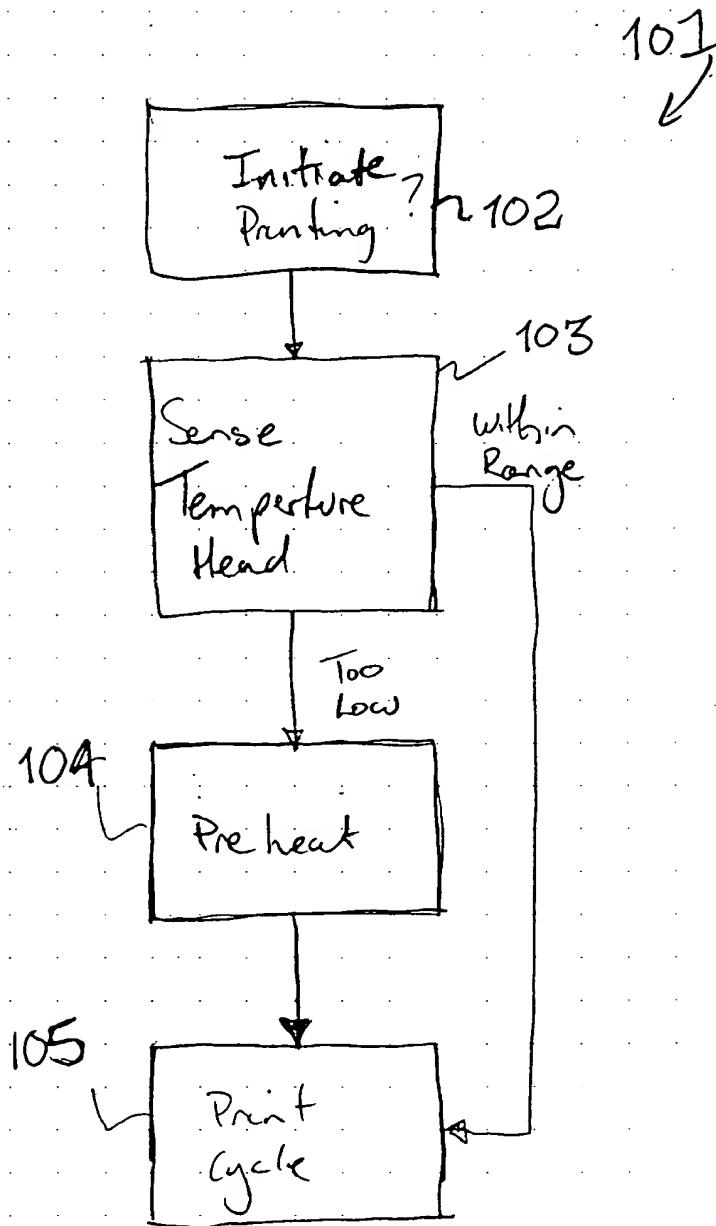


FIG. 12

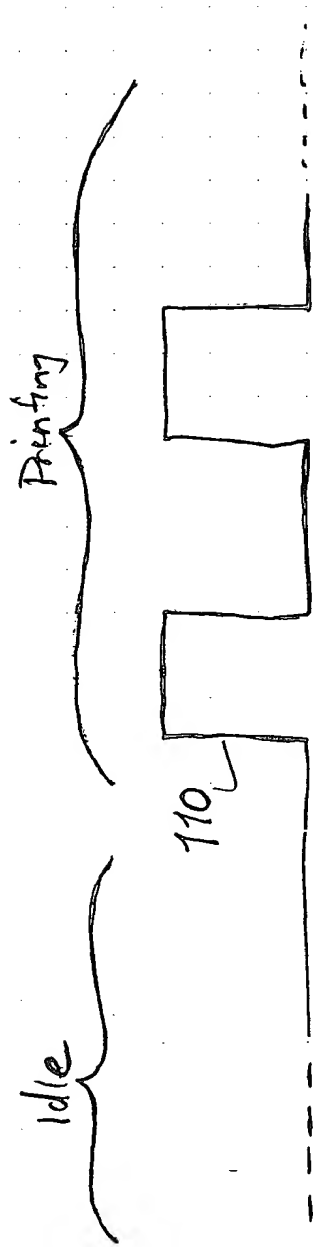


FIG. 13

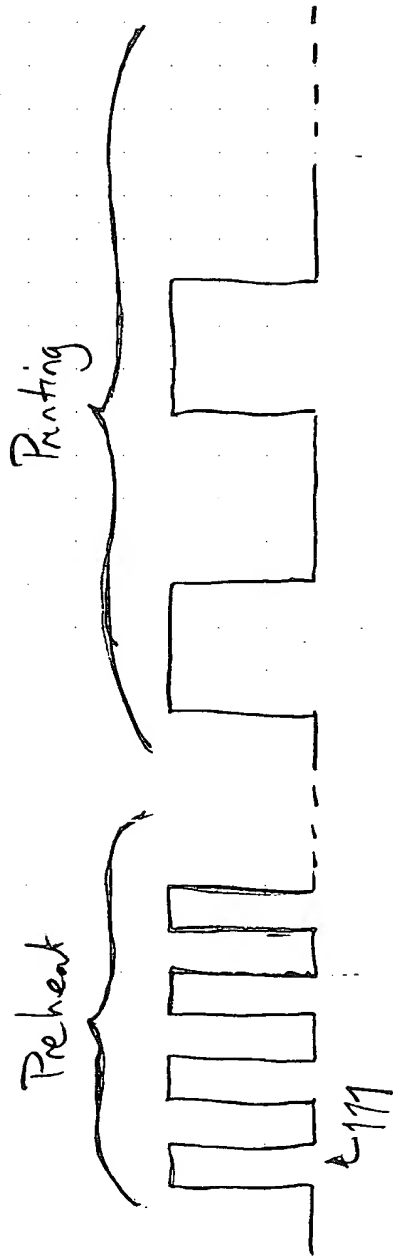


FIG. 14

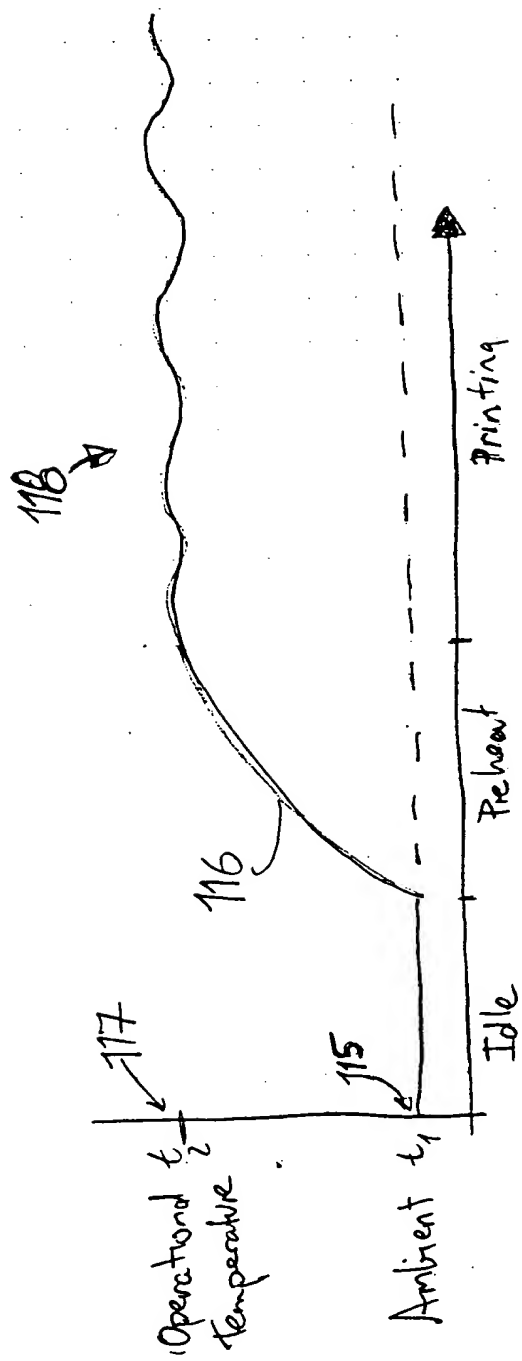


FIG. 15

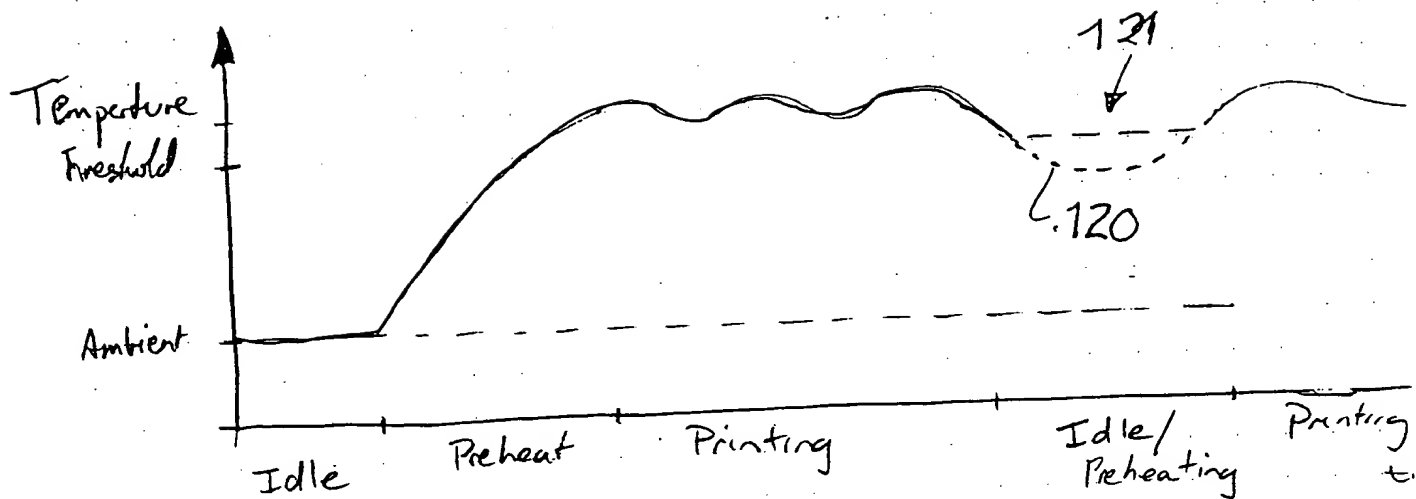


FIG. 16

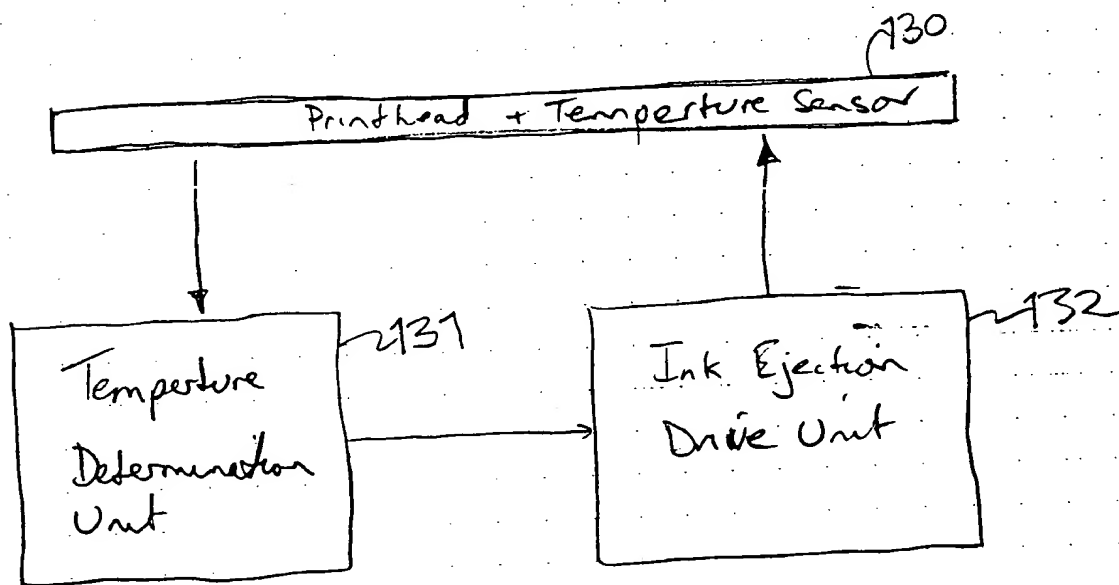


FIG. 17

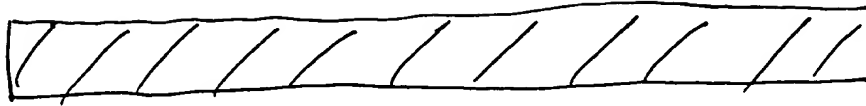


FIG. 18

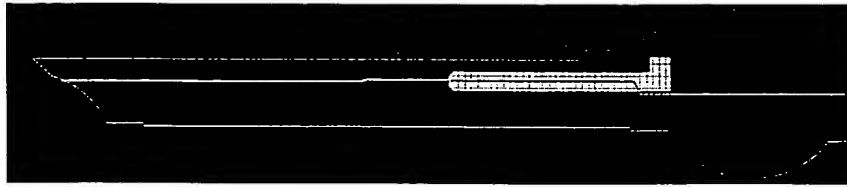


FIG. 19

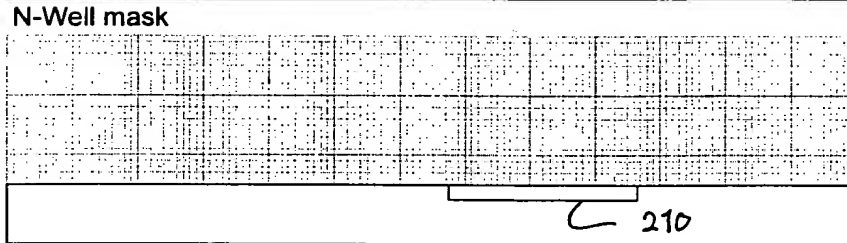


FIG. 20

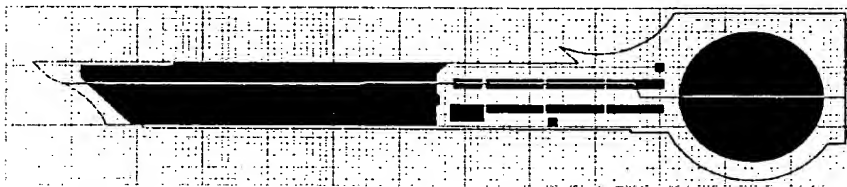


FIG. 22



FIG. 23

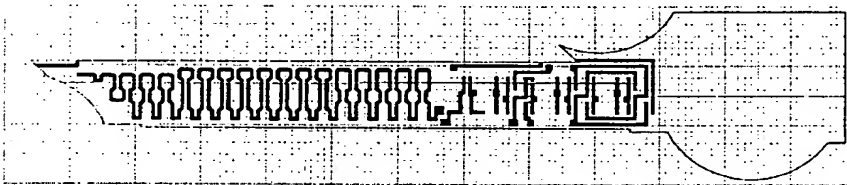


FIG. 25

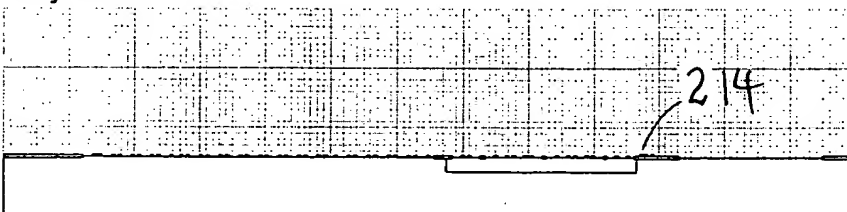


FIG. 26

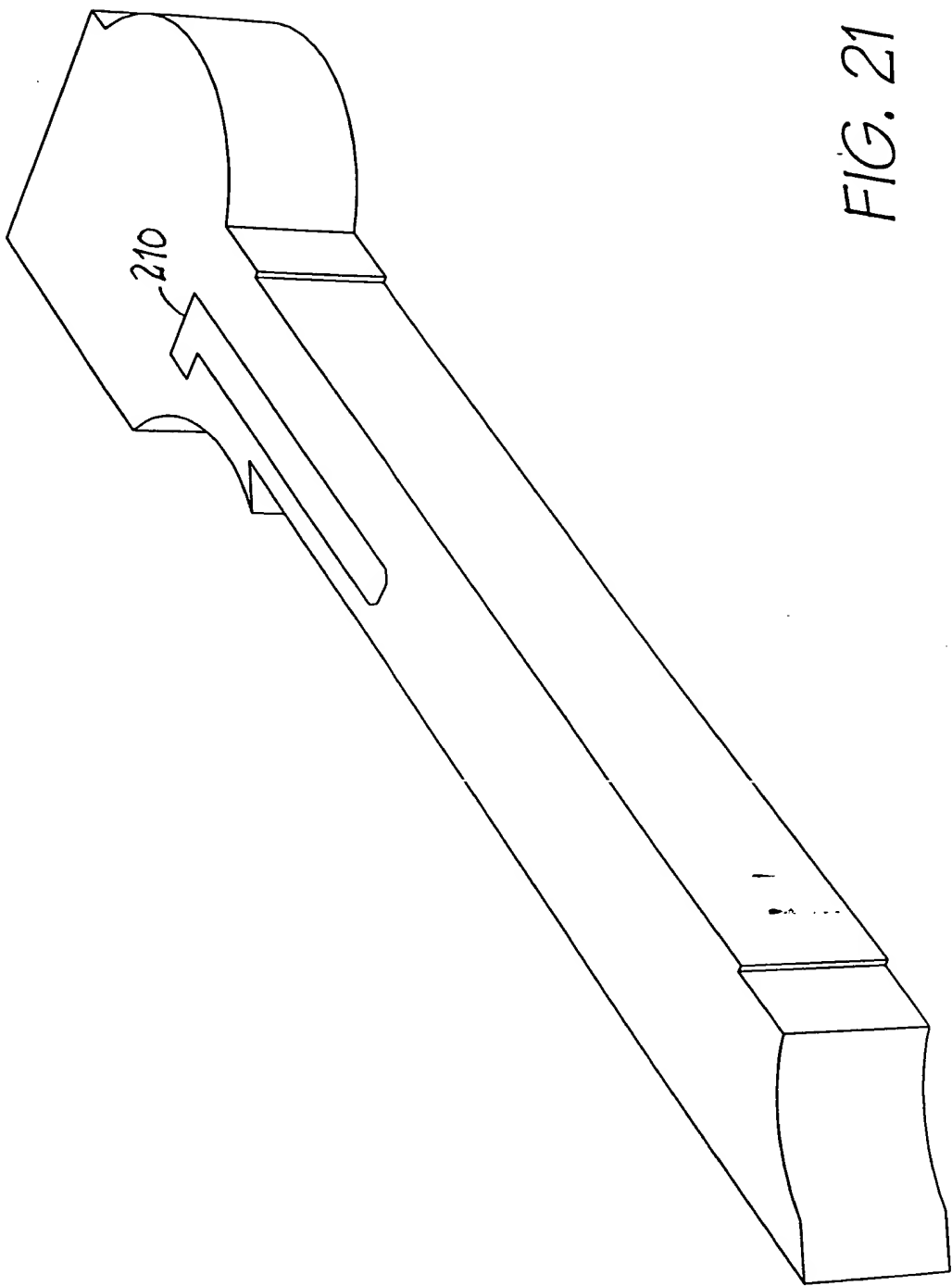


FIG. 21

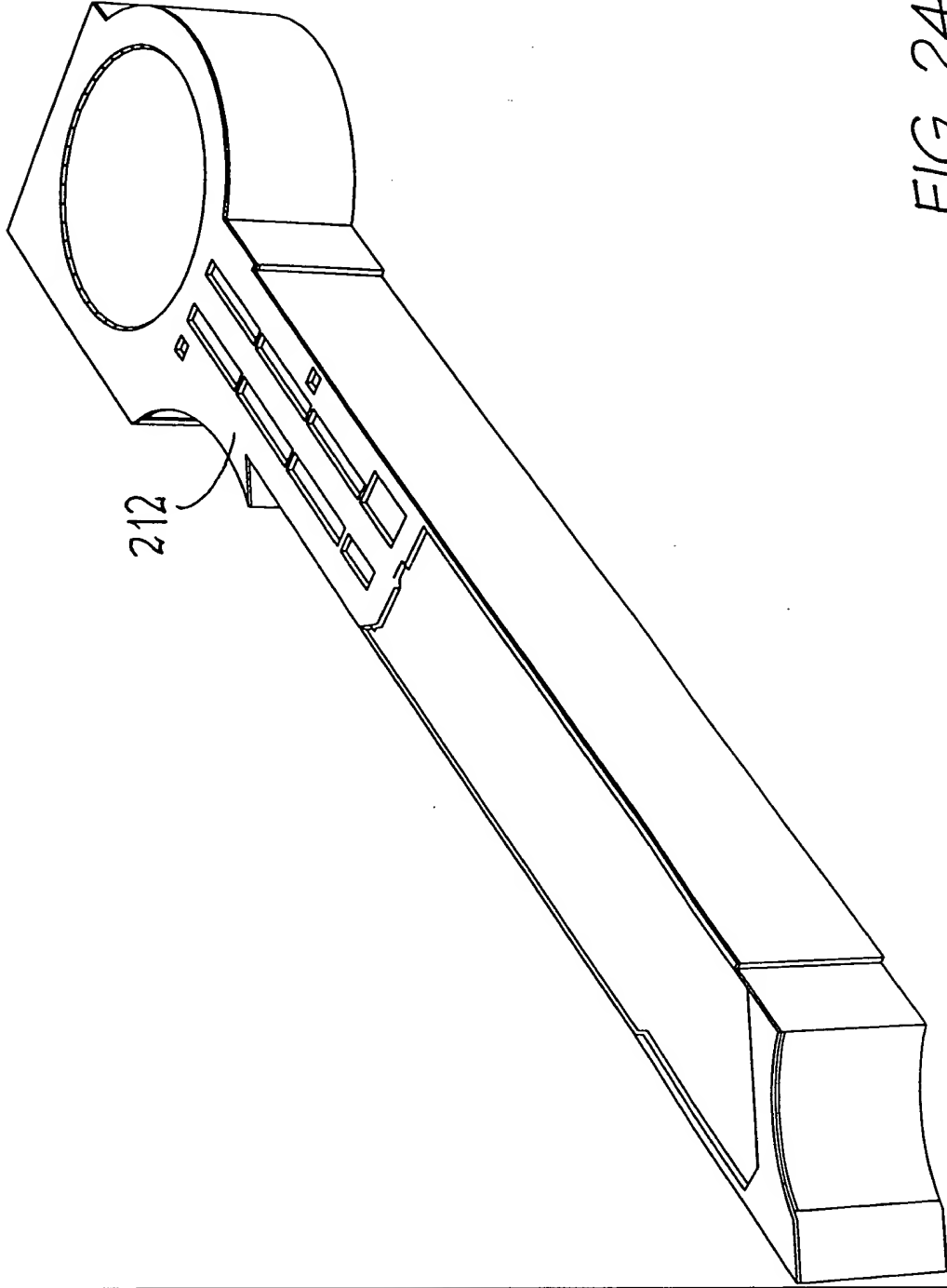


FIG. 24

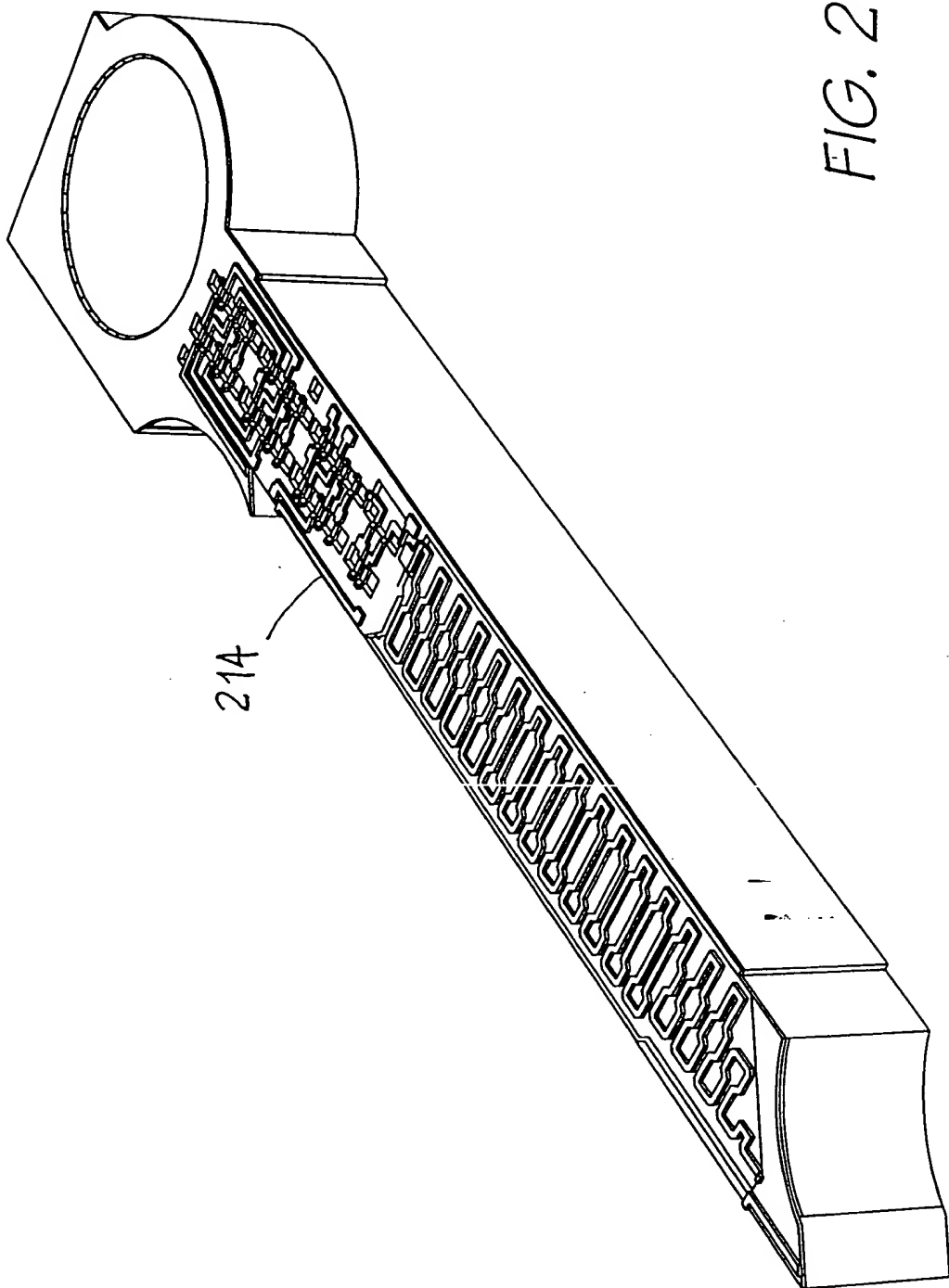


FIG. 27

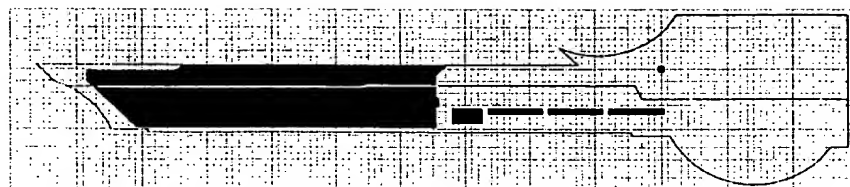


FIG. 28

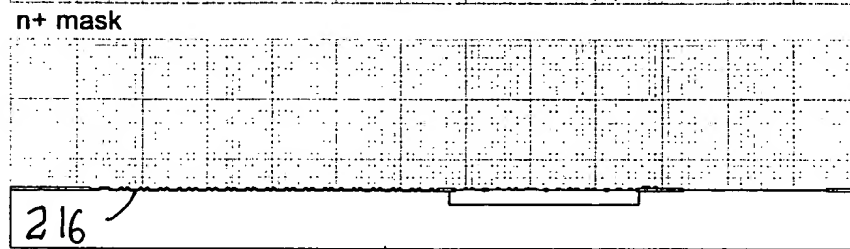


FIG. 29



FIG. 31

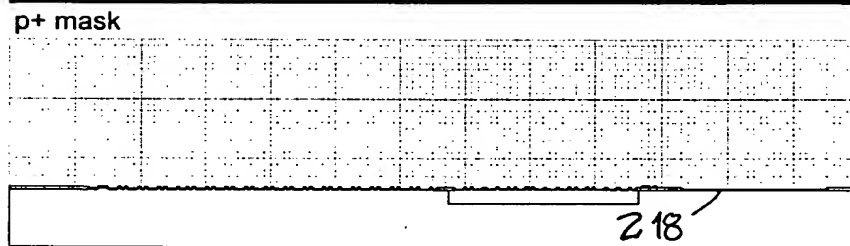


FIG. 32

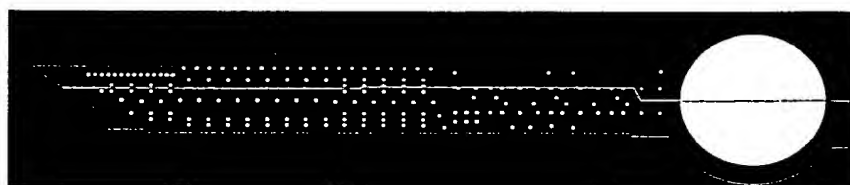


FIG. 34

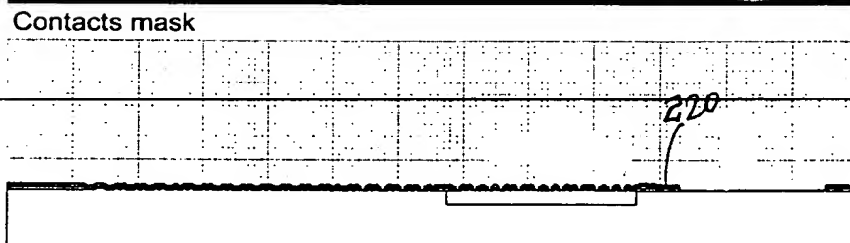


FIG. 35

Deposit ILD 1, etch contacts

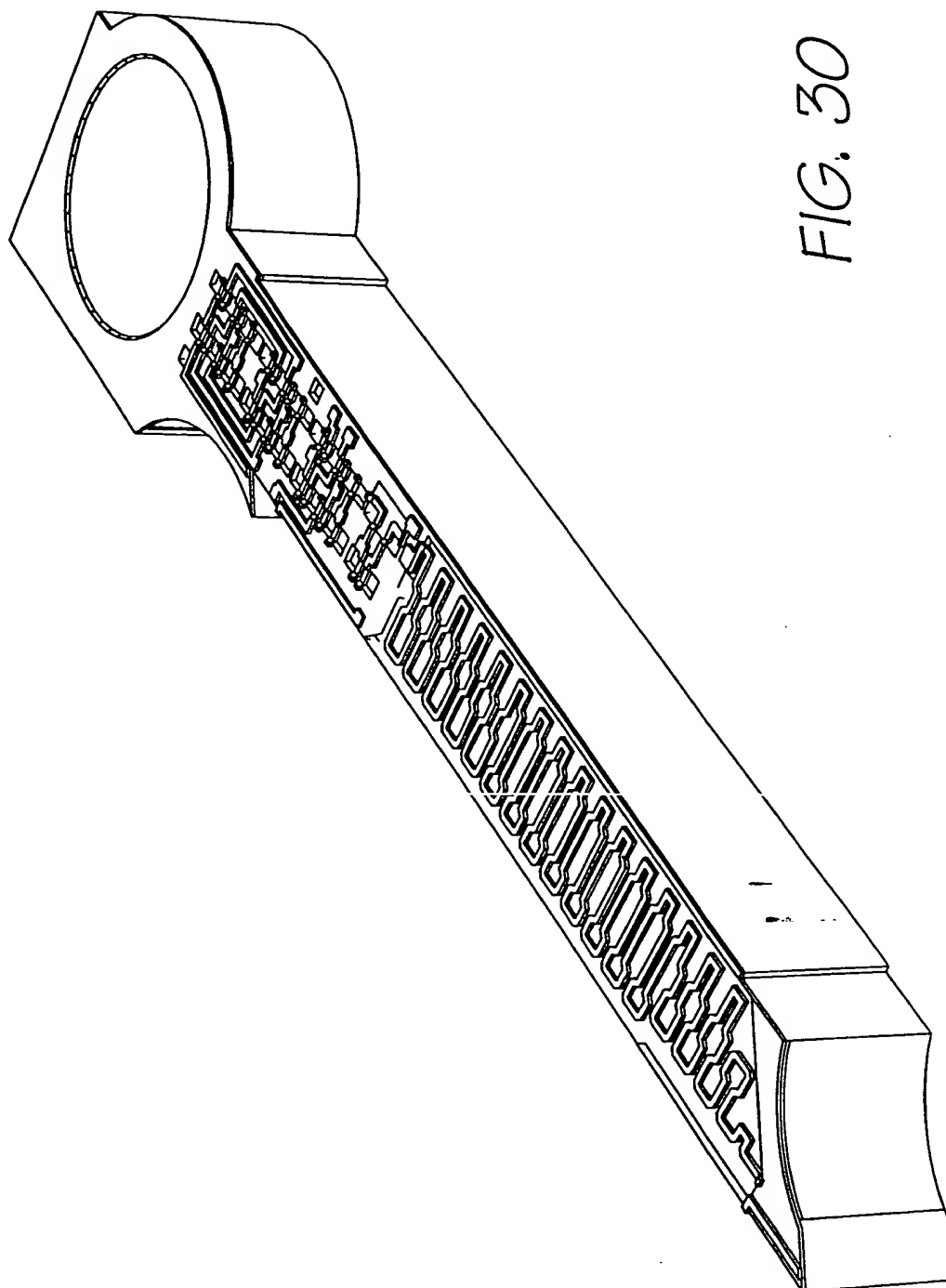


FIG. 30

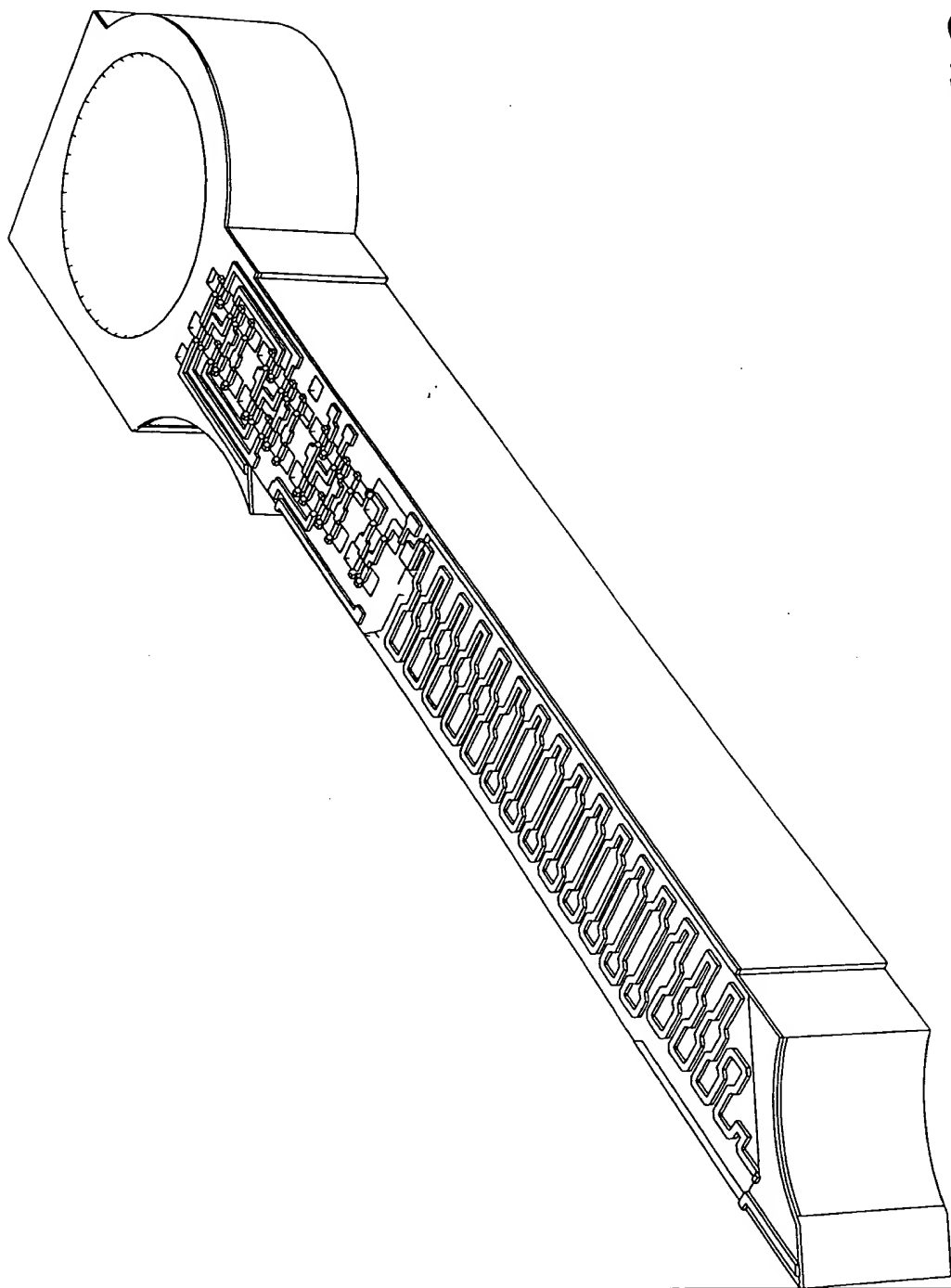


FIG. 33

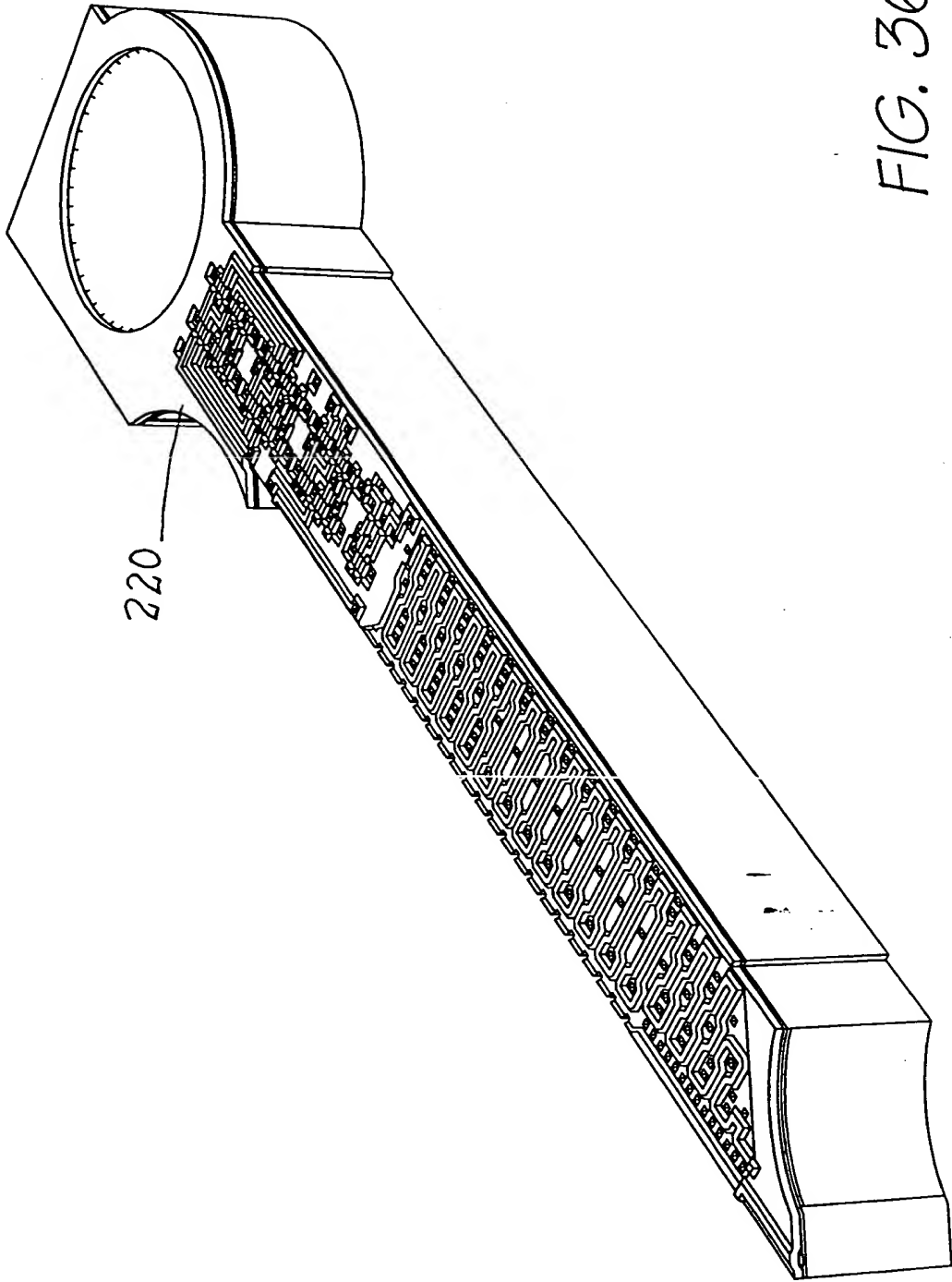


FIG. 36

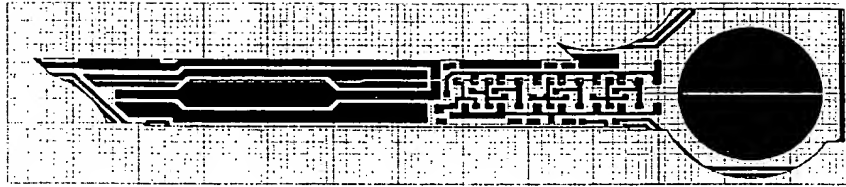


FIG. 37

Metal 1 mask

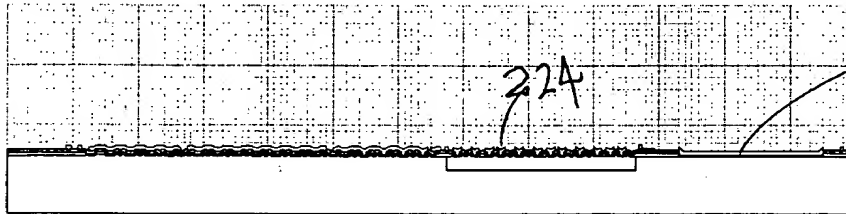


FIG. 38

Deposit Metal 1

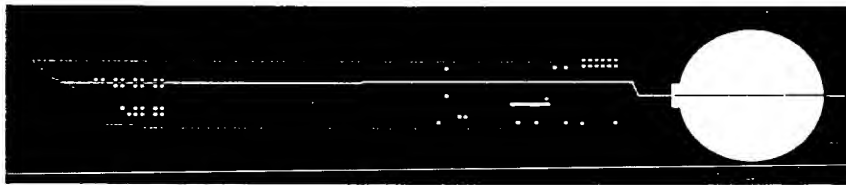


FIG. 40

Via 1 mask

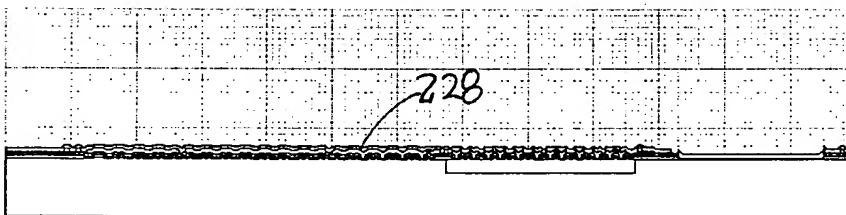


FIG. 41

Deposit ILD 2, etch vias

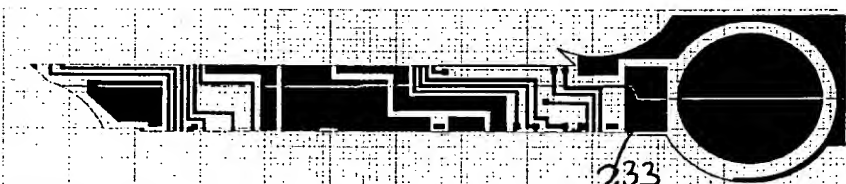


FIG. 42

Metal 2 mask

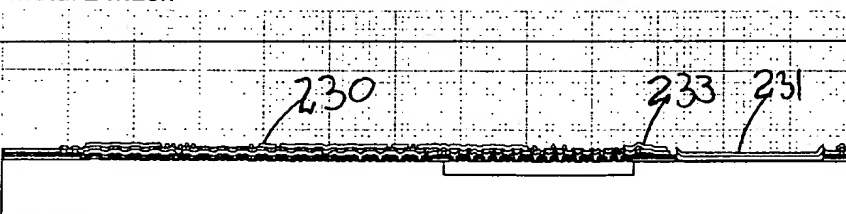


FIG. 43

Deposit metal 2

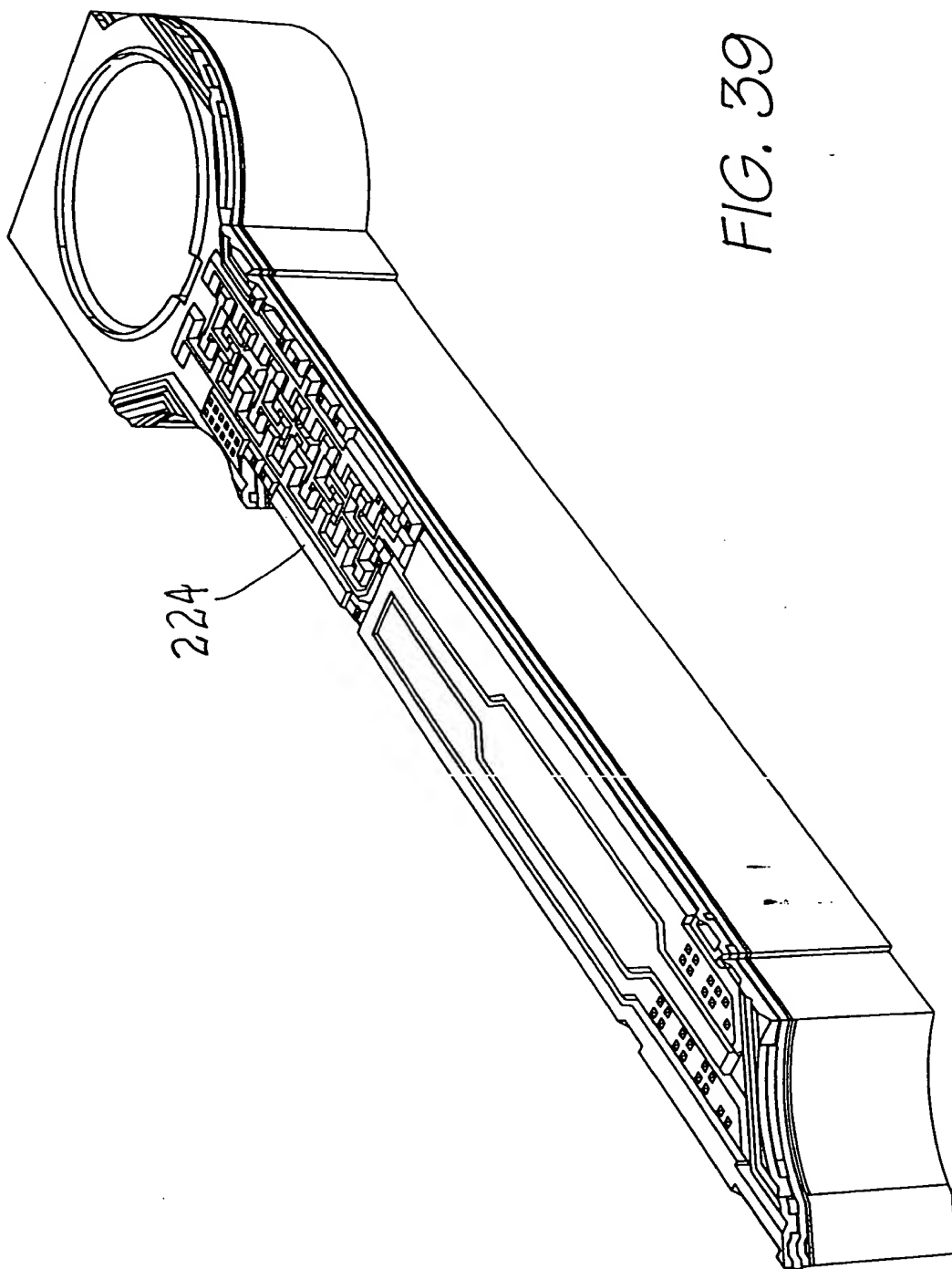


FIG. 39

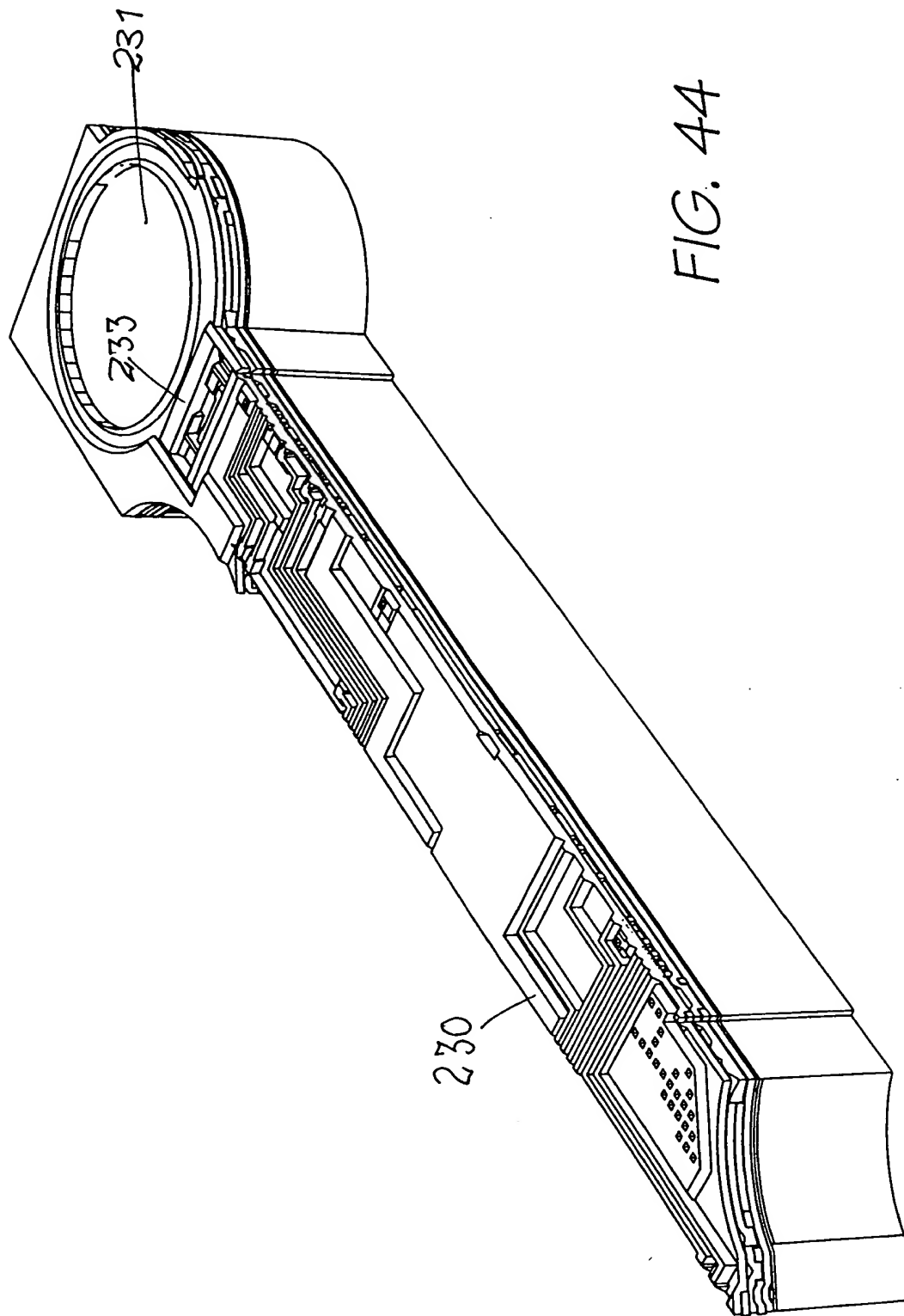


FIG. 44



FIG. 45

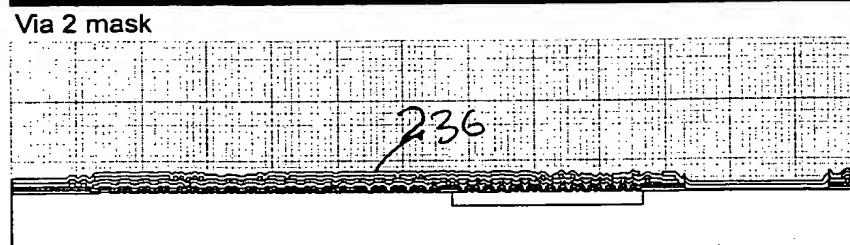


FIG. 46

Deposit ILD 3, etch vias

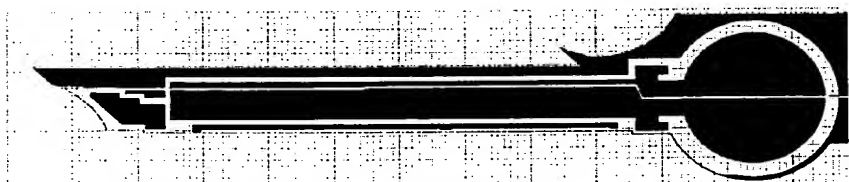


FIG. 47

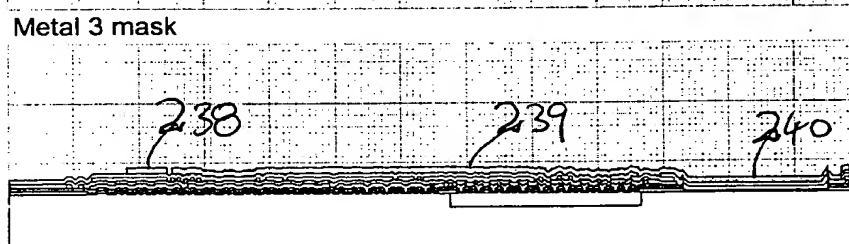


FIG. 48

Deposit metal 3



242

FIG. 50

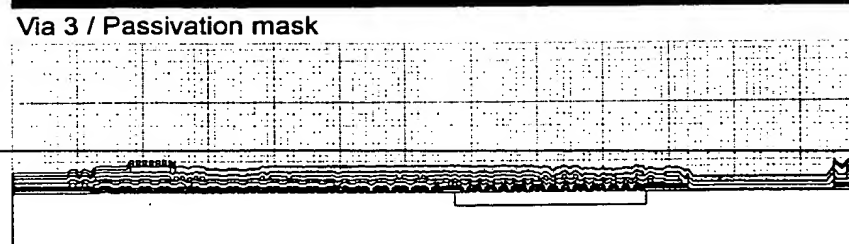


FIG. 51

Deposit passivation oxide & nitride, etch vias

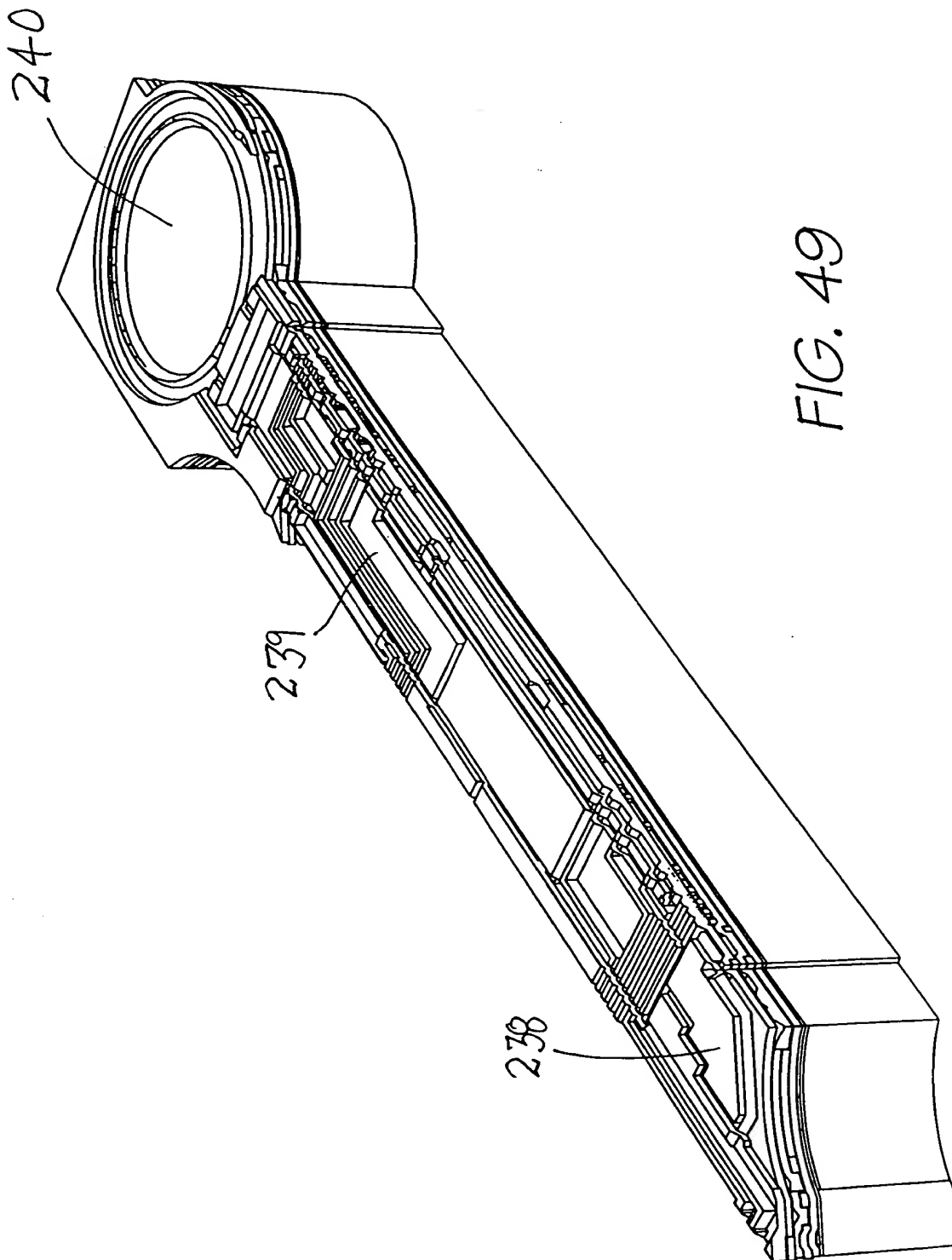


FIG. 49

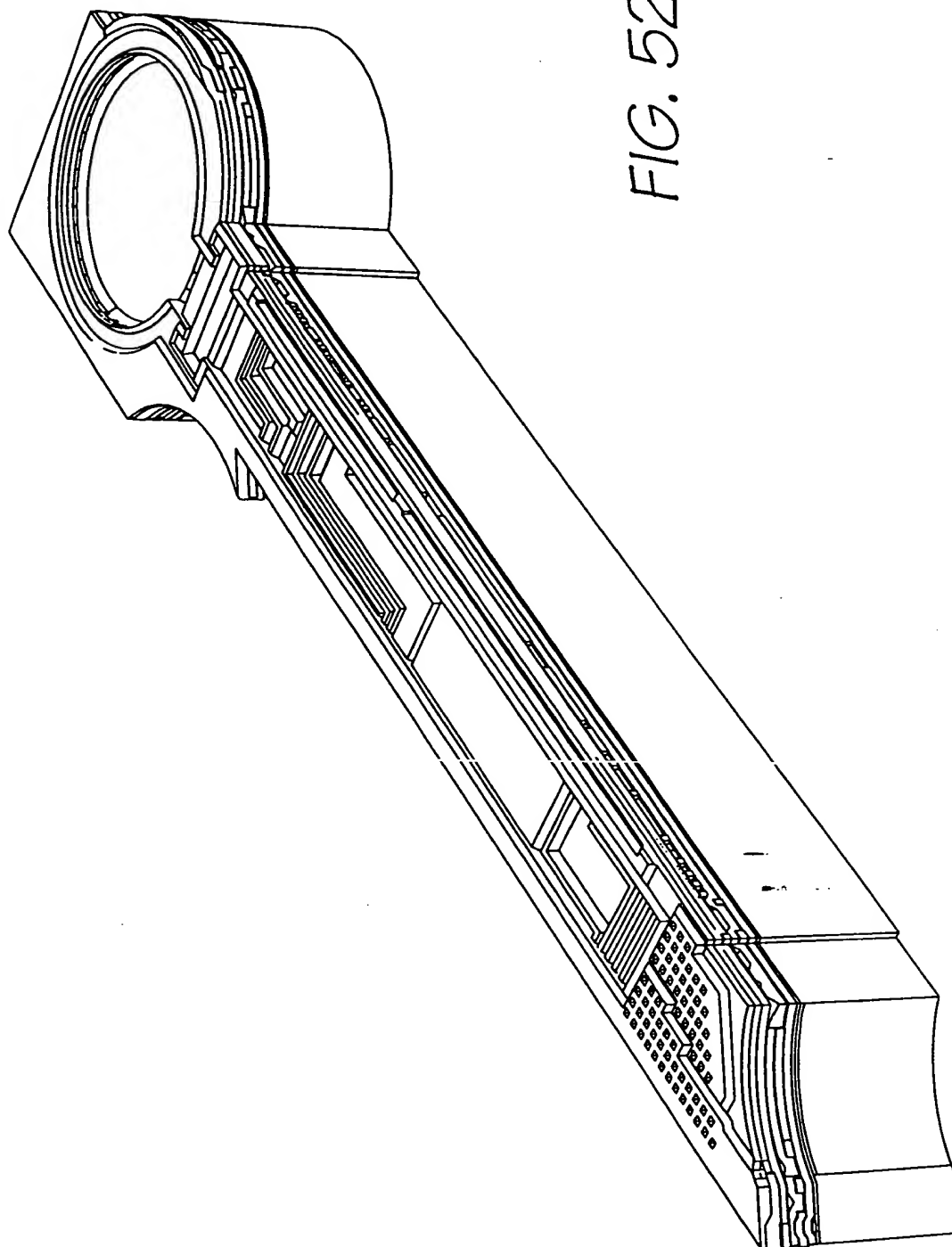


FIG. 52

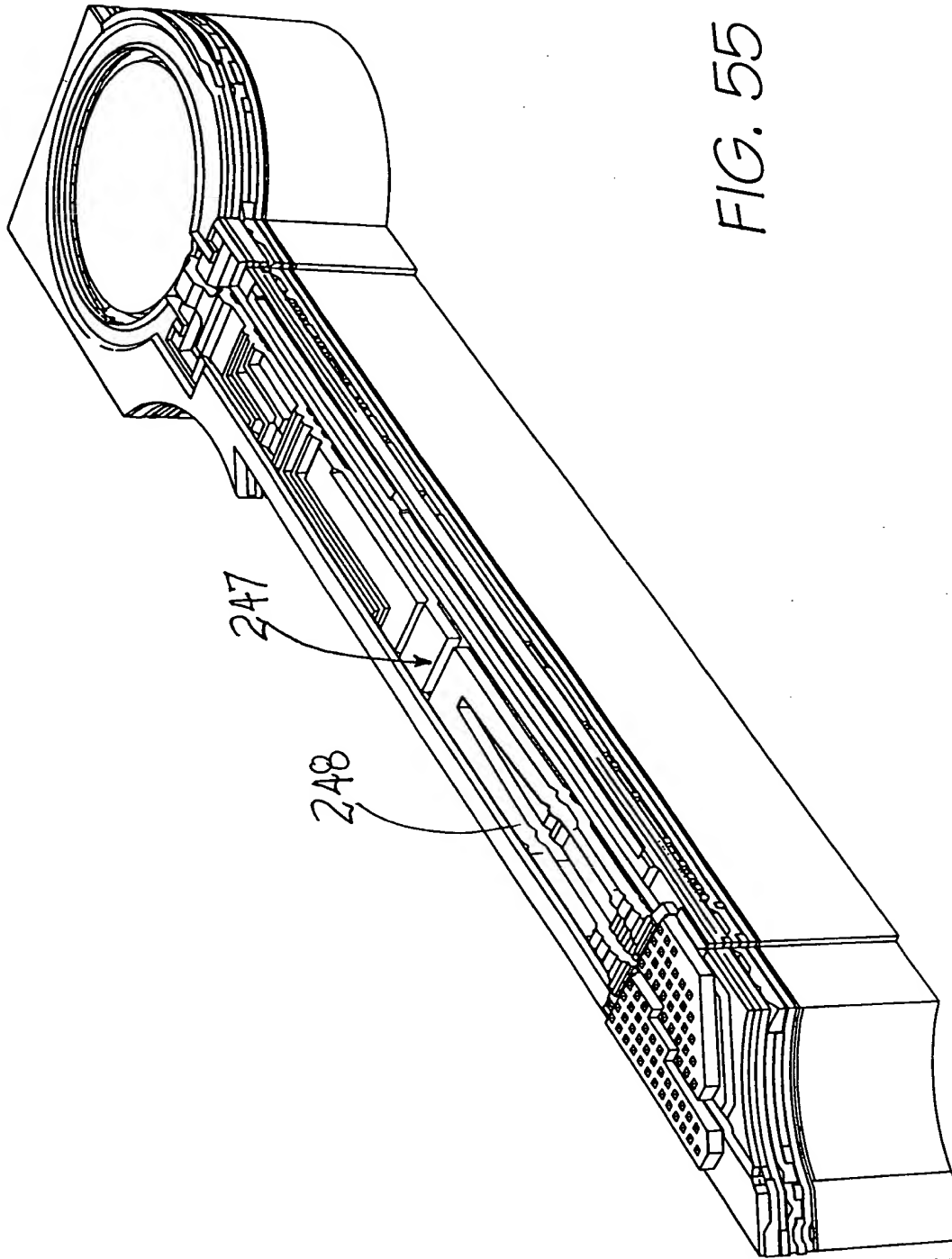


FIG. 55

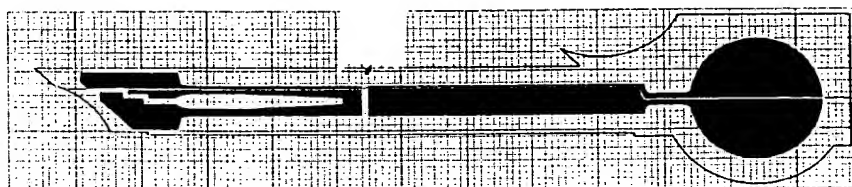


FIG. 53

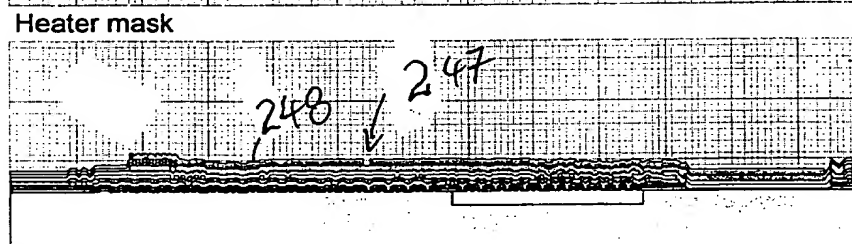


FIG. 54

Deposit heater TiN

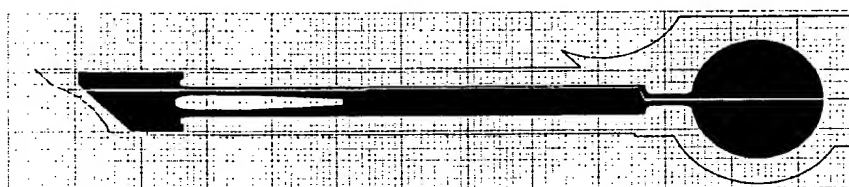


FIG. 56

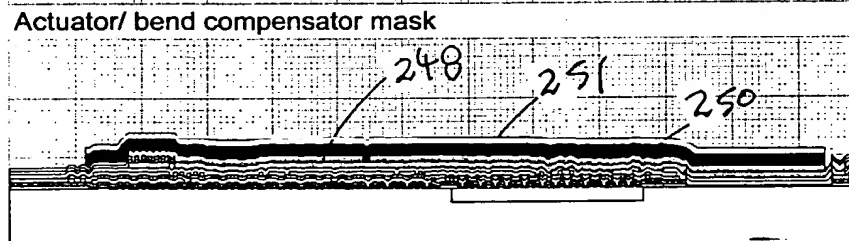


FIG. 57

Deposit actuator glass and bend compensator TiN, etch together

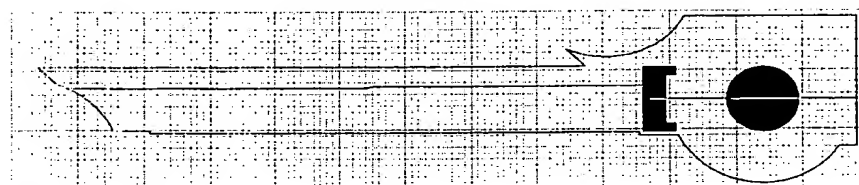
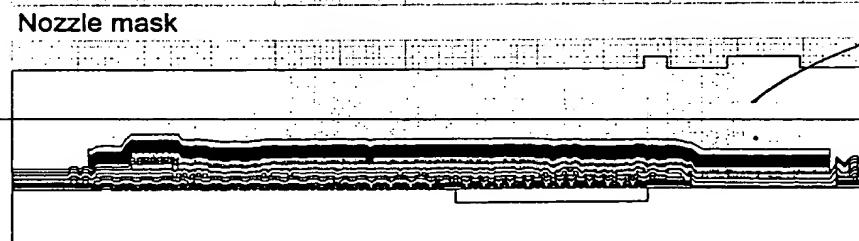


FIG. 59



254

FIG. 60

Deposit sacrificial layer, etch nozzles

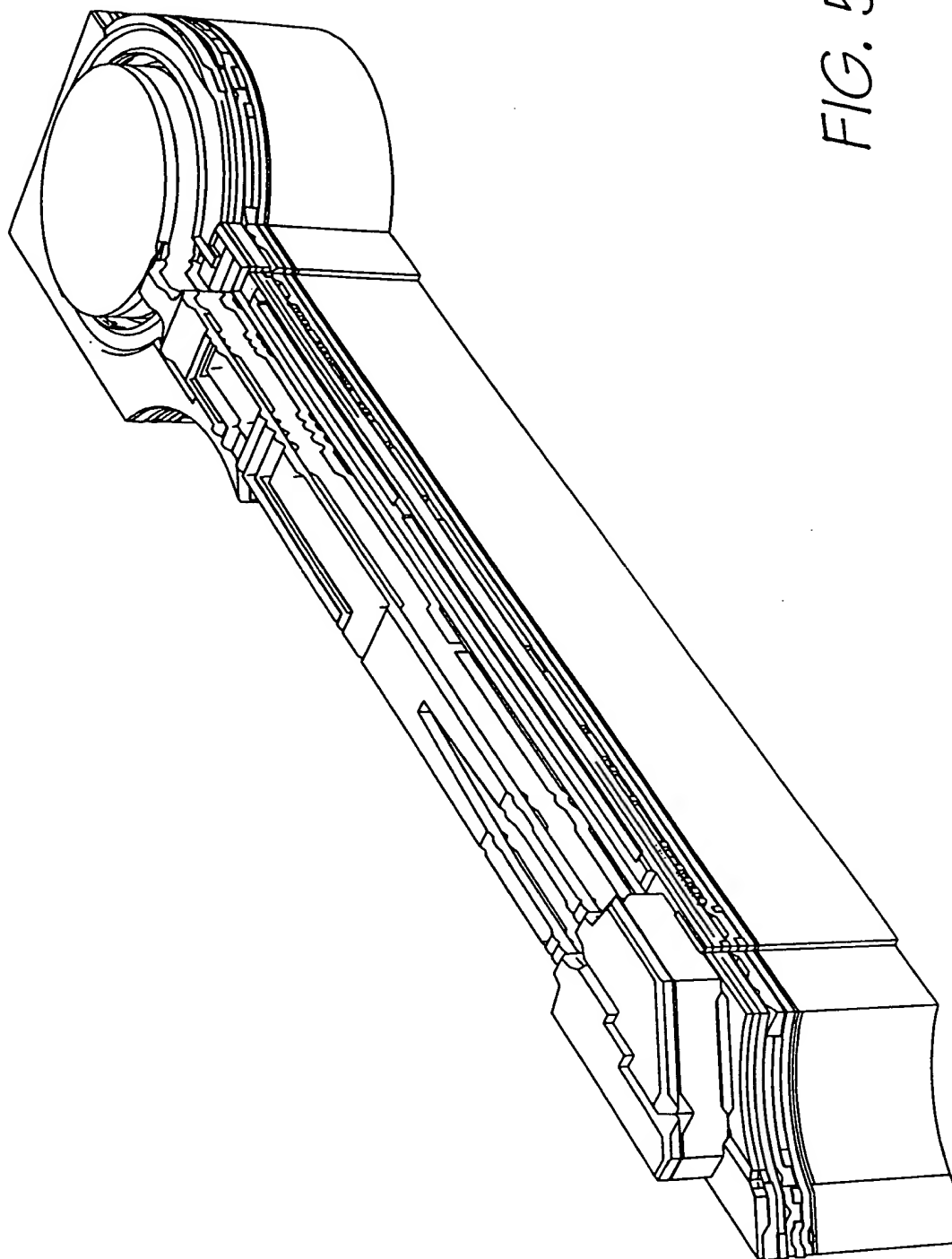


FIG. 58

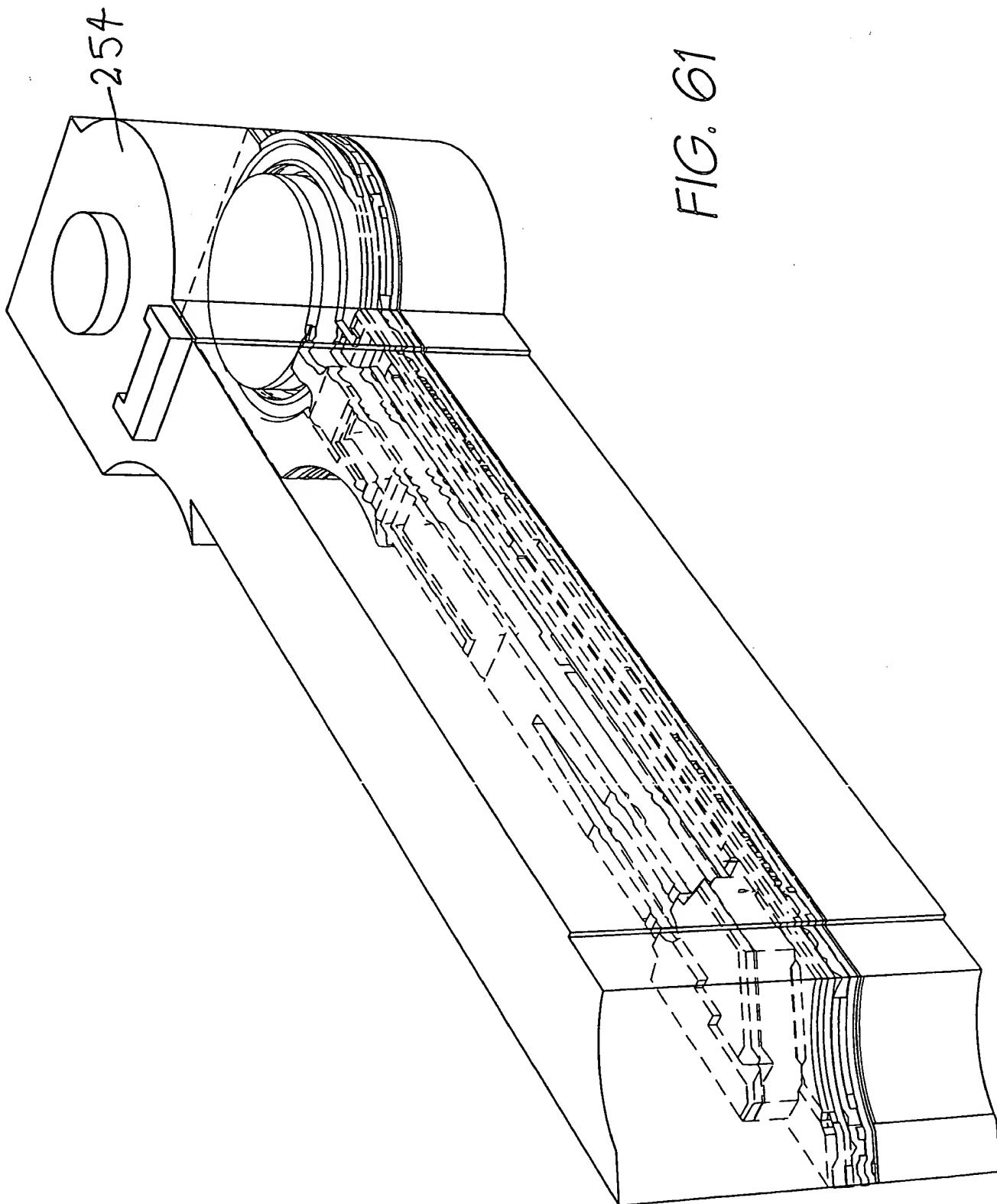


FIG. 61

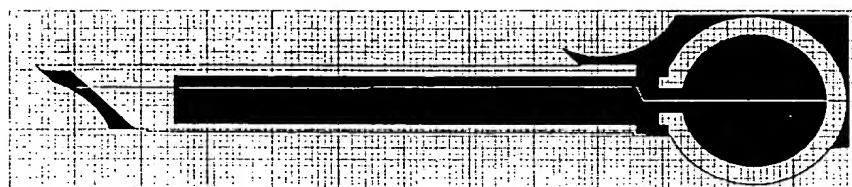
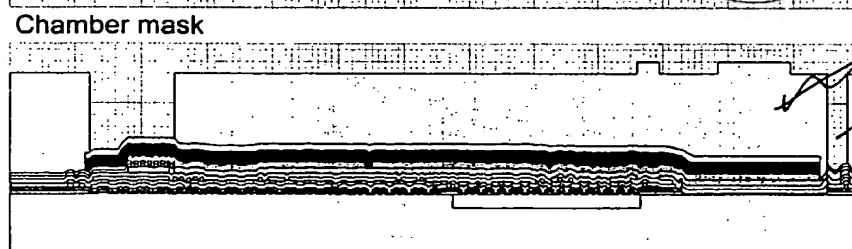


FIG. 62

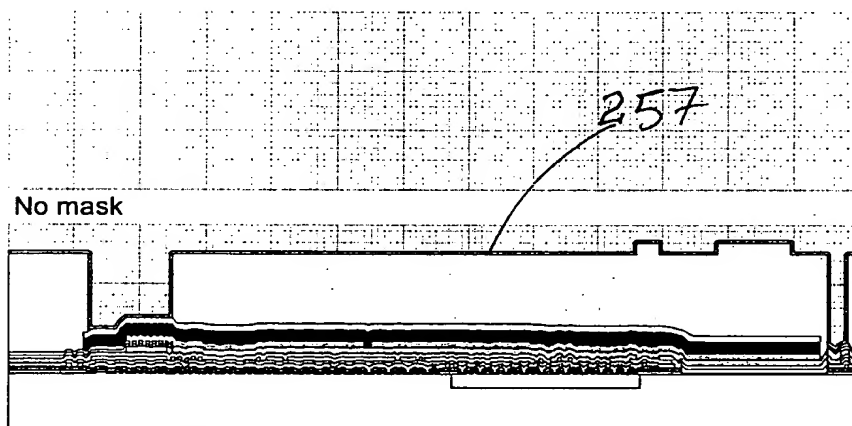


Chamber mask

Etch chambers in sacrificial layer

255

FIG. 63

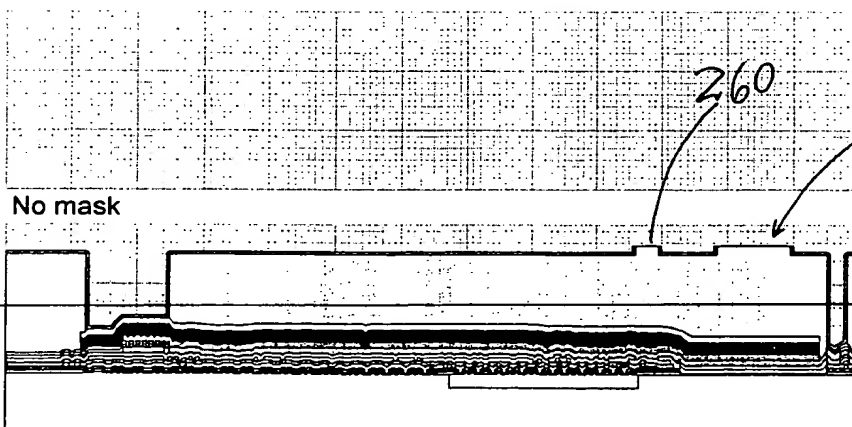


No mask

Deposit chamber walls

257

FIG. 65



No mask

Form self-aligned nozzles using CMP

260

259

FIG. 67

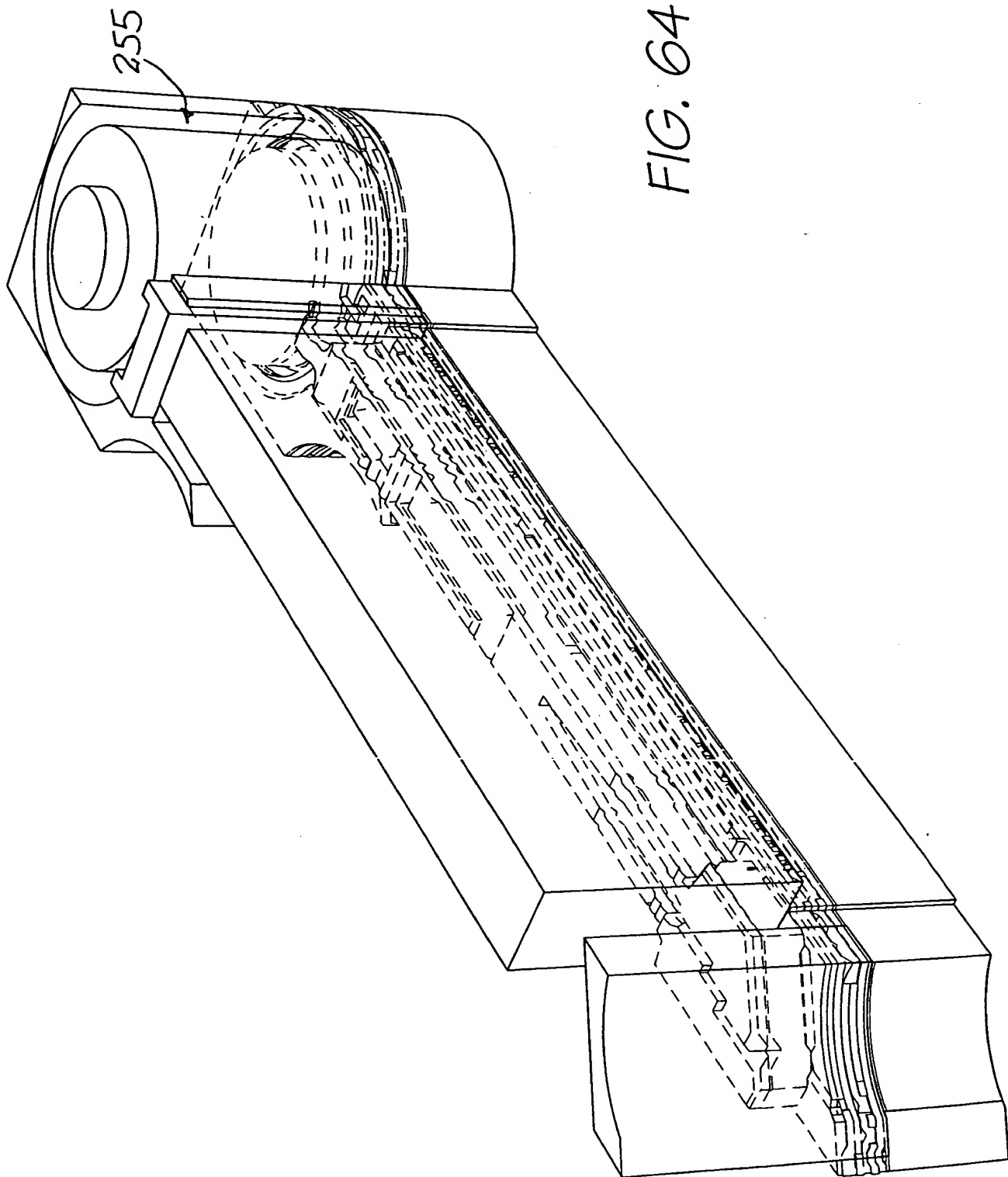


FIG. 64

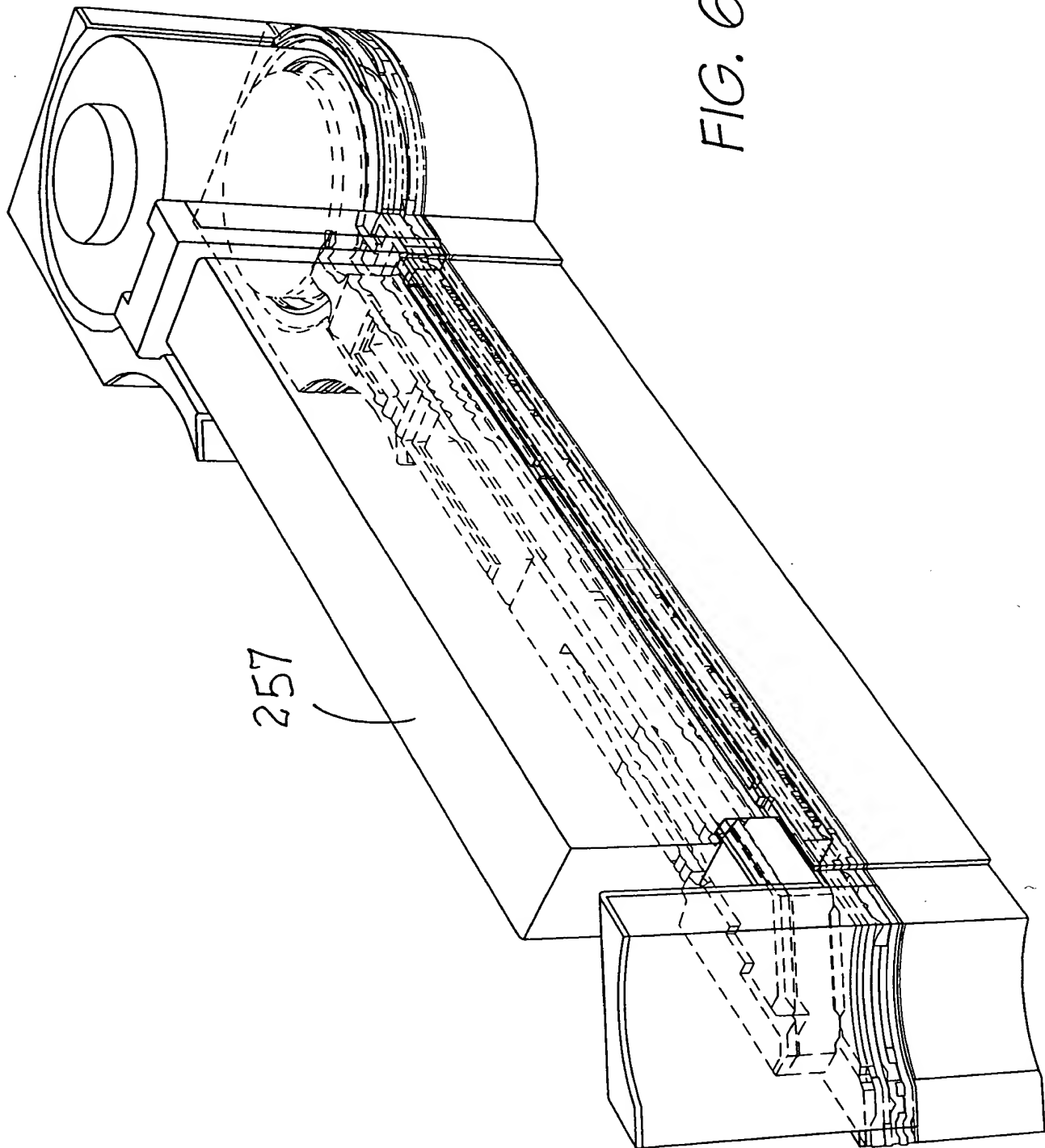


FIG. 66

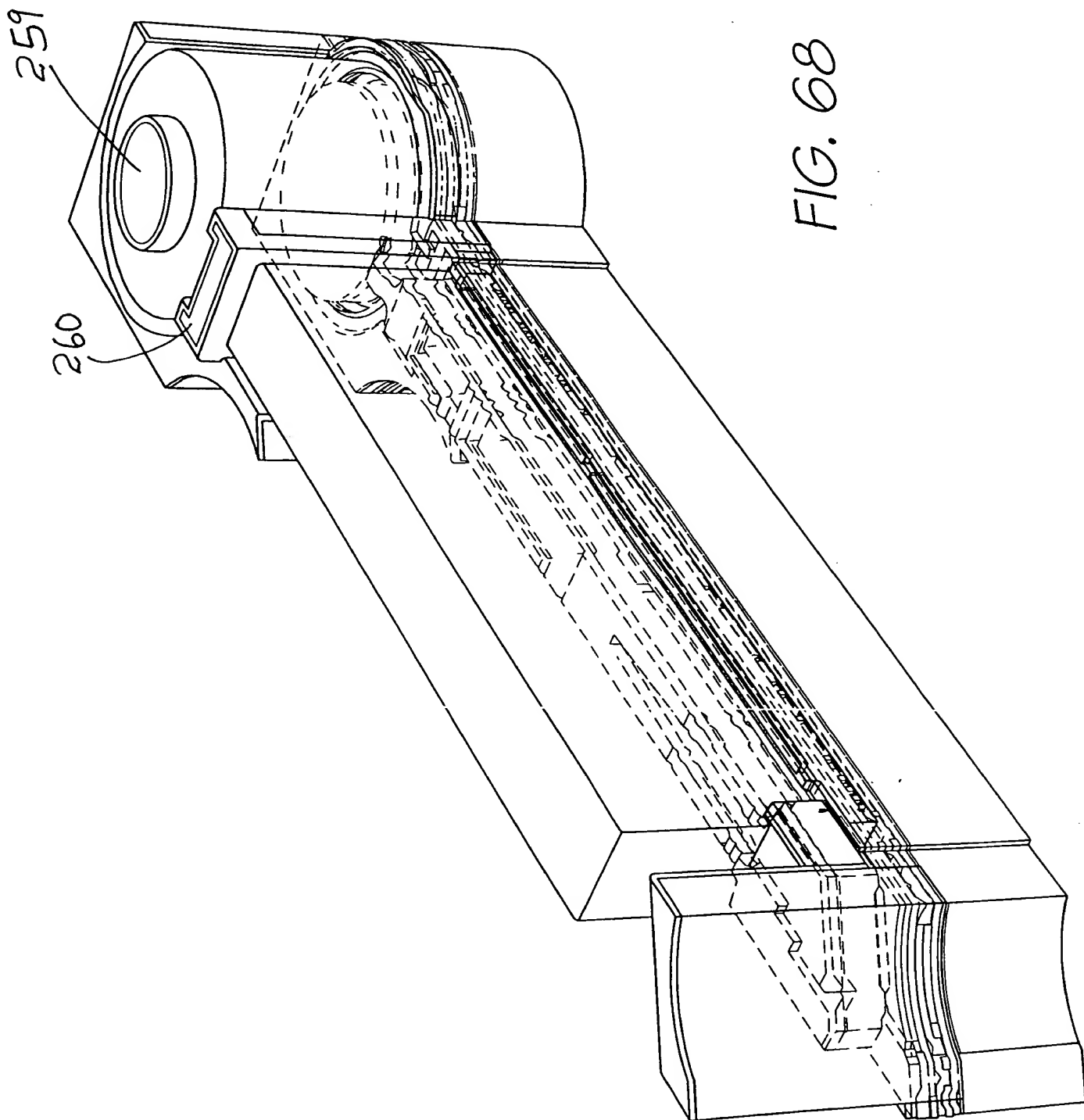


FIG. 68

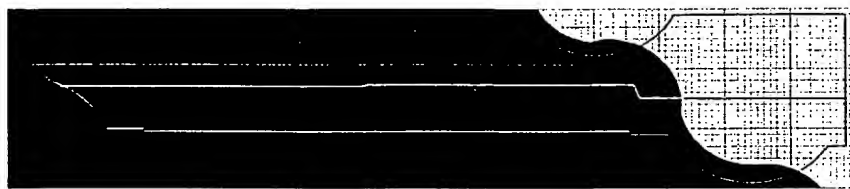
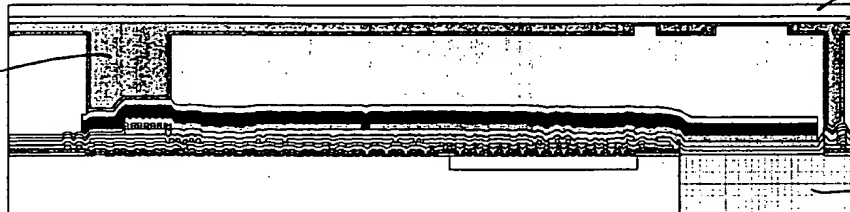


FIG. 70

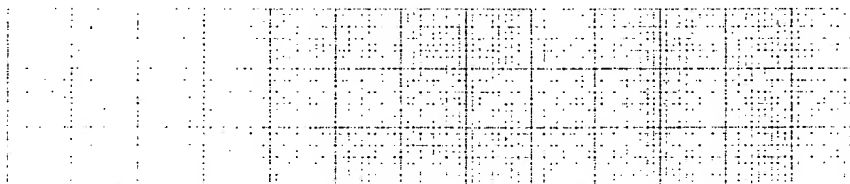
Back-etch inlet mask



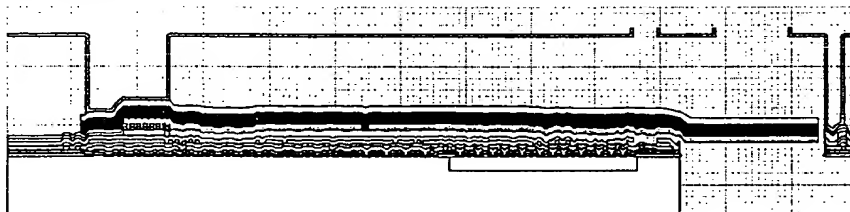
262
263

FIG. 69

Mount on wafer blank, back-etch inlets

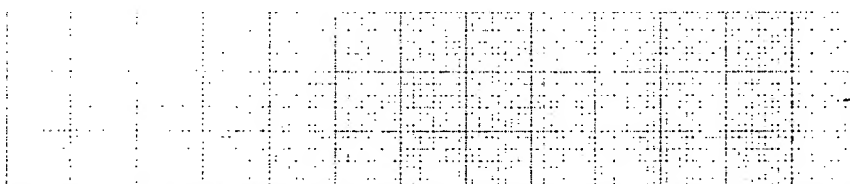


No Mask

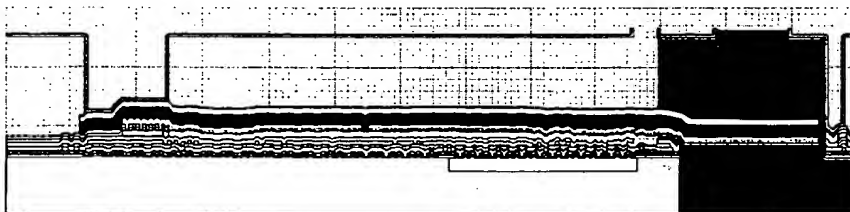


Detach from wafer blank, etch sacrificial material

FIG. 71



No Mask



Package, fill with ink, test

FIG. 74

268

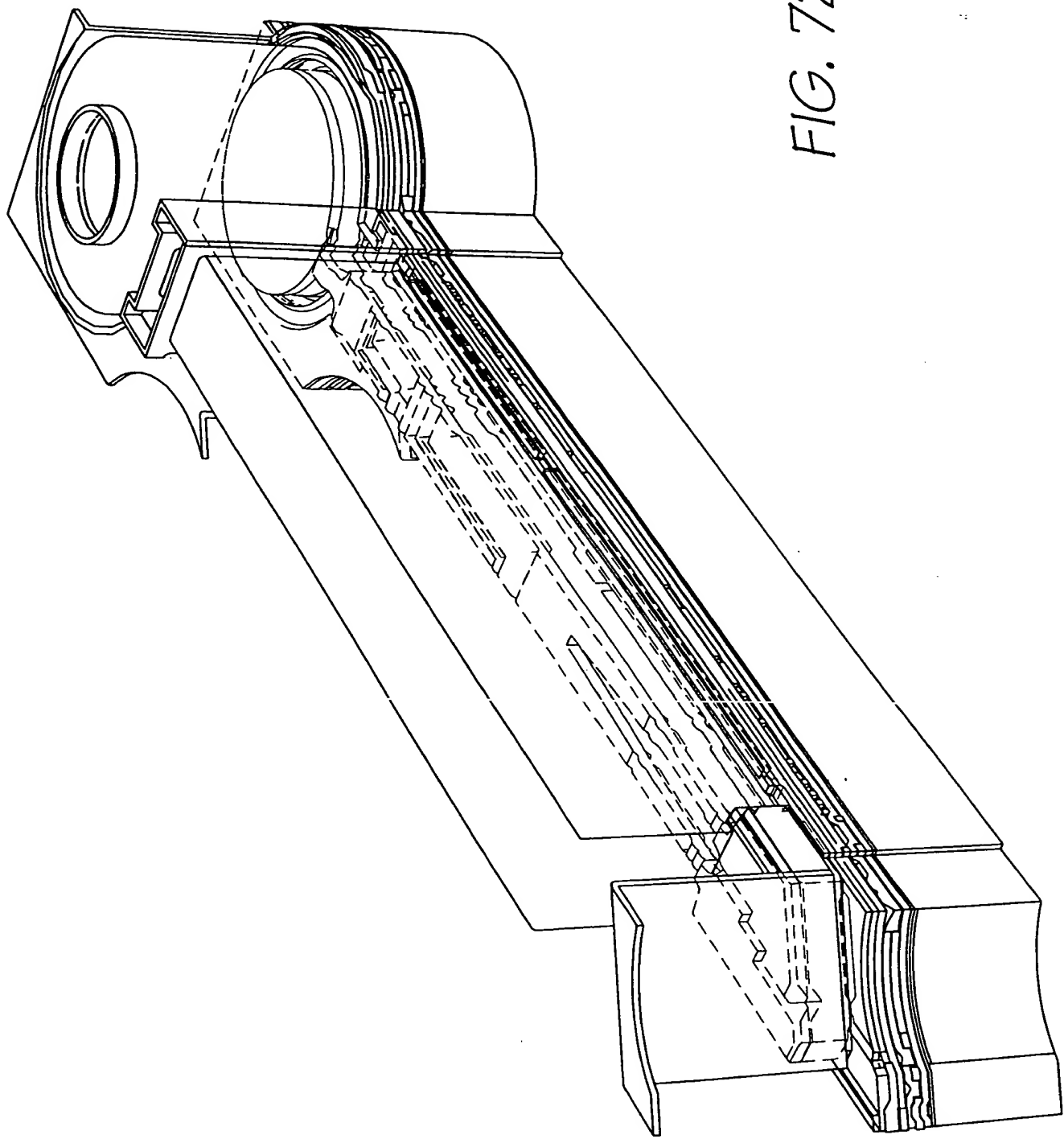
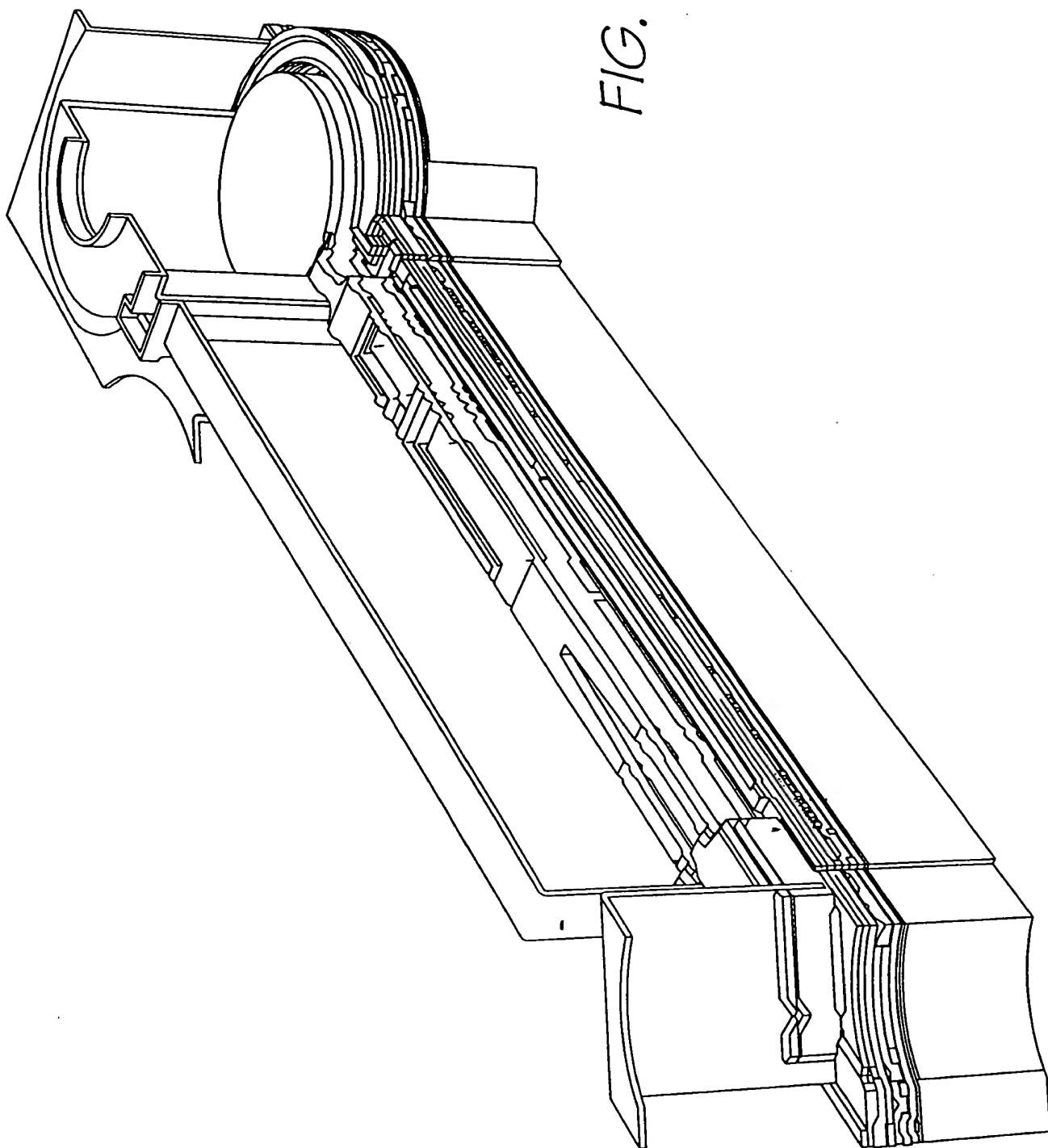


FIG. 72

FIG. 73



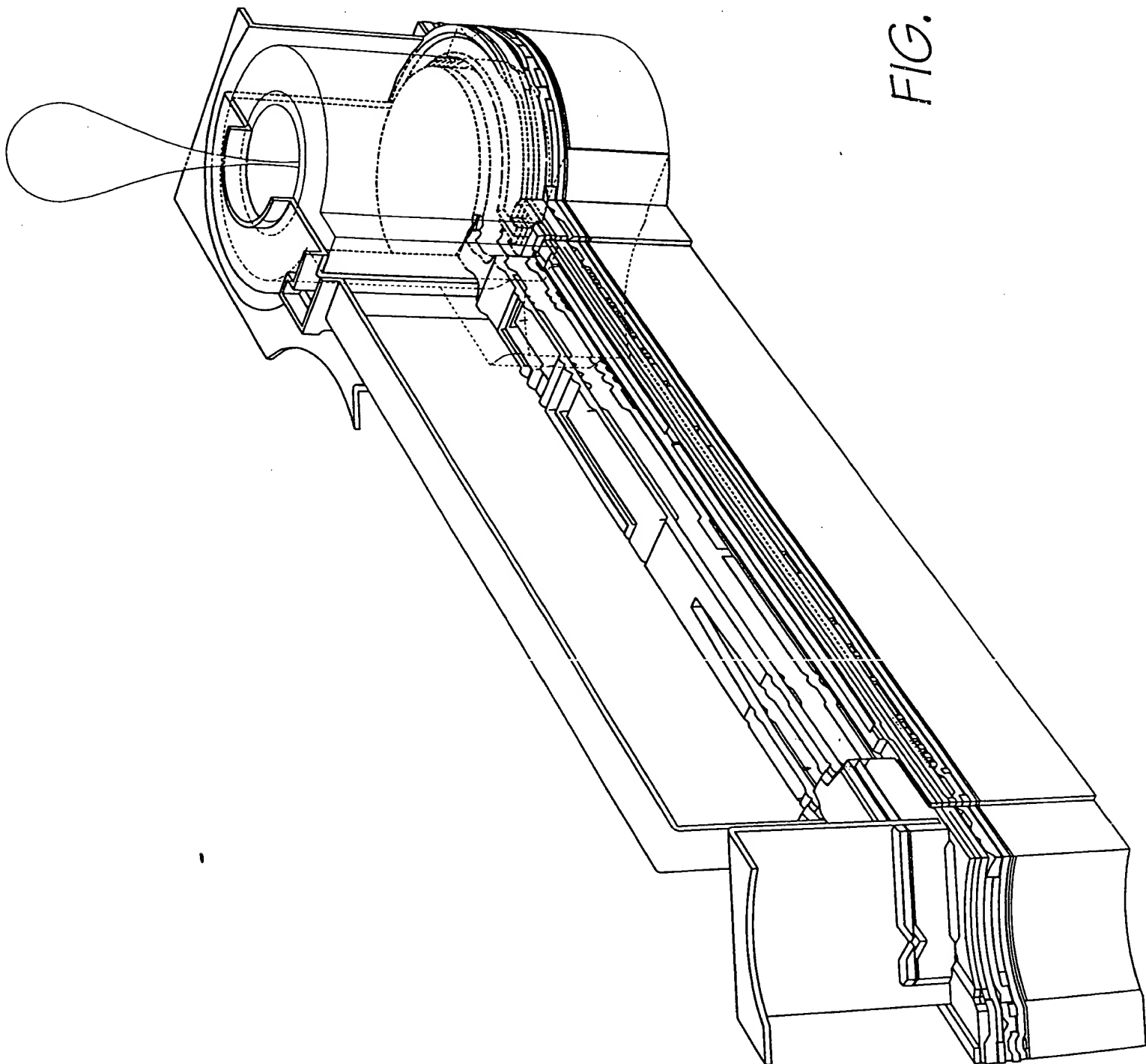


FIG. 75

280

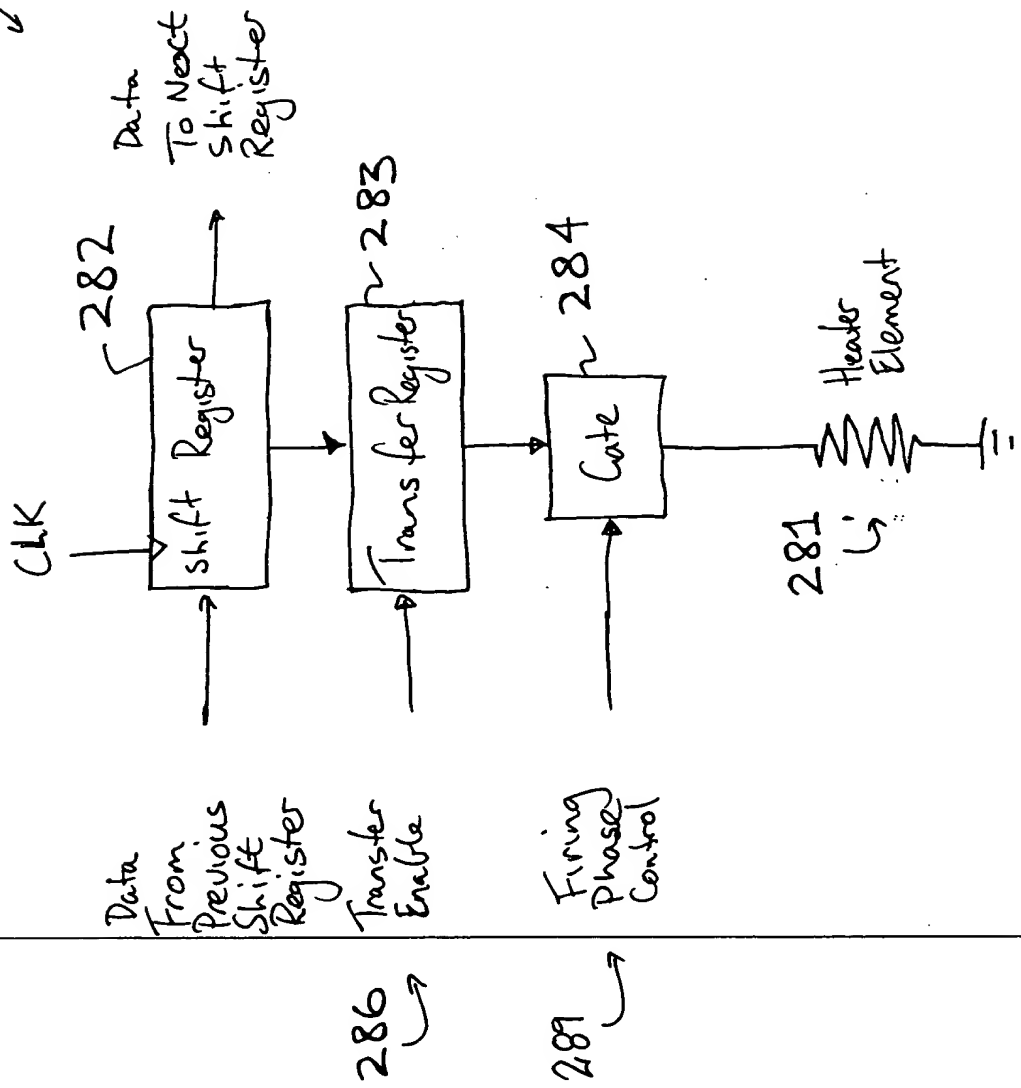


FIG. 76

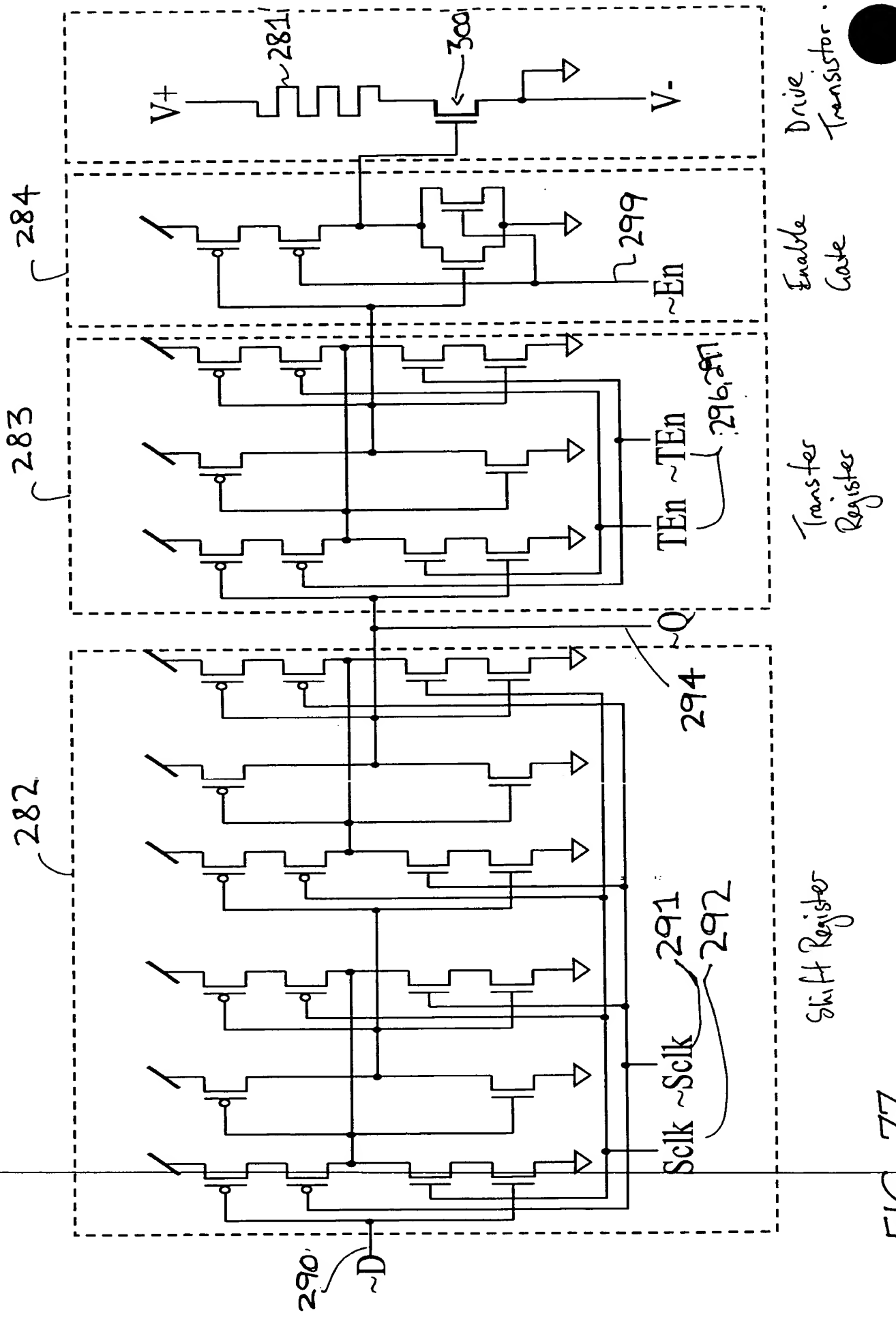


FIG. 77

KEY









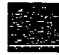





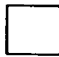









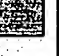

	Silicon		Poly		Via 2		Actuator TiN		Cyan Ink
	N-Well		Contacts		Metal 3		Actuator Glass		Magenta Ink
	Active		Metal 1		Via 3		Compensator TiN		Yellow Ink
	p+		Via 1				Sacrificial		Floor
	n+		Metal 2				Sacrificial-nozzle		Wall
									Roof
									Rim
									Shroud

FIG. 78

Shift Register Transfer Enable Register Gate Drive Transistor

306

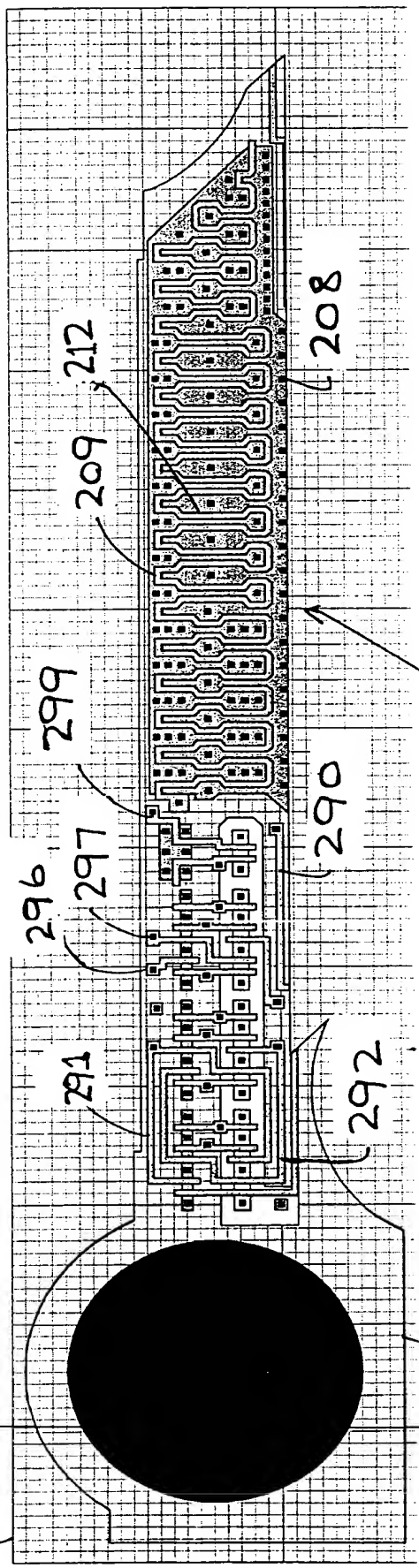


FIG. 79

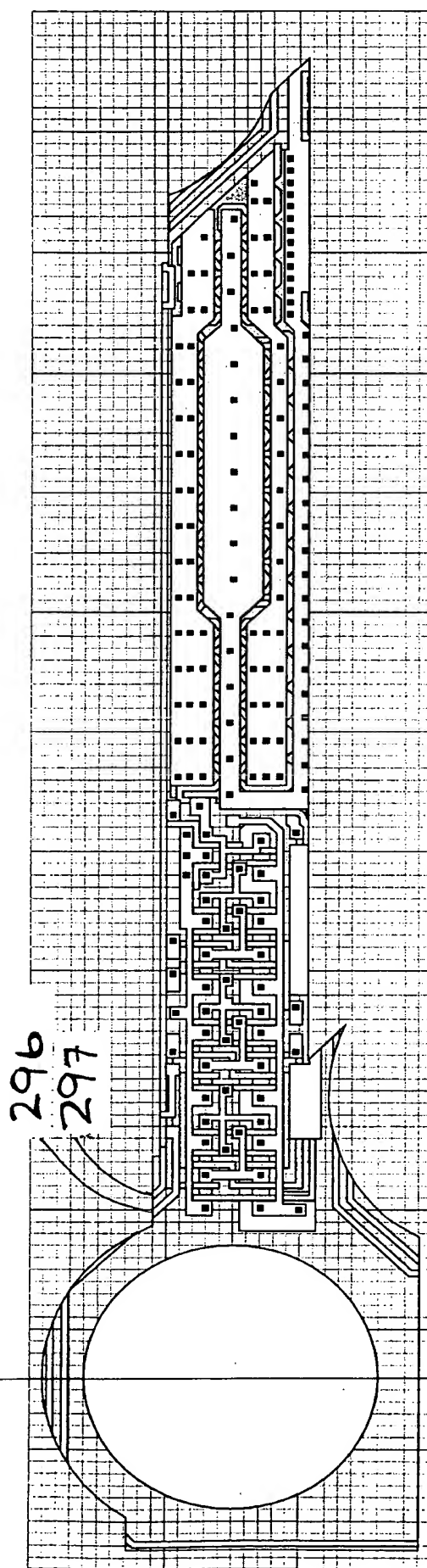


FIG. 80

330 331

294 291

292

290 291 296 297

328

326

325

324

322

321

323

297

296

291

290

292

291

296

297

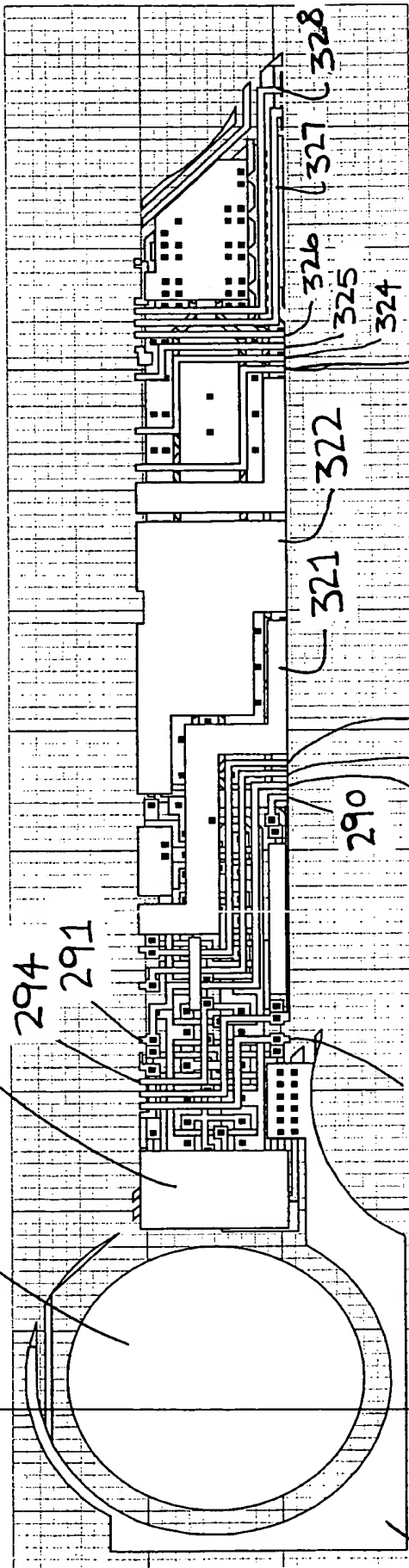
290

291

296

297

FIG. 81



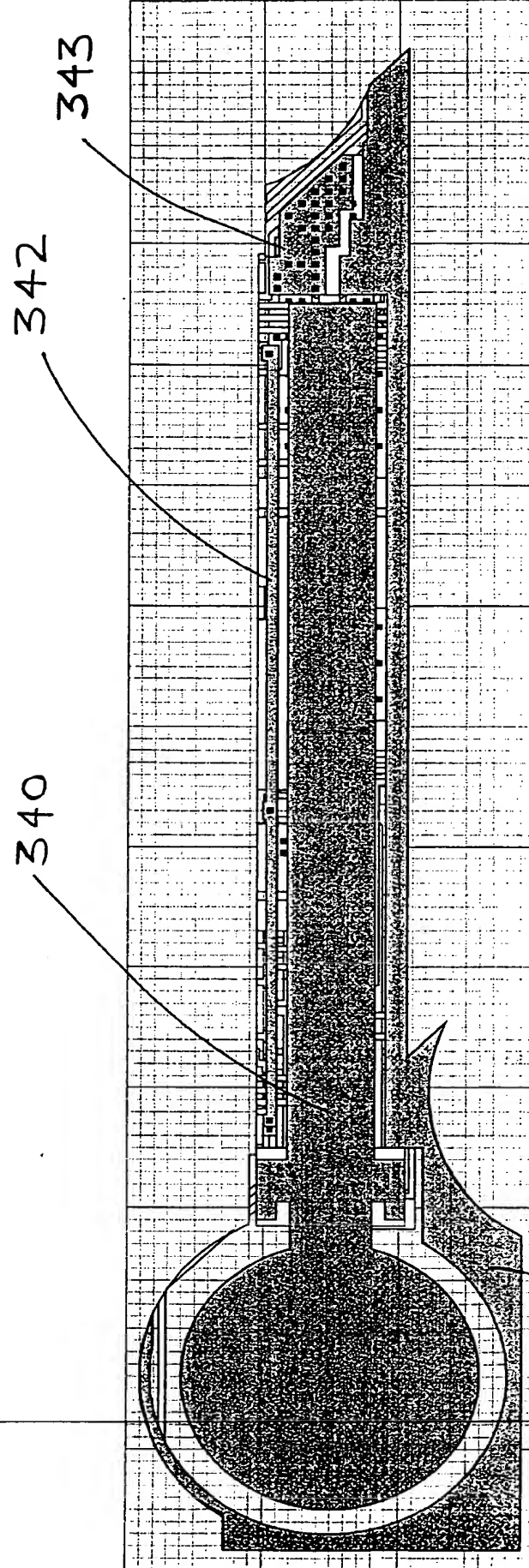


FIG. 82

341

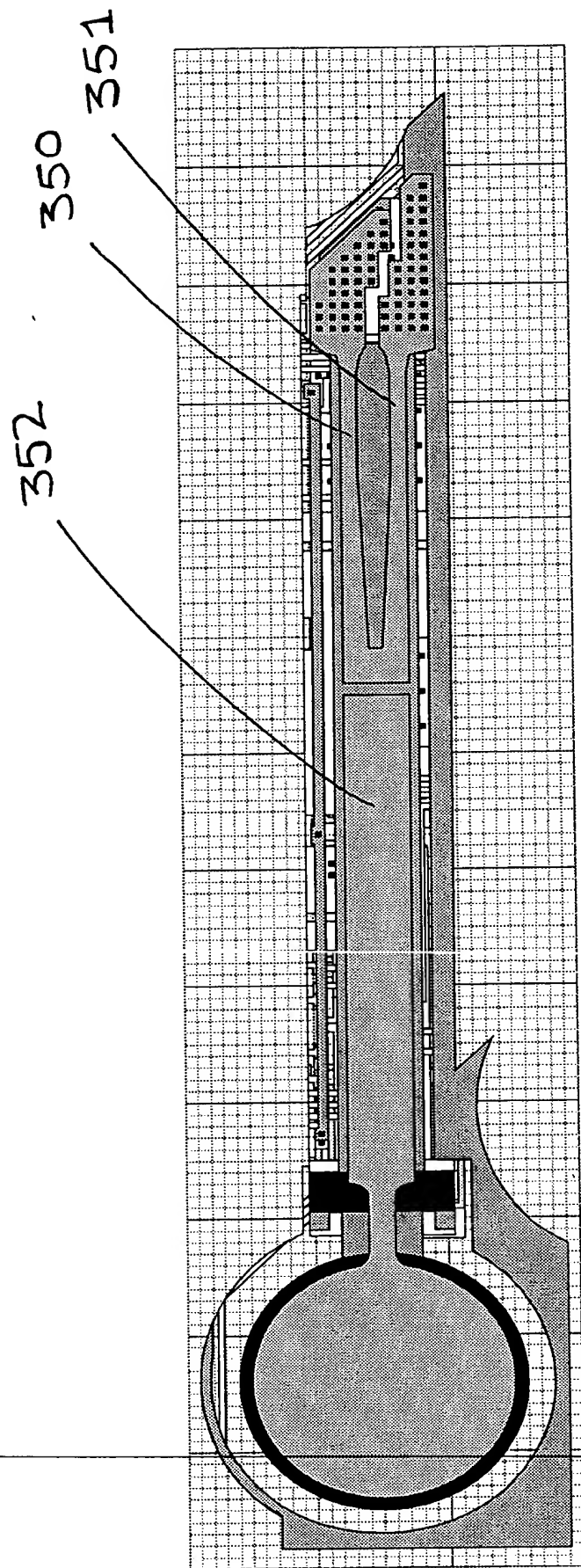


FIG. 83

350

351

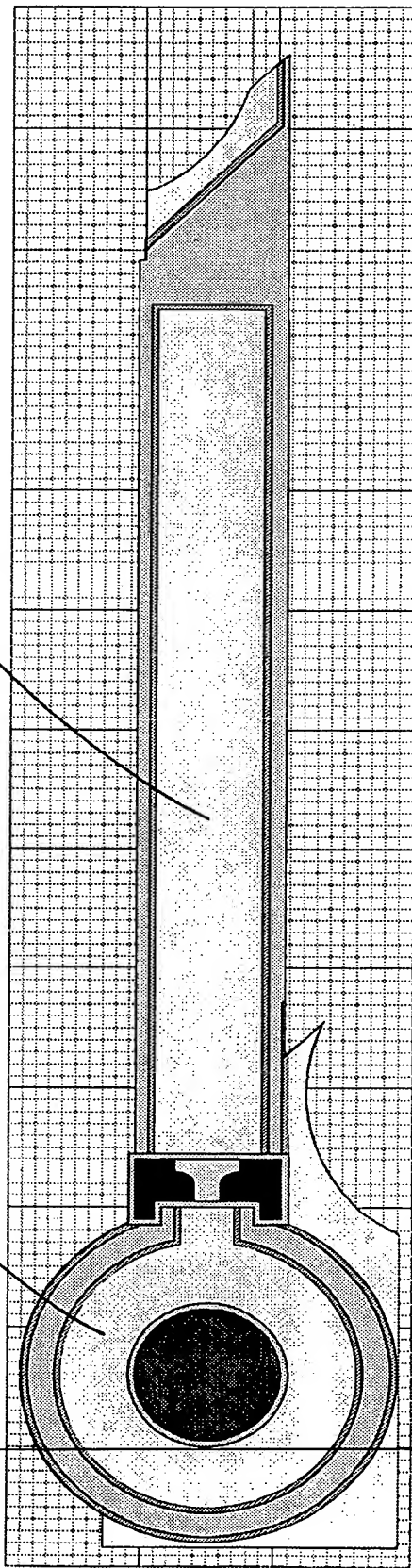


FIG. 84

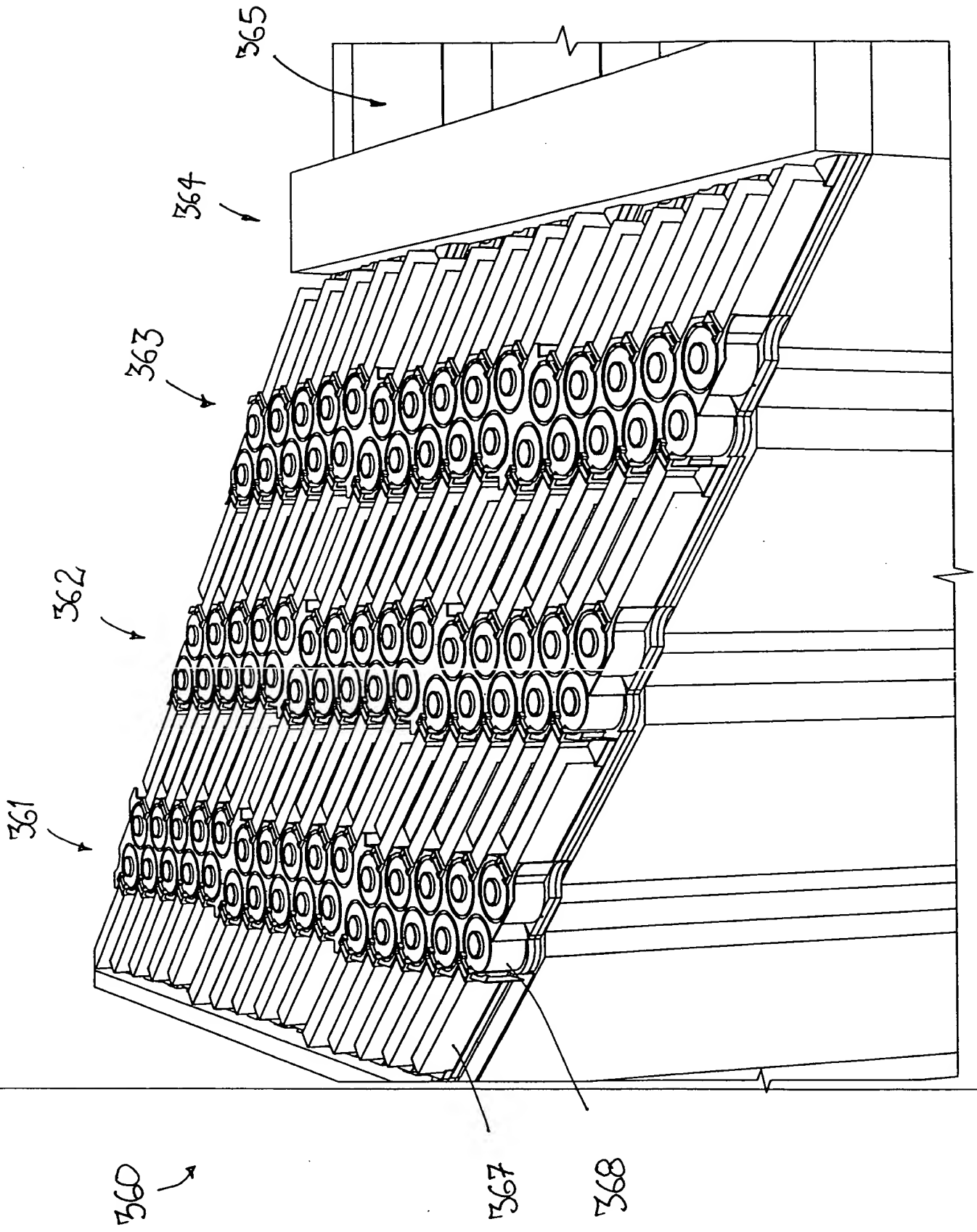
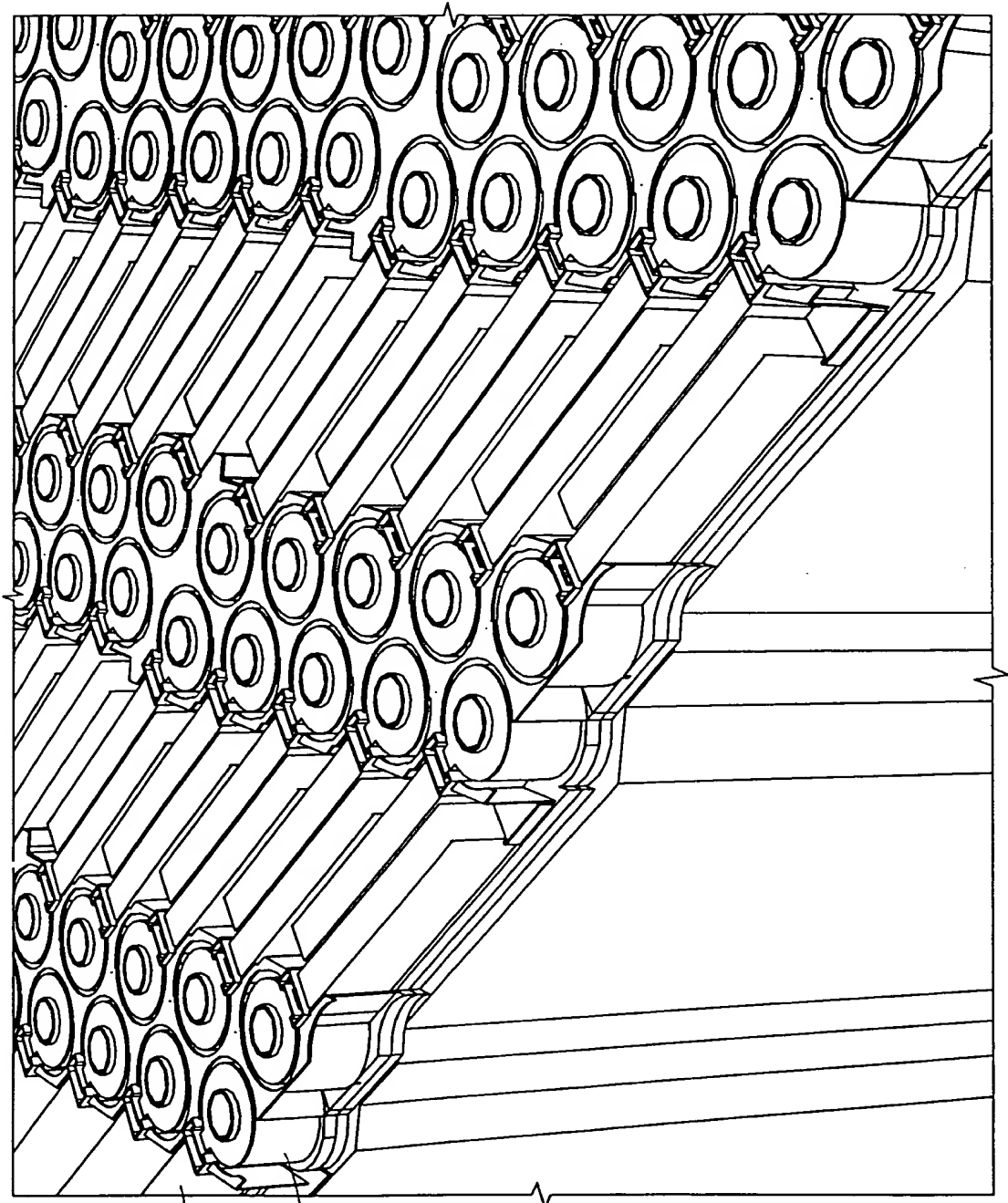


FIG. 85



367

368

FIG. 86

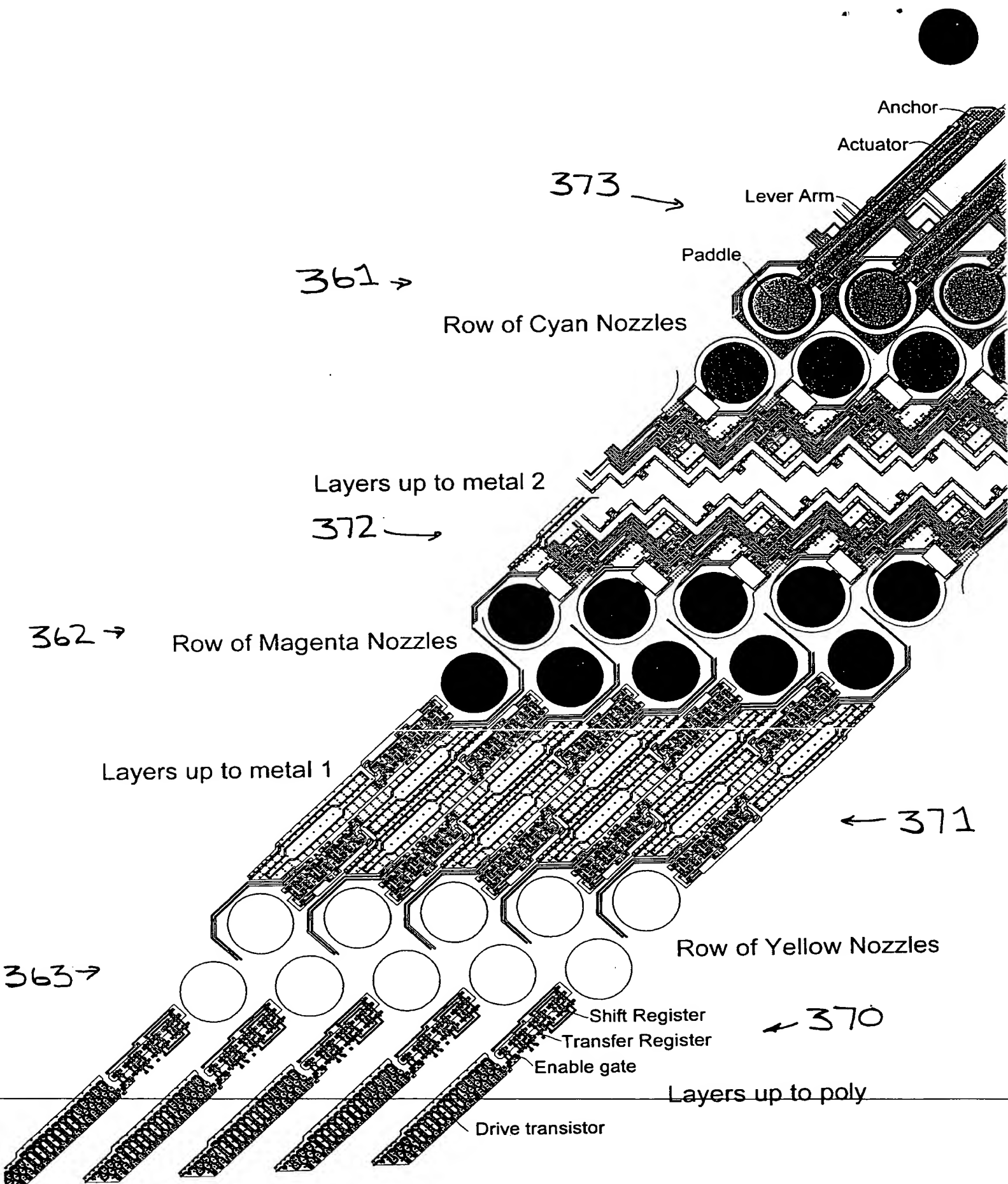


FIG. 87

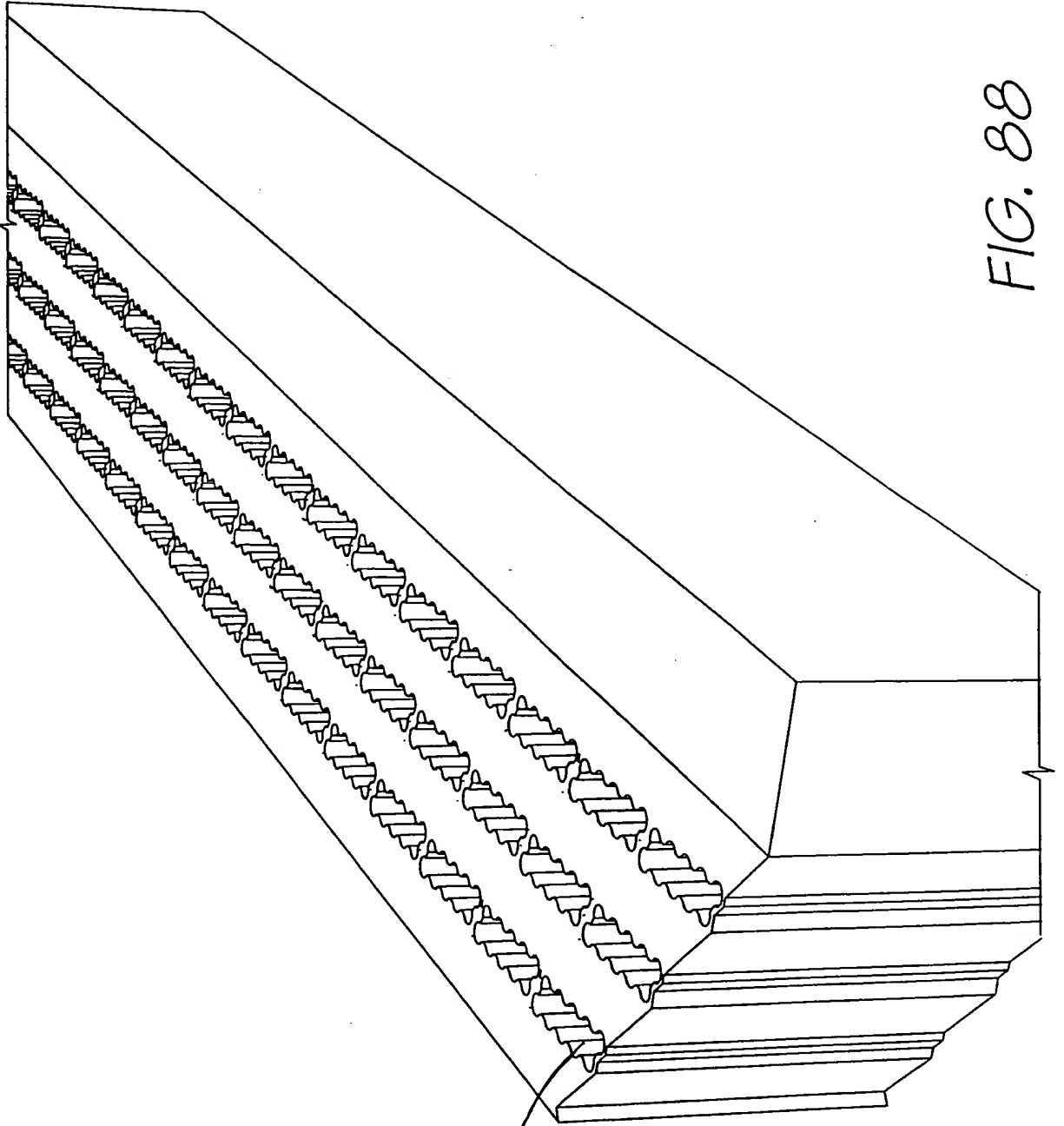


FIG. 88

380

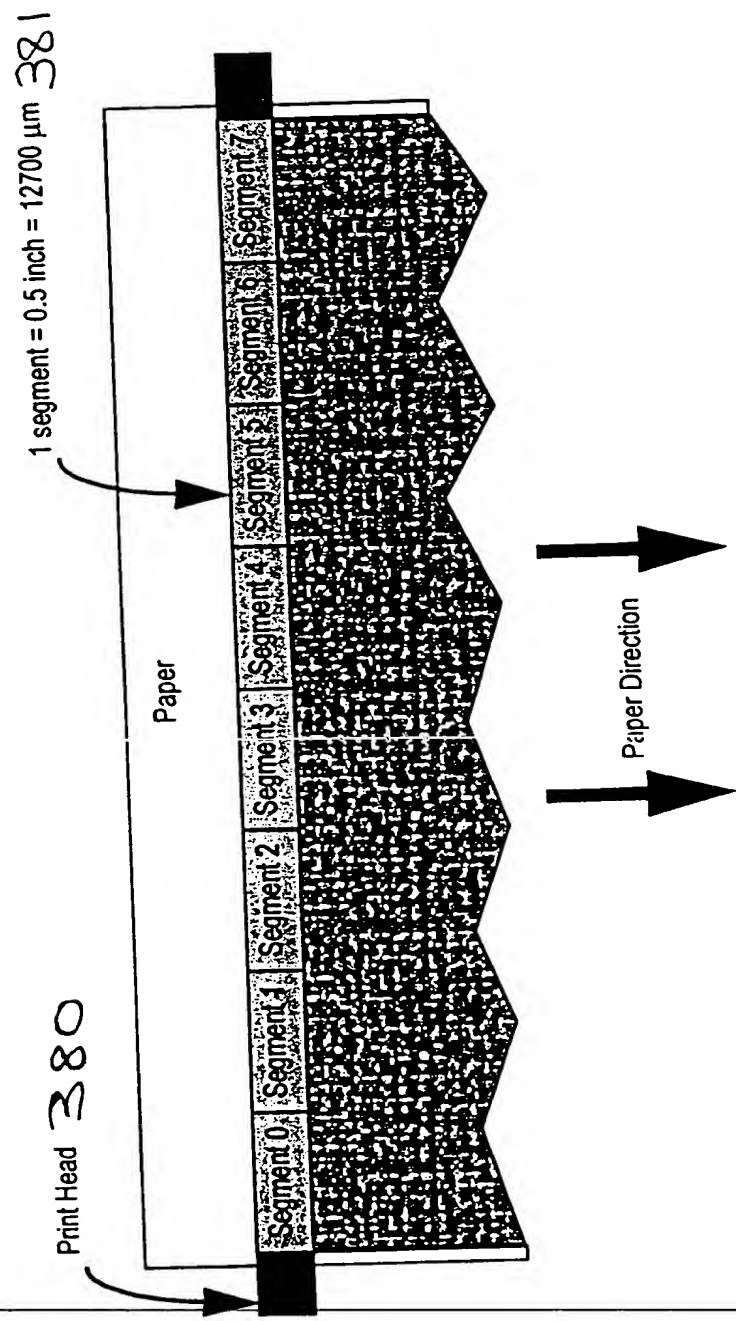


FIG. 89

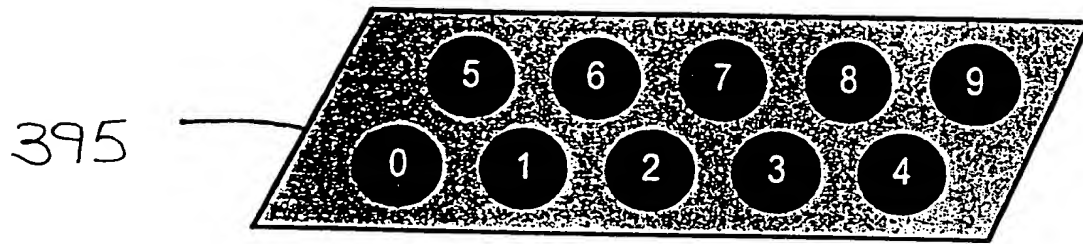


FIG. 90

Figure 3. A single pod, numbered by firing order

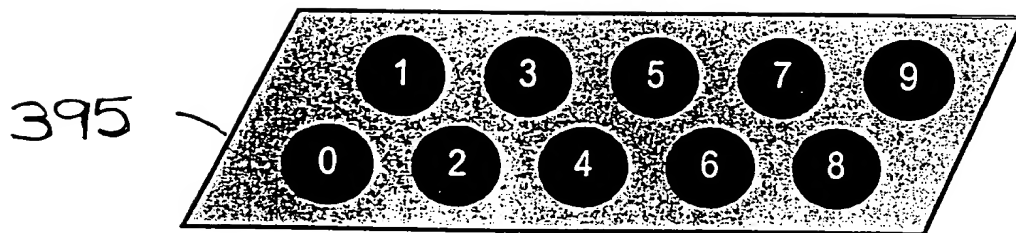


FIG. 91

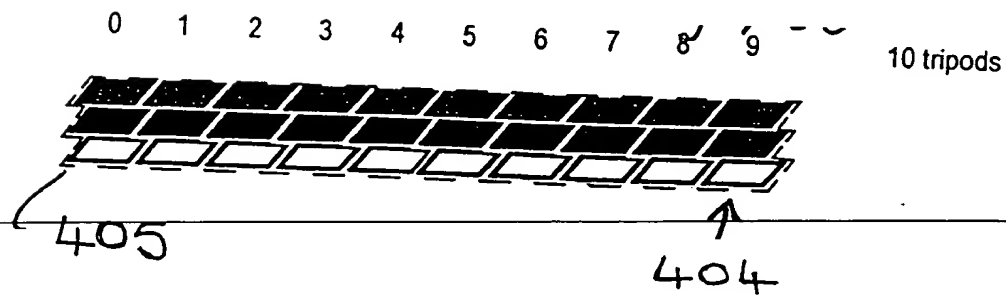


FIG. 93

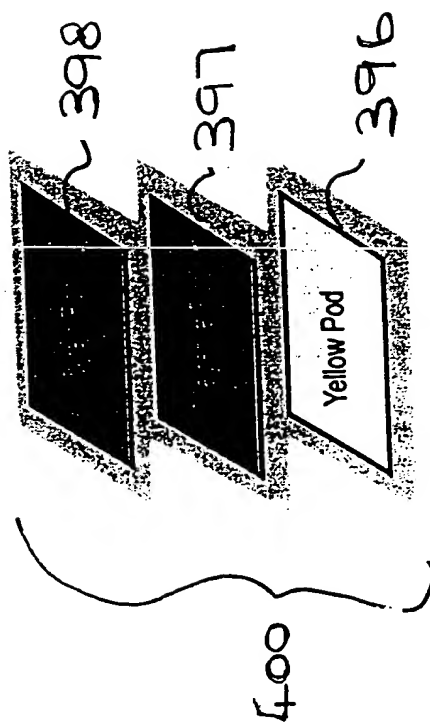


FIG. 92

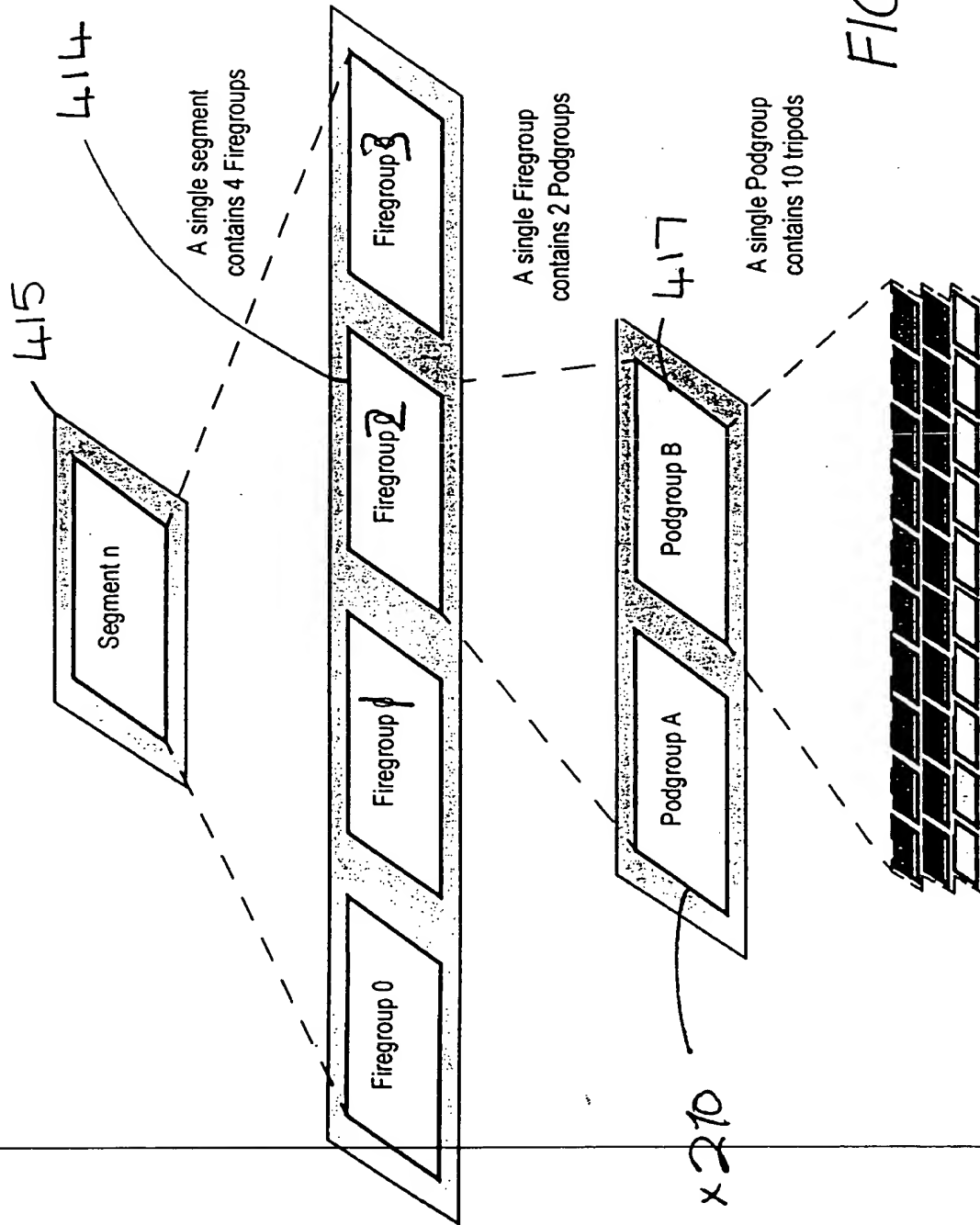


FIG. 94

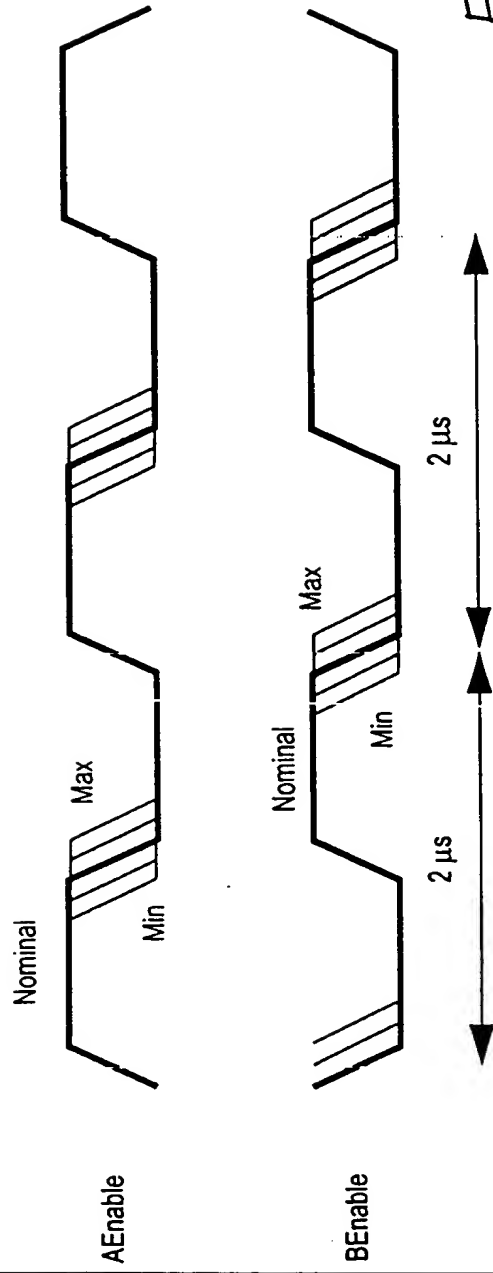


FIG. 95

Figure 8. AEnable and BEnable during a Typical Print Cycle

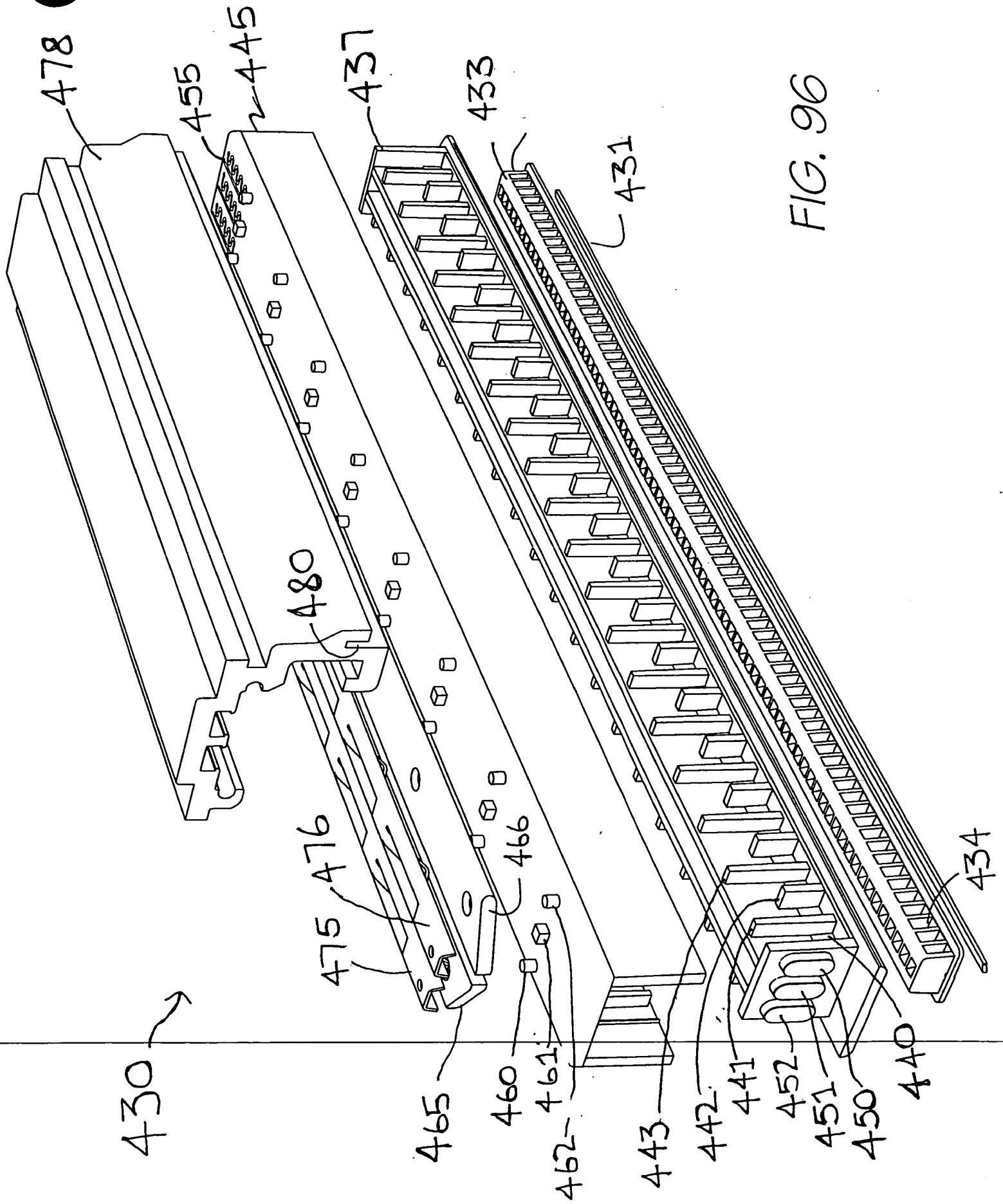


FIG. 96

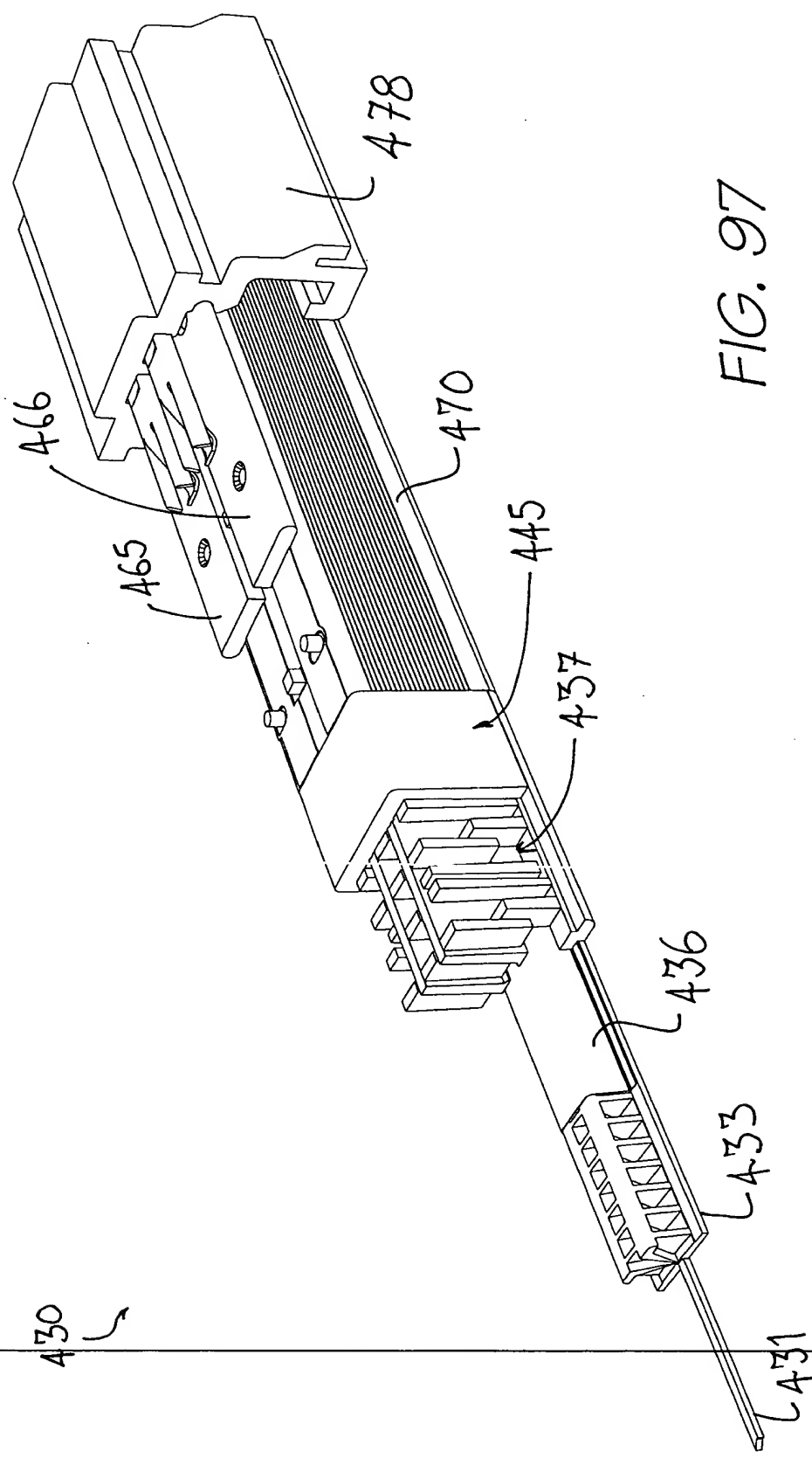


FIG. 97

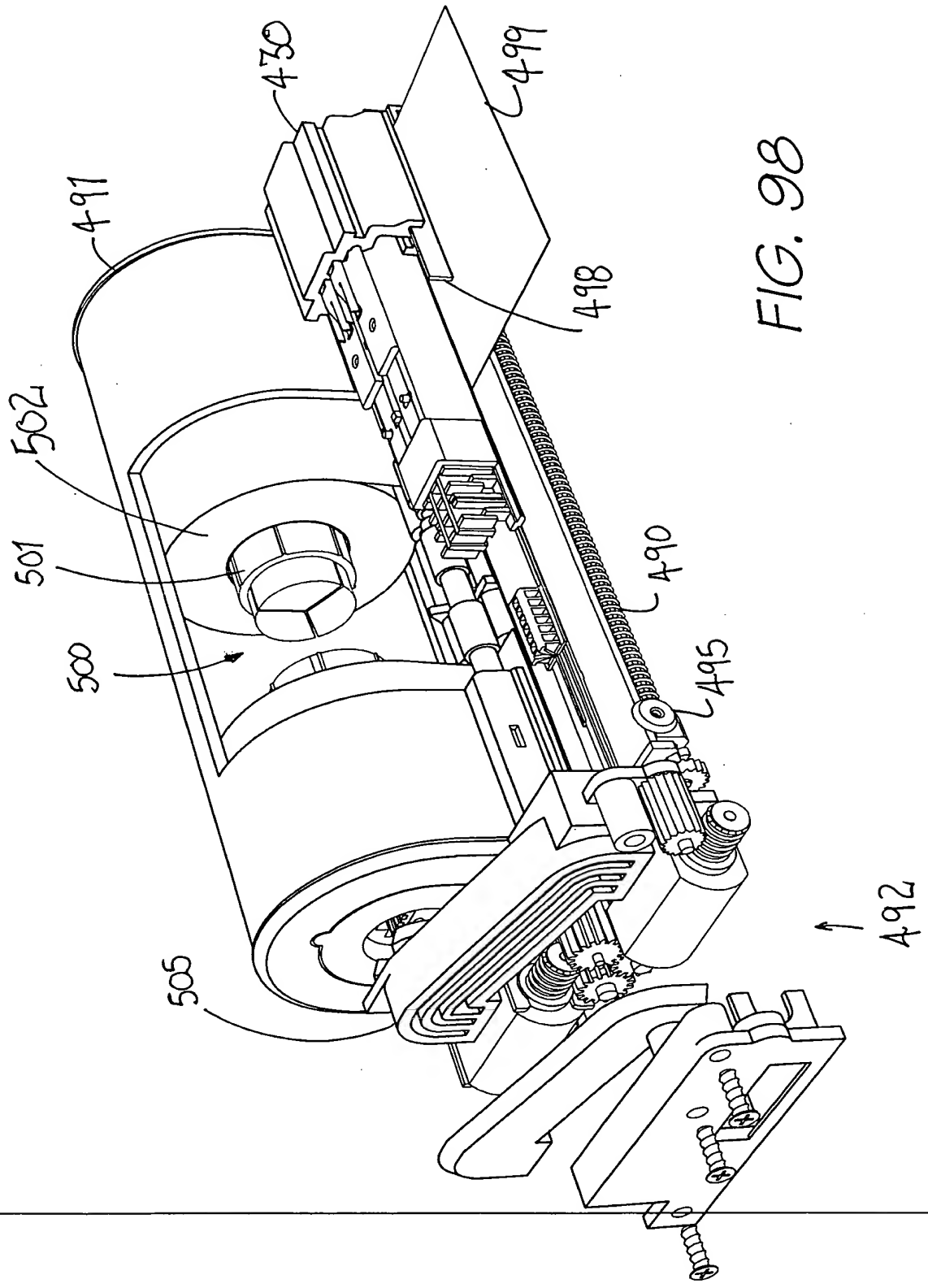


FIG. 98

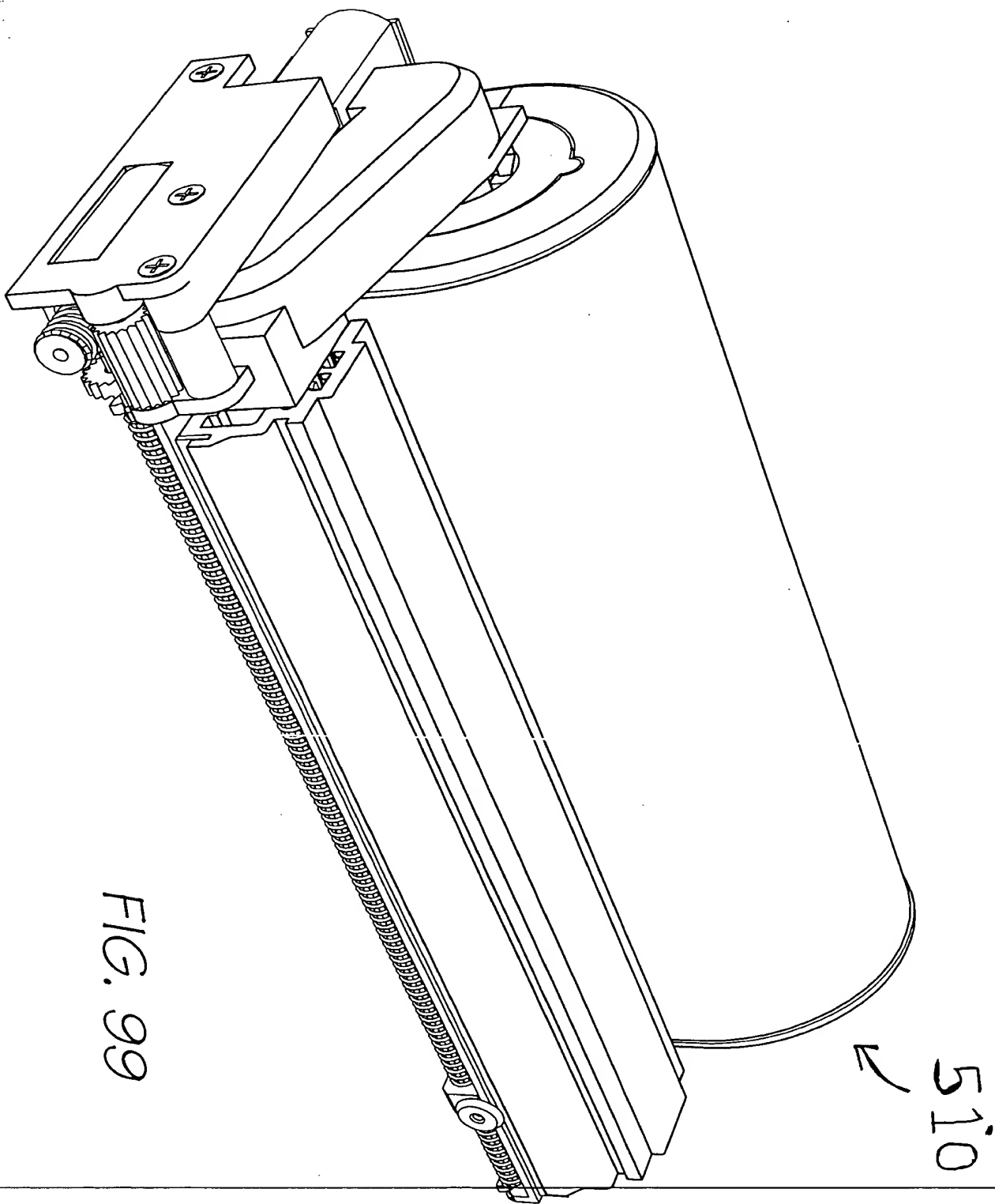
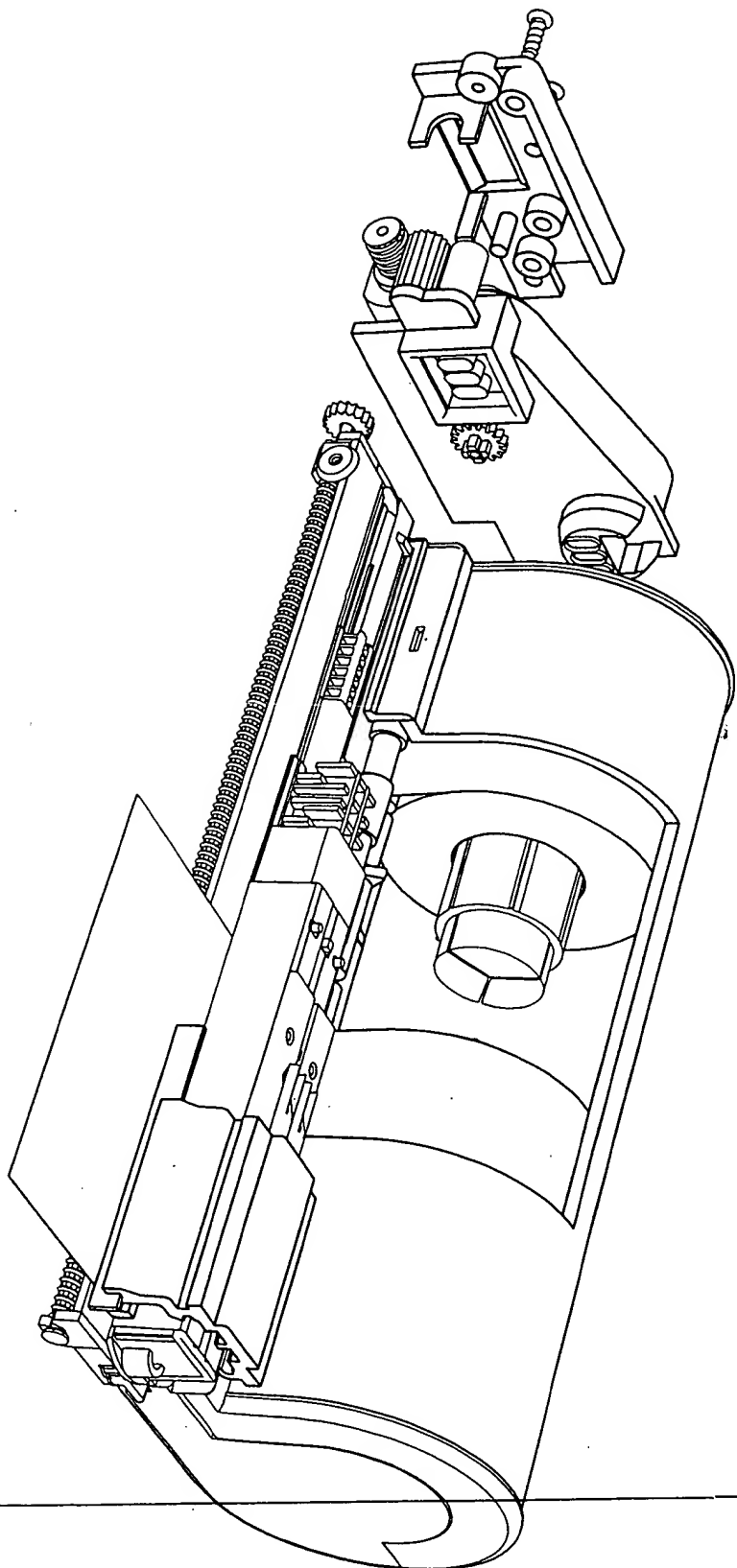


FIG. 99

FIG. 100



Abstract

In a moveable micromechanical device including a bending member having a first bending direction having a planar bottom surface, the bending member formed on a
05 plane substrate on top of a number of deposited lower layers, a method of forming the bending member comprising the step of: forming a series of structures in the deposited lower layers, the series of structures having a surface profile including a series of elongated ribs
10 running in a direction substantially transverse to the bending direction. The bending member can comprise a thermal bend actuator. The deposited layers can include a conductive circuitry layer.